“Spectra and Photometry: Windows into Exoplanet Atmospheres”

A. Burrows
Dept. of Astrophysical Sciences
Princeton University

Transiting Planets

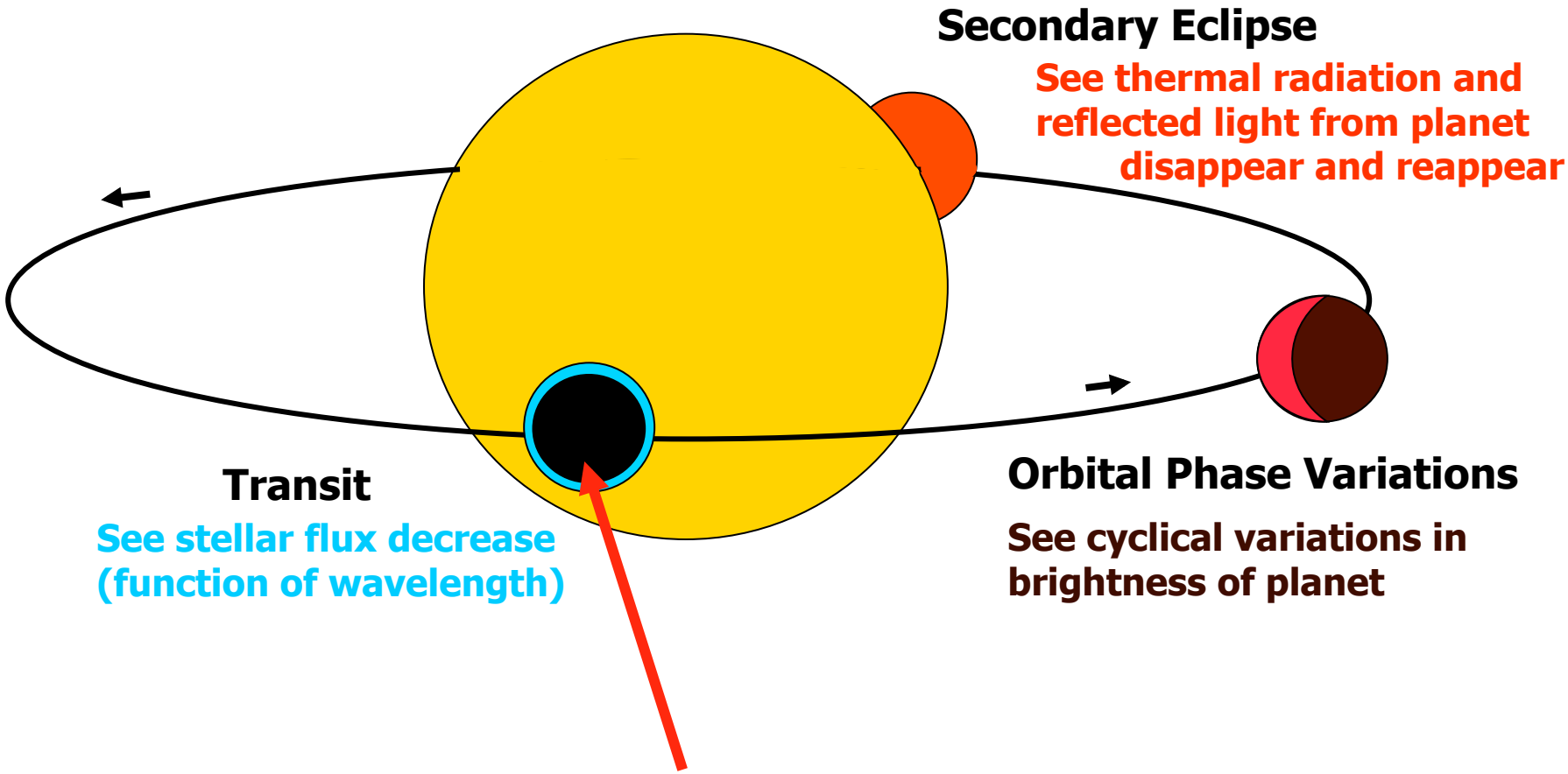

figure taken from H. Knutson

With upper-atmosphere optical absorber

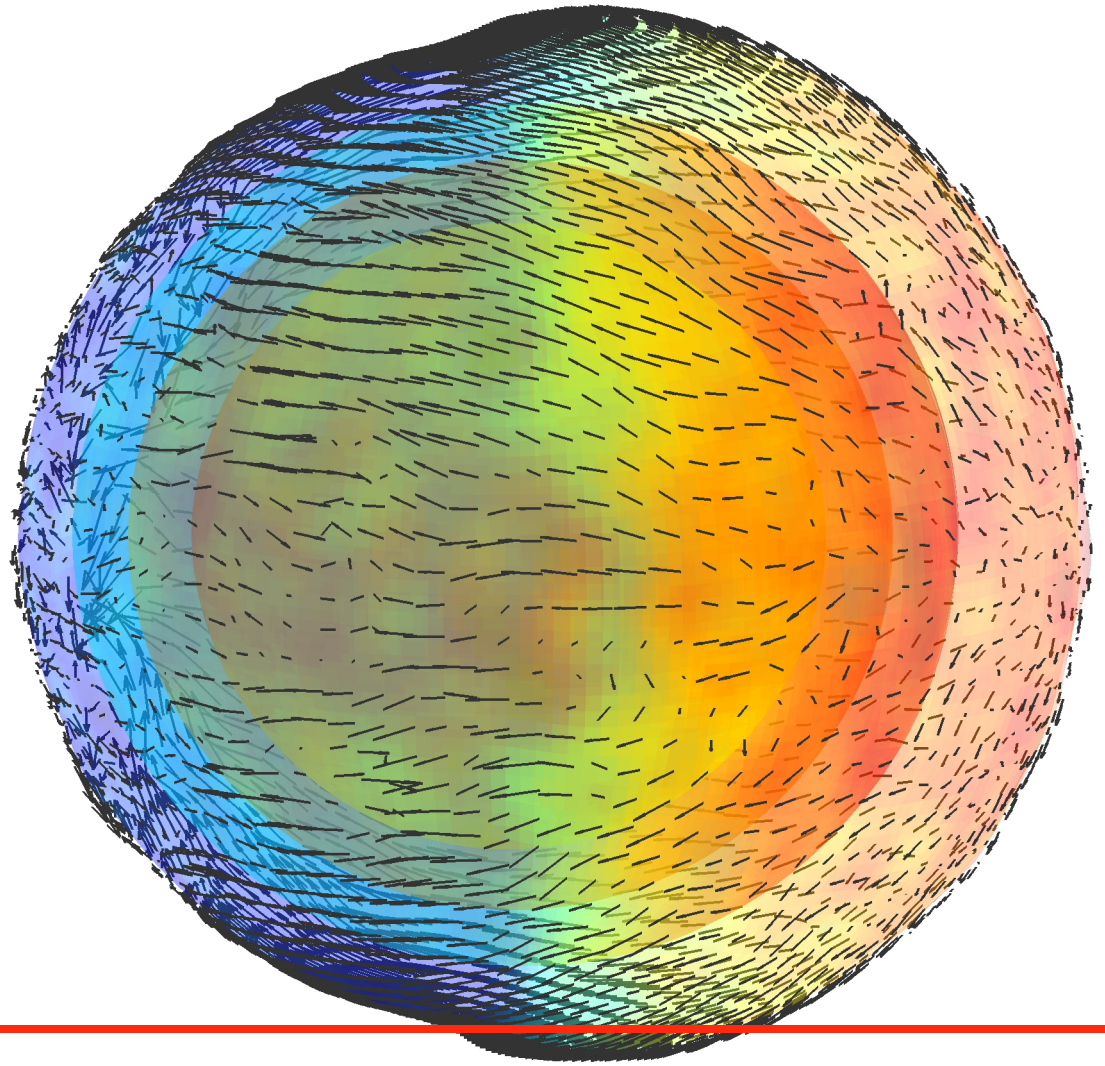

Transit chord

Graphics by D. Spiegel

P = 0.02 mbar, 5.7 mbar, 0.14 bar, 3.6 bar

Central Longitude: -90

Haze on HD 189733b

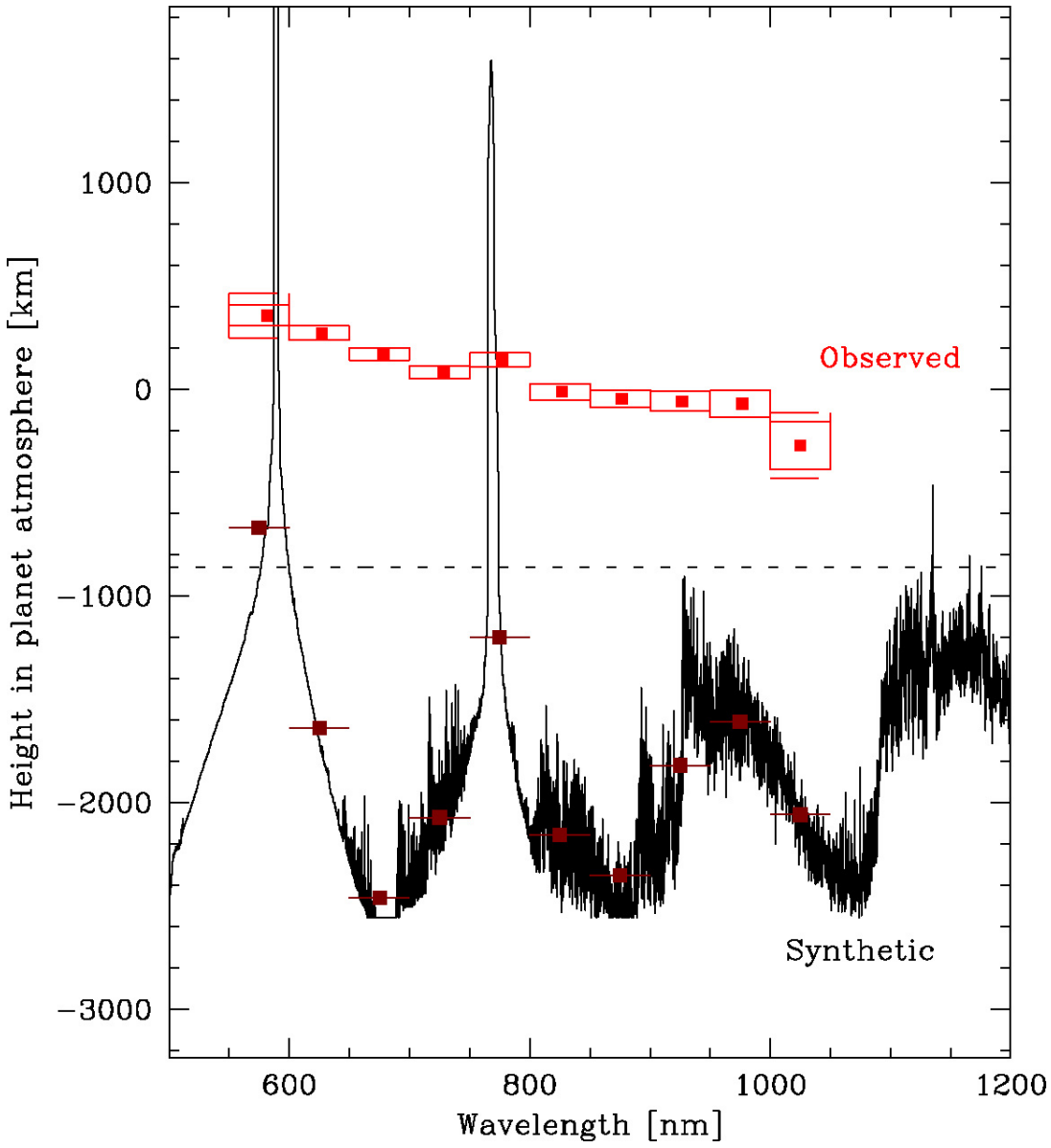

Pont et al .2013: Haze on HD 189733b

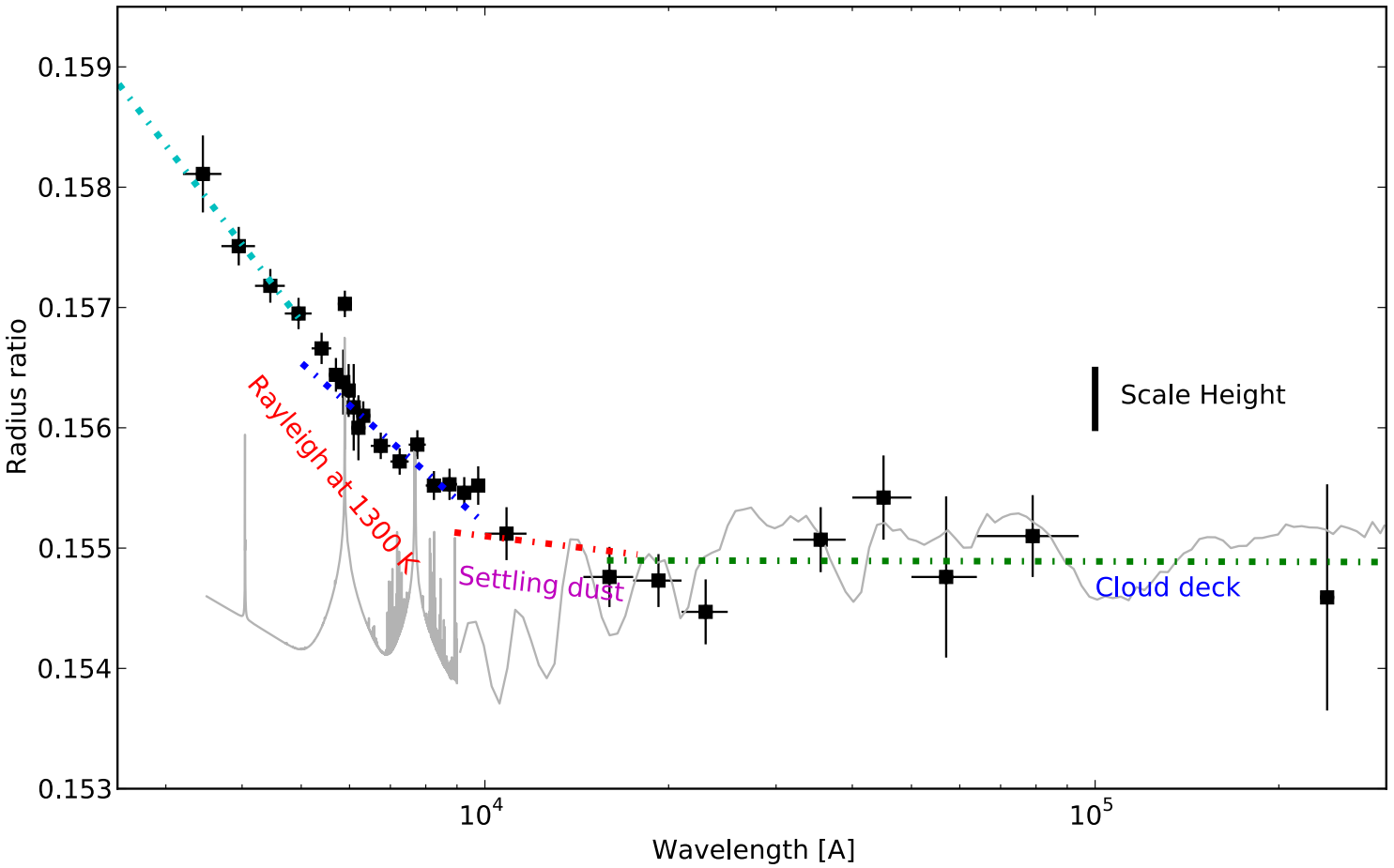

GJ 1214b: Transit Radius vs. Wavelength

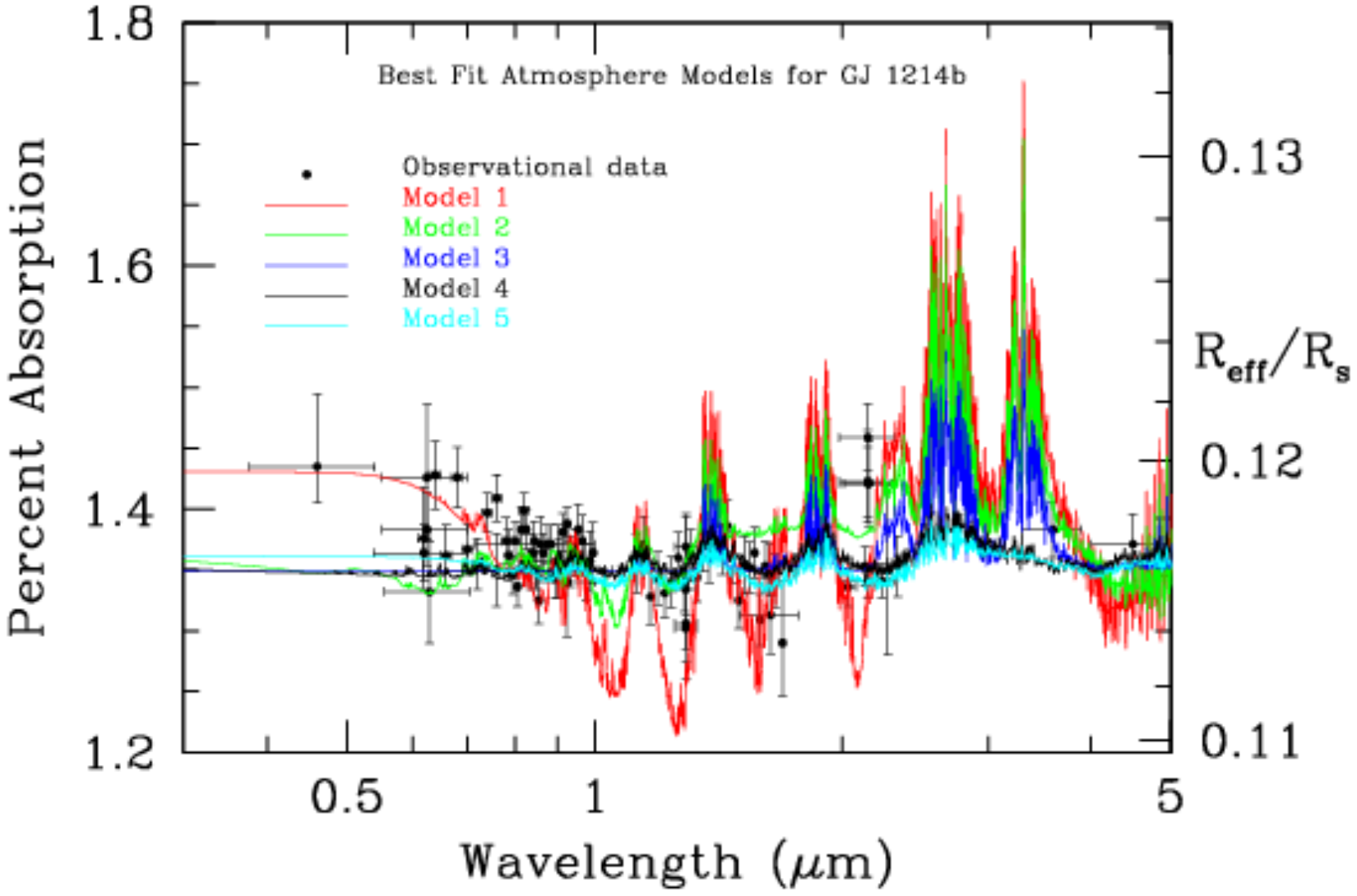

Howe & Burrows 2012, in press

HST GJ1214b transit spectrum – Kreidberg et al. 2014

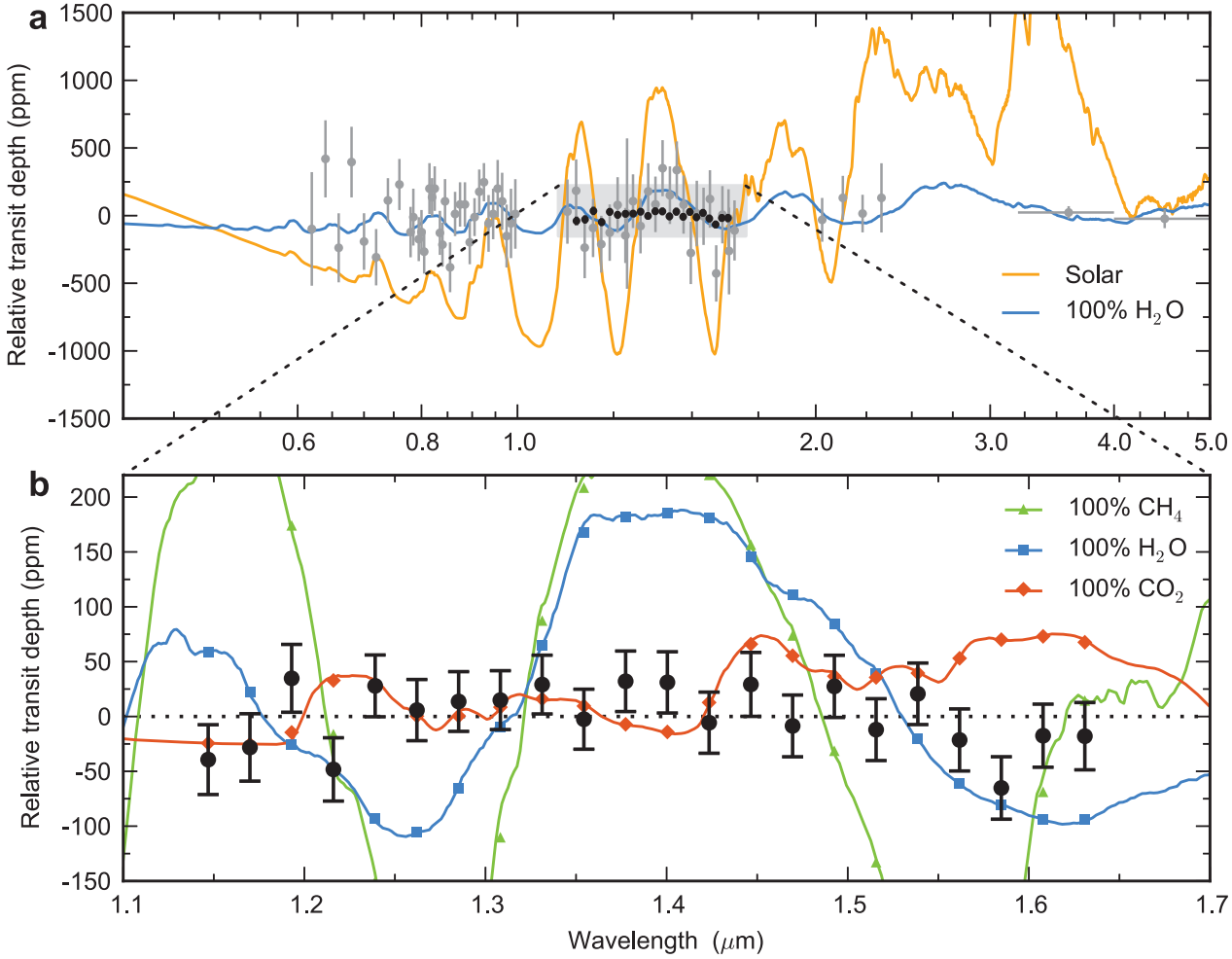

Hazes!

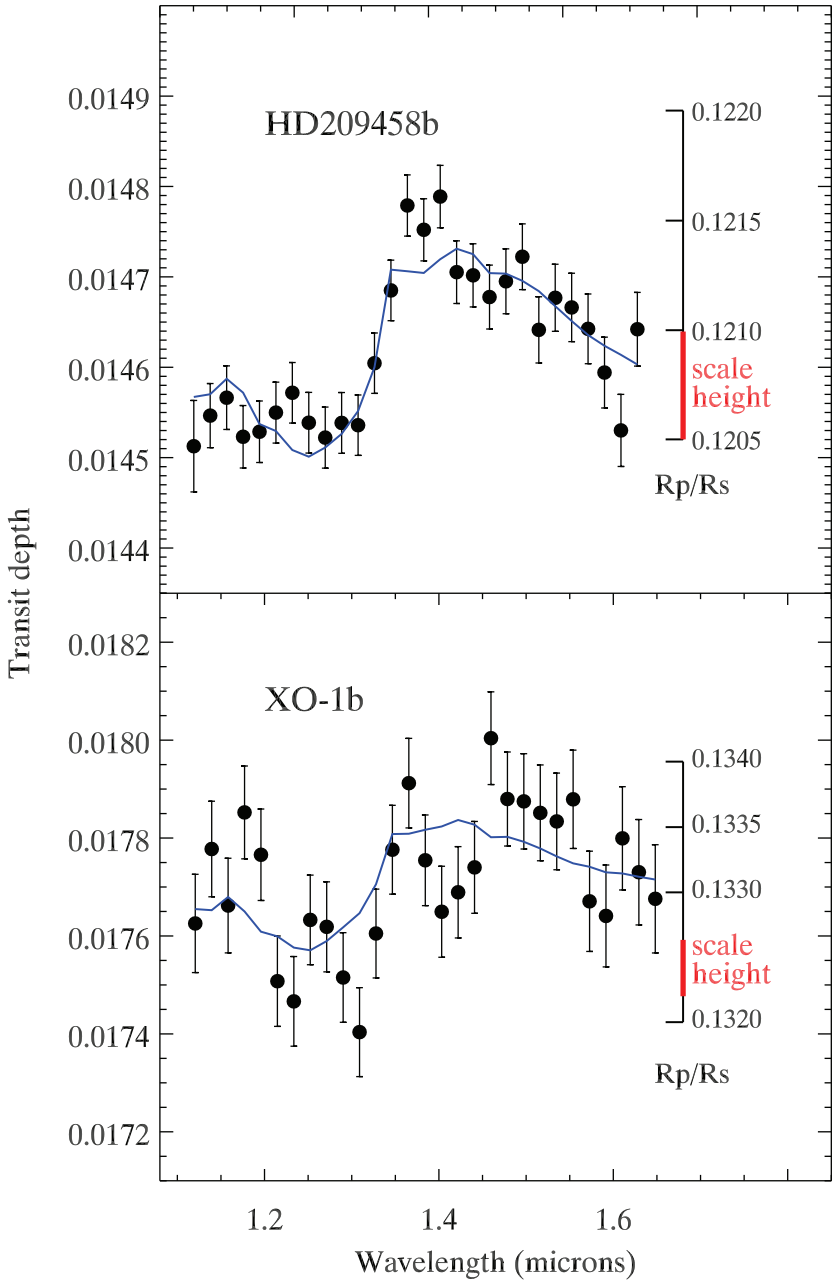

Deming et al. 2013:

HST transit spectra for HD209458b & XO-1b - Water

HST HD 209458b transit spectrum – Deming et al. 2013

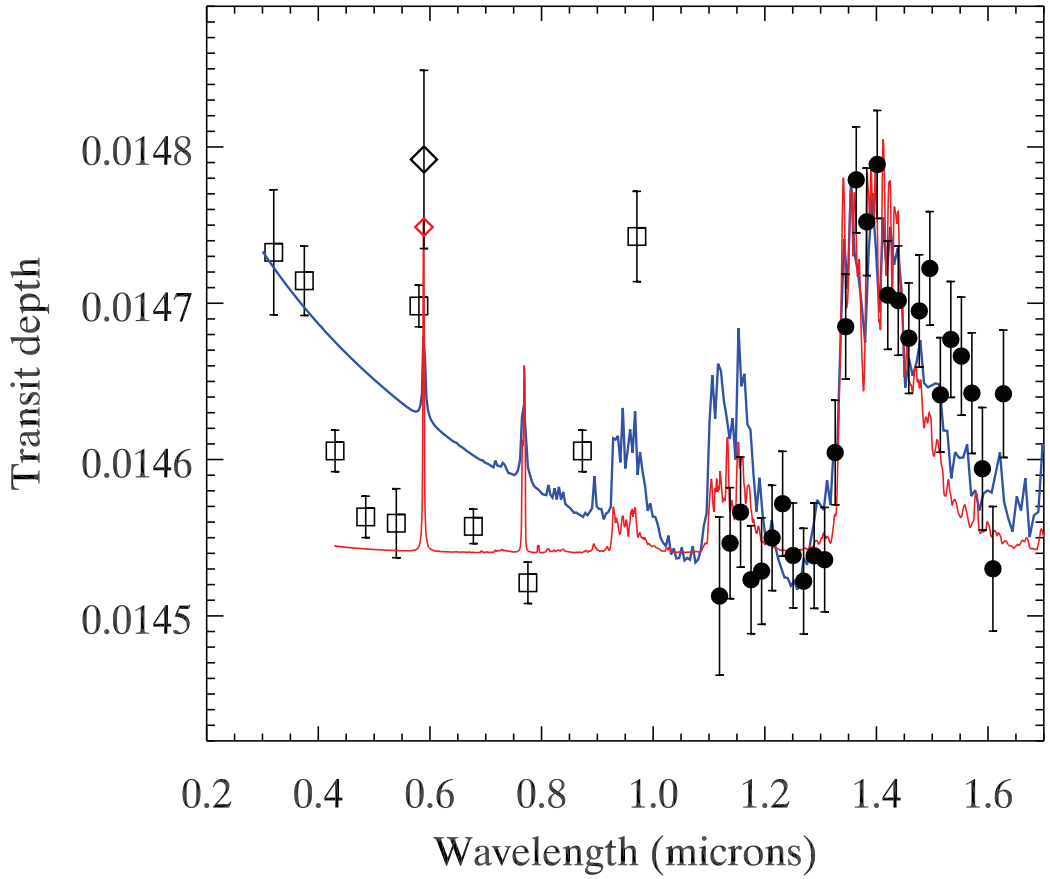

Hazes!

FIG. 14.— Transmission spectrum of HD 209458b derived from Hubble spectroscopy. Our WFC3 results are the solid points. The open squares are our reanalysis of the STIS bands defined by Knutson et al. (2007a), and the diamond is the narrow sodium band absorption from Charbonneau et al. (2002). The red line is the transmittance spectrum from an isothermal Burrows model, having an extra opacity of gray character and magnitude $0.012\,\mathrm{cm^2\,g^{-1}}$. The red diamond integrates the red model over the sodium bandpass. The blue line is a Dobbs-Dixon model for HD 209458b, with no gray opacity, but with λ^{-4} (Rayleigh) opacity, normalized to magnitude $0.001\,\mathrm{cm^2\,g^{-1}}$ at $0.8\,\mu$m. Because the blue model has no gray opacity, we scale-down the modulation in this spectrum by a factor of 3 for this comparison (see text).

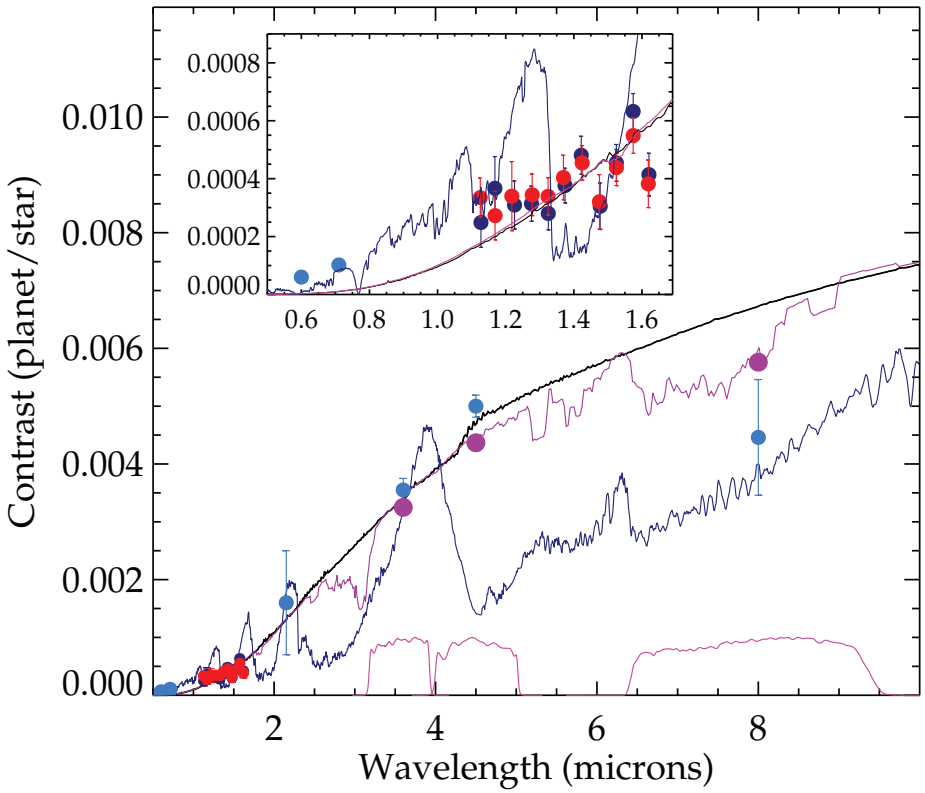

CoRoT2 HST spectrum
– Wilkins et al. 2014

Figure 14. Our WFC3 results for CoRoT-2b shown in the context of ground-based 2 μm results (Alonso et al. 2010), the Spitzer results from Deming et al. (2011), and the optical eclipse depths from Alonso et al. (2009). The black line is an 1788K blackbody for the planet, and the dark blue line is a conventional Burrows model used to interpret the Spitzer data (Deming et al. 2011). The magenta model is from Madhusudhan as a best-fit to the totality of the data illustrated here. It has equal carbon and oxygen abundances, but lacks a temperature inversion (see text). The inset shows our WFC3 results, from both our α (red points) and β (blue) analyses.

HST GJ436b transit spectrum – Knutson et al. 2014

Hazes!

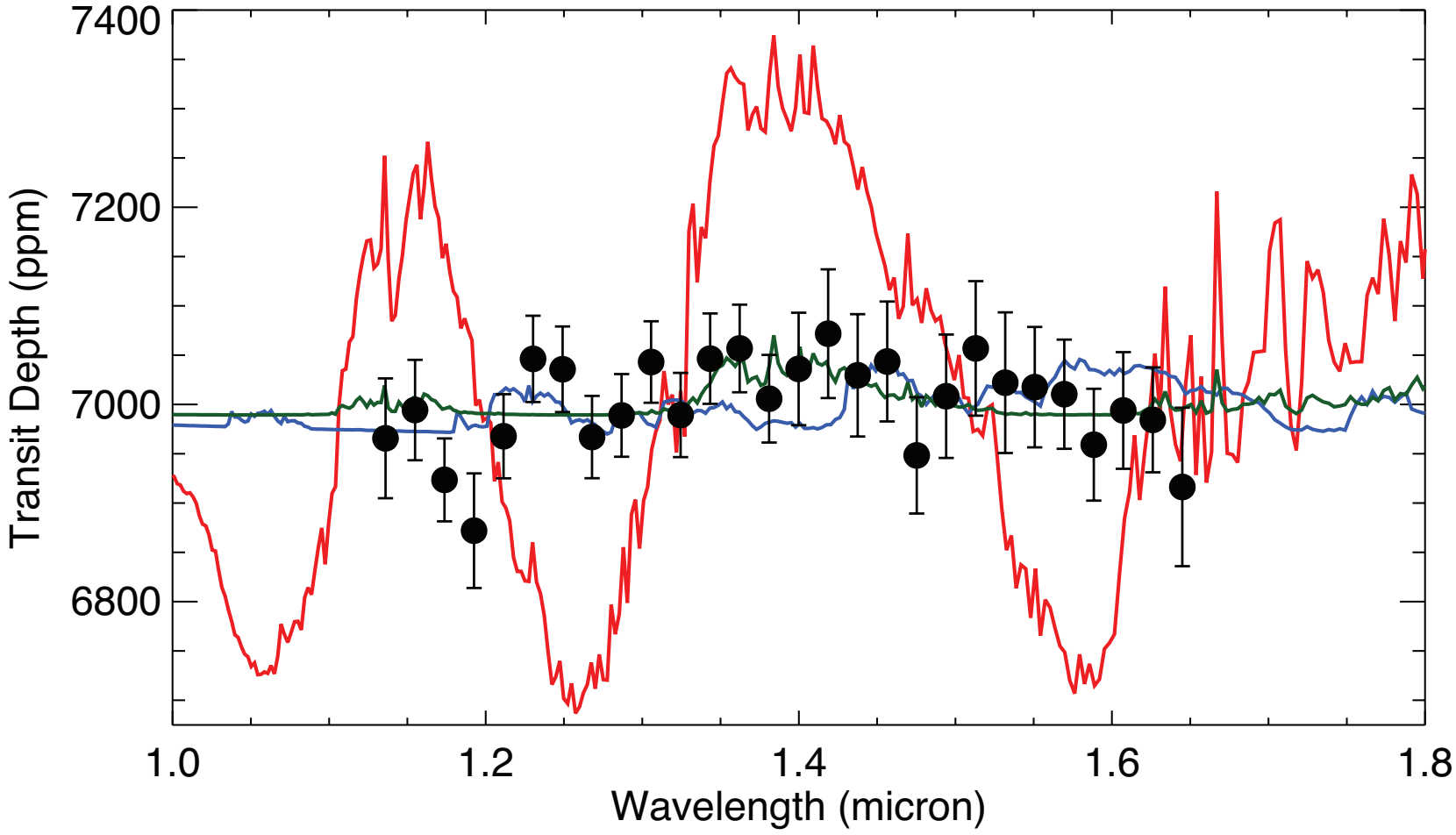

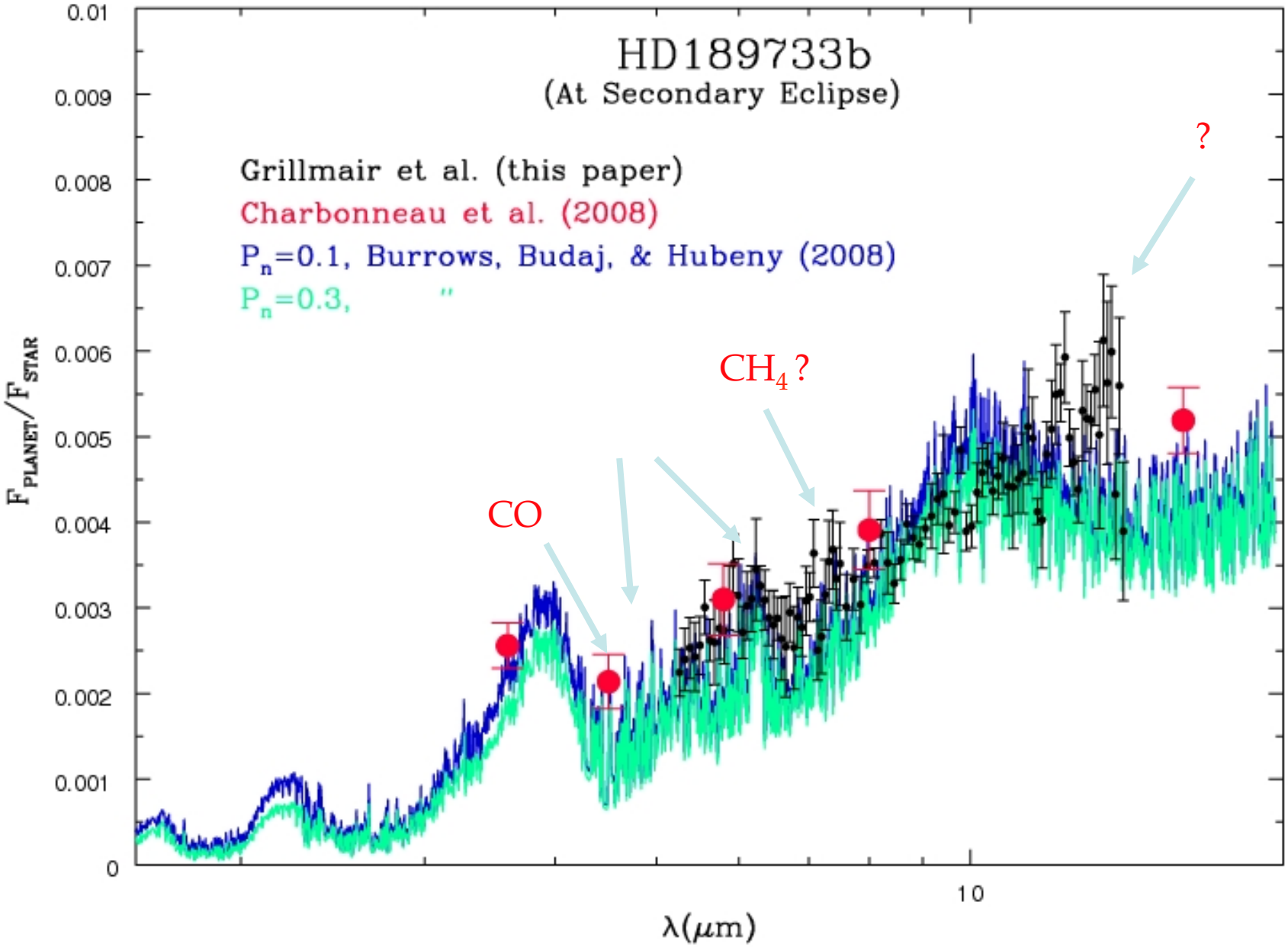
HD189733b
(At Secondary Eclipse)
Grillmair et al. (this paper)
Charbonneau et al. (2008)
P_n=0.1, Burrows, Budaj, & Hubeny (2008)
P_n=0.3, "
?
CH4 ?
CO
F_PLANET/F_STAR
λ(μm)
0.01
0.009
0.008
0.007
0.006
0.005
0.004
0.003
0.002
0.001
0
10

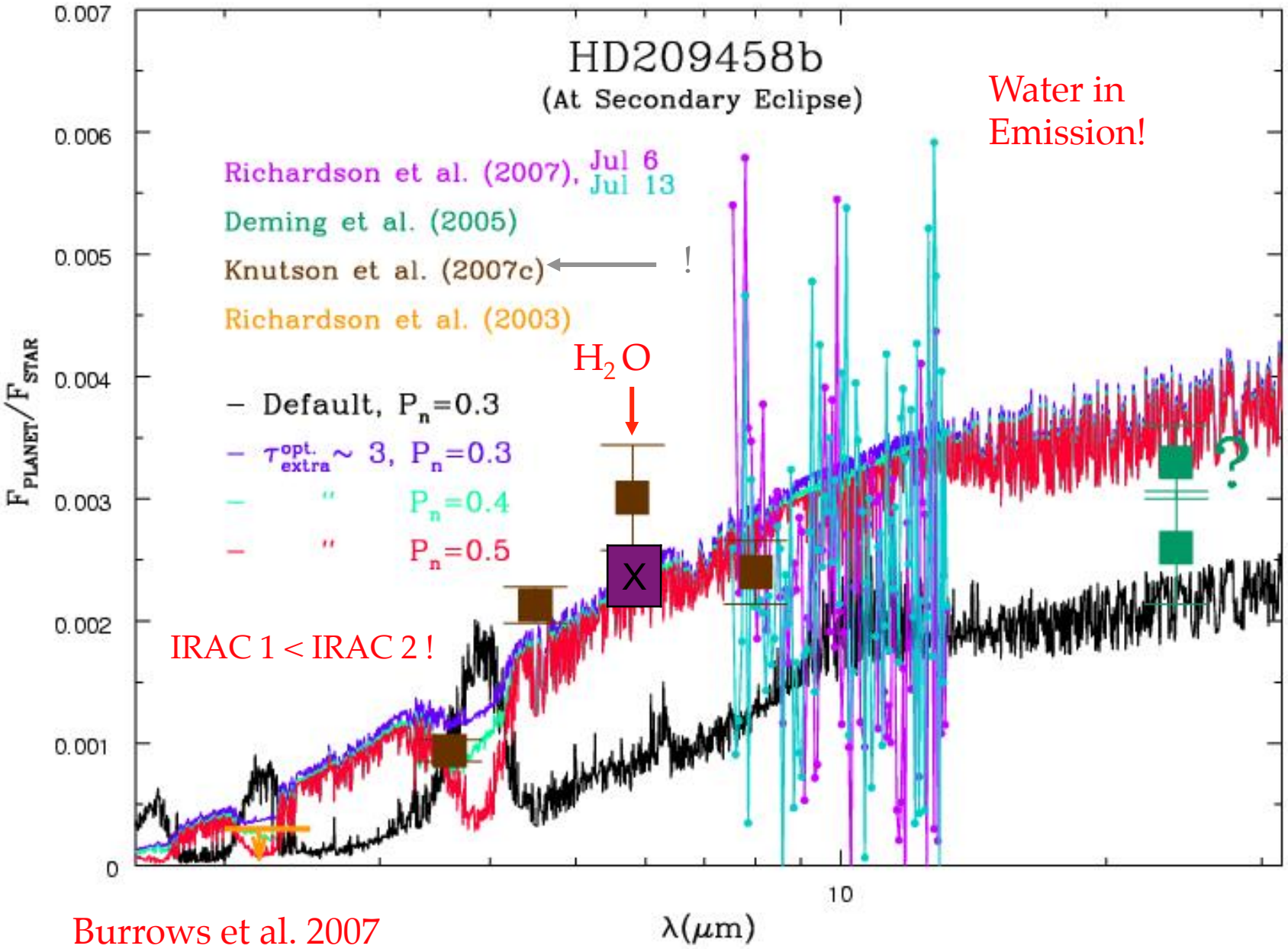

Burrows et al. 2007

First Longitudinal Temperature Profile for an Exoplanet: HD 189733b's Warm Night Side

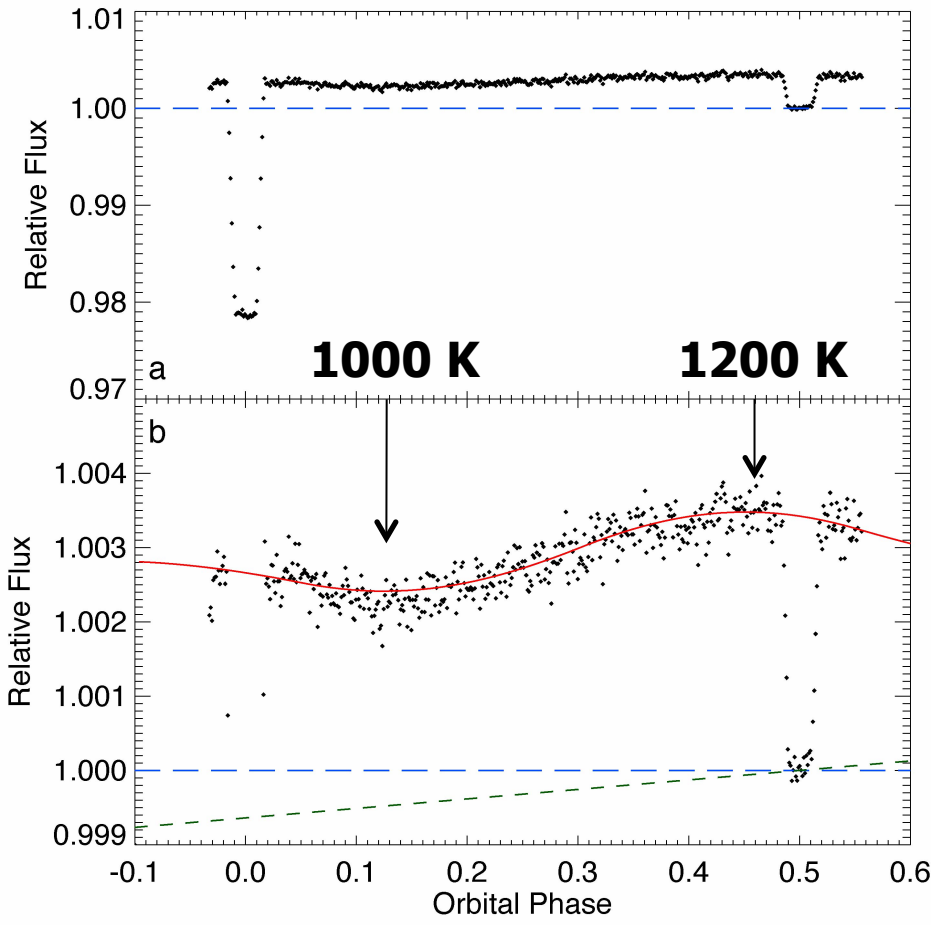

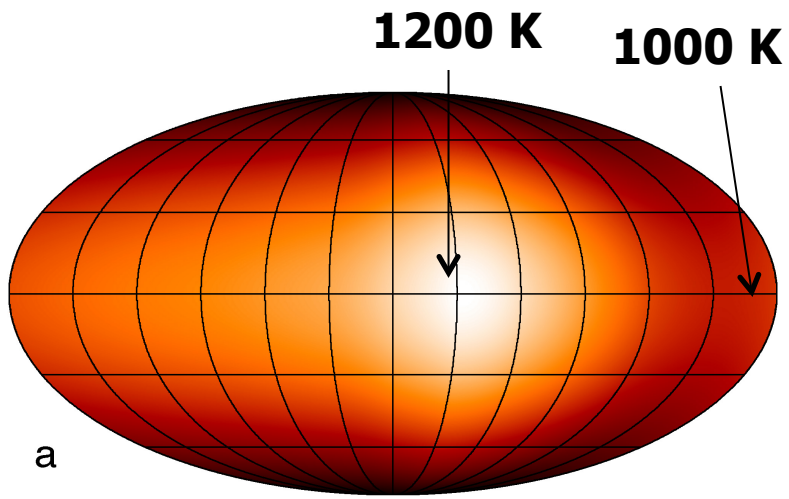

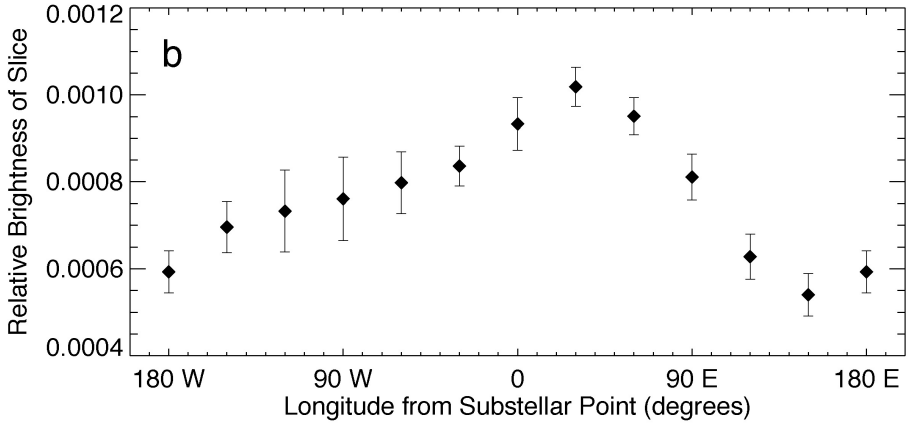

Spitzer 8 μm observations of HD 189733b (Knutson et al. 2007b, *Nature* 447, 183).

New Ups And b Phase Curve at 24 μm

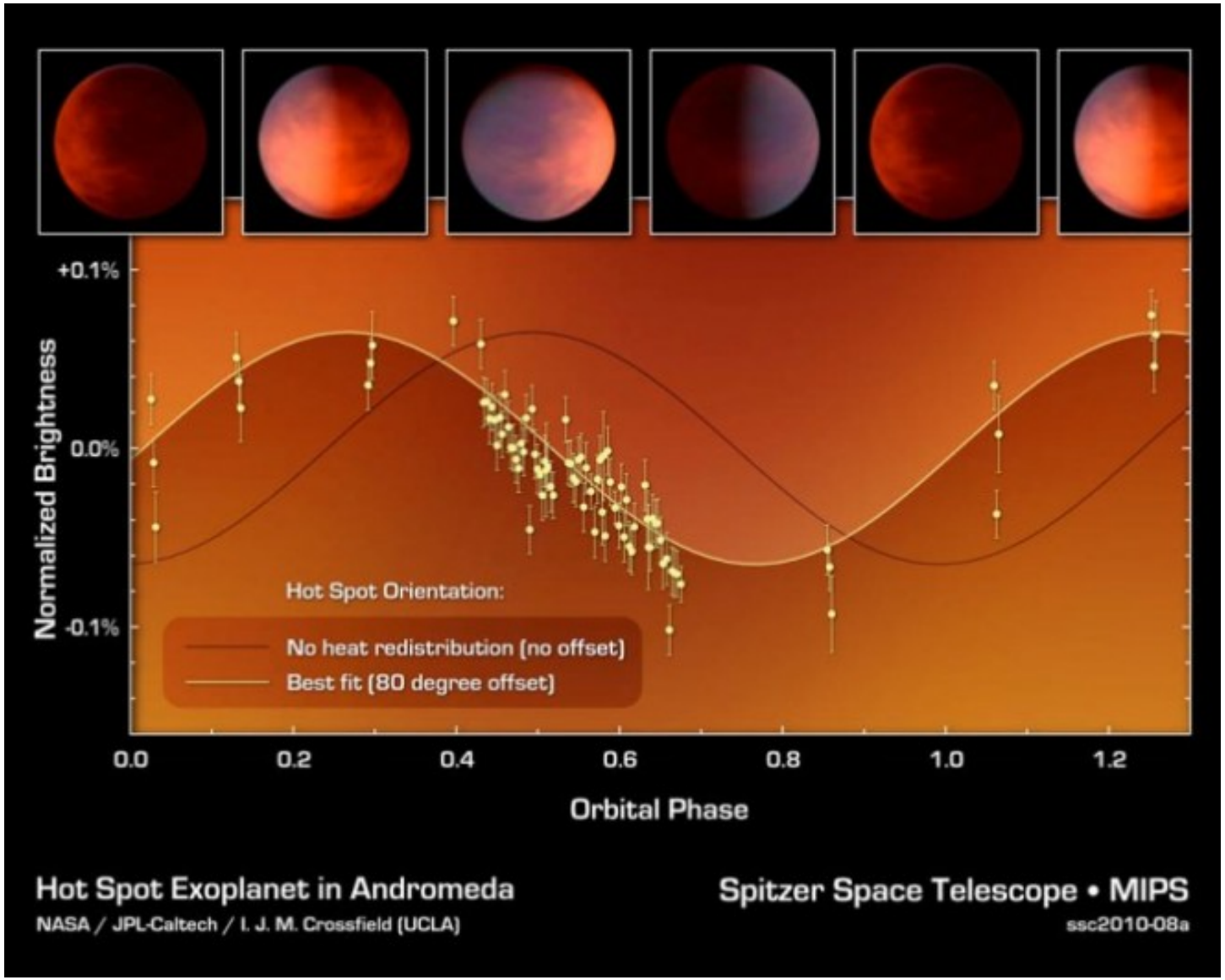

Harrington et al. 2010

Evidence for a Diversity of Day-Night Circulation Patterns

Large day-night brightness gradient
HAT-P-7 / Kepler

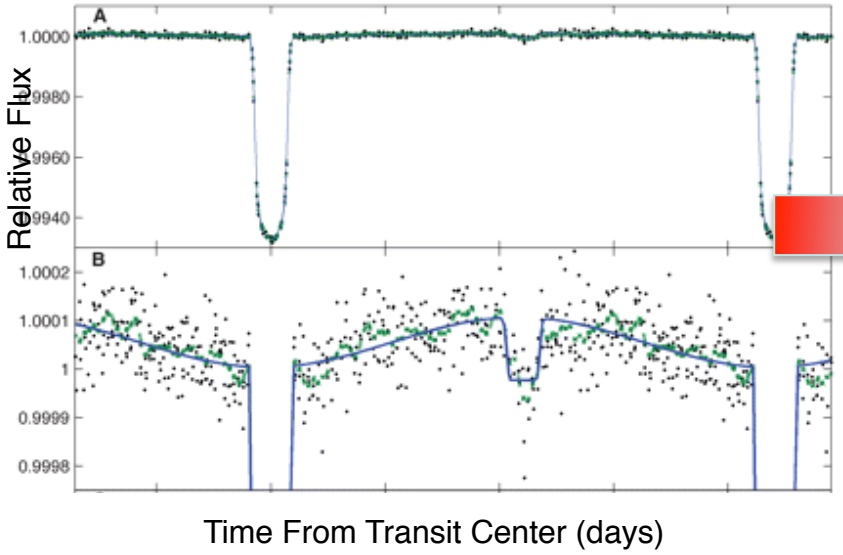

Small day-night brightness gradient
HD 189733b / Spitzer

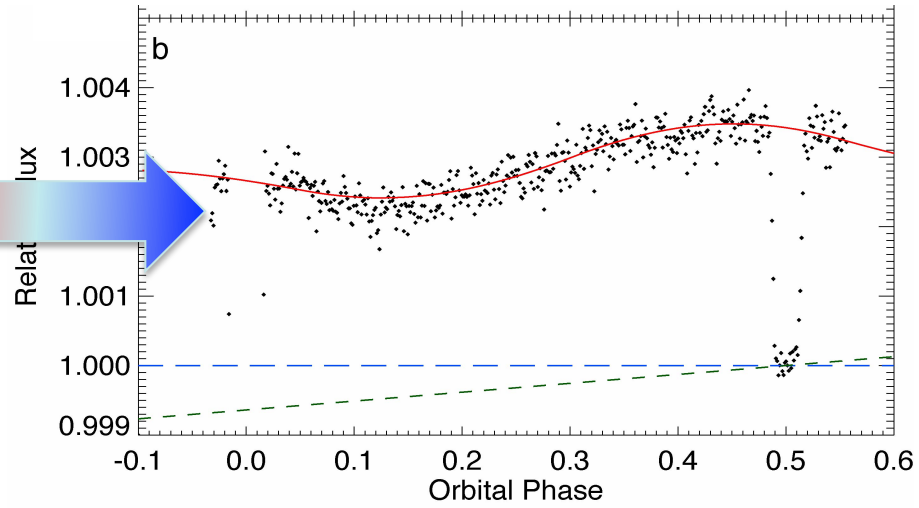

Large gradients:

u And b* (Harrington et al. 2007)

HD 179949* (Cowan et al. 2008)

HAT-P-7 (Borucki et al. 2009)

* non-transiting planet, brightness/ temperature gradient degenerate with unknown orbital inclination and planet radius

Intermediate gradients:

HD 149026 (Knutson et al. 2009)

Small gradients:

HD 189733b (Knutson et al. 2007)

HD 209458 (Zellem et al. 2014)

I-band HD 209458b Map (model a03)

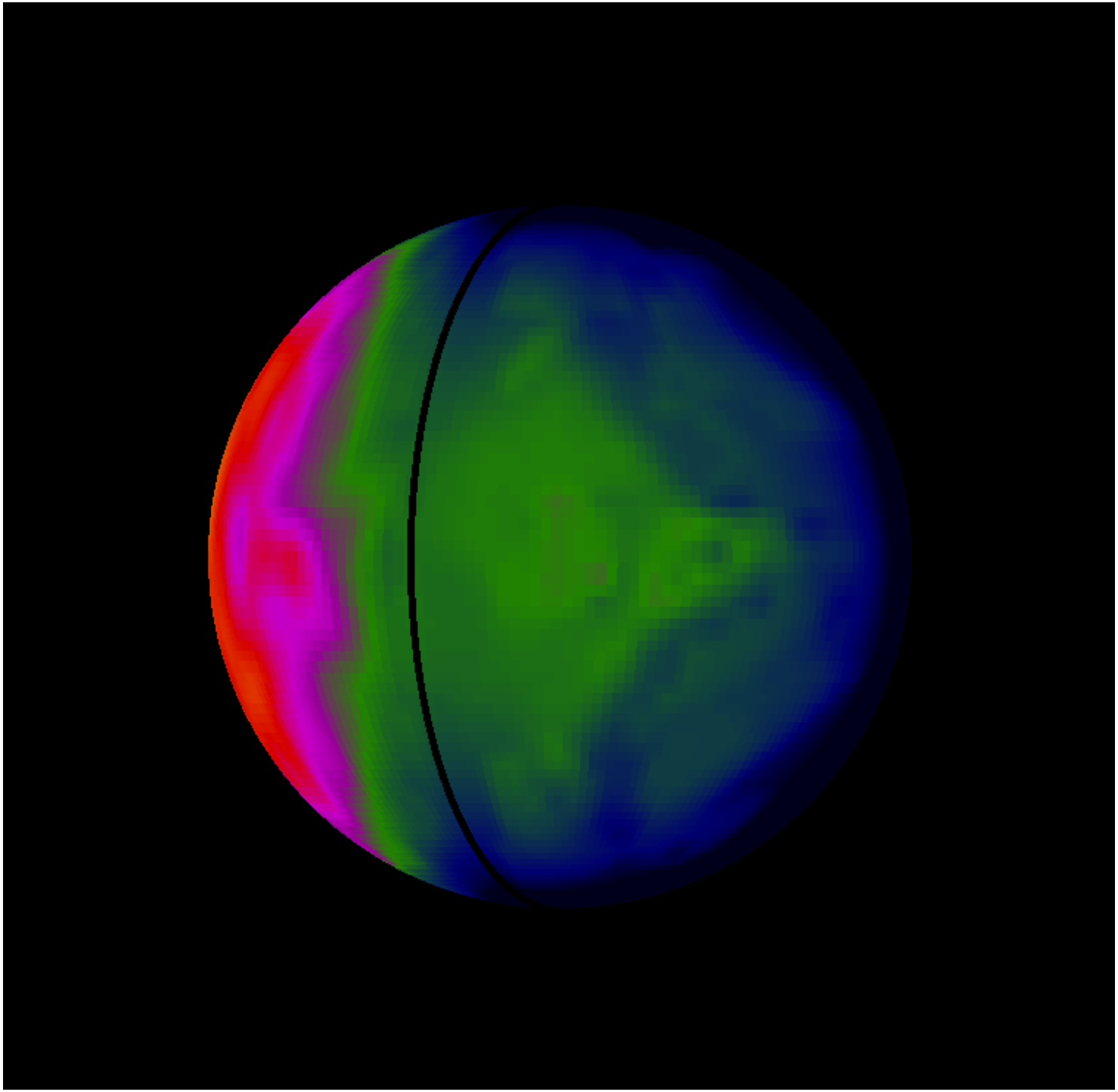

Burrows et al. 2010

J-band HD 209458b Map (model a03)

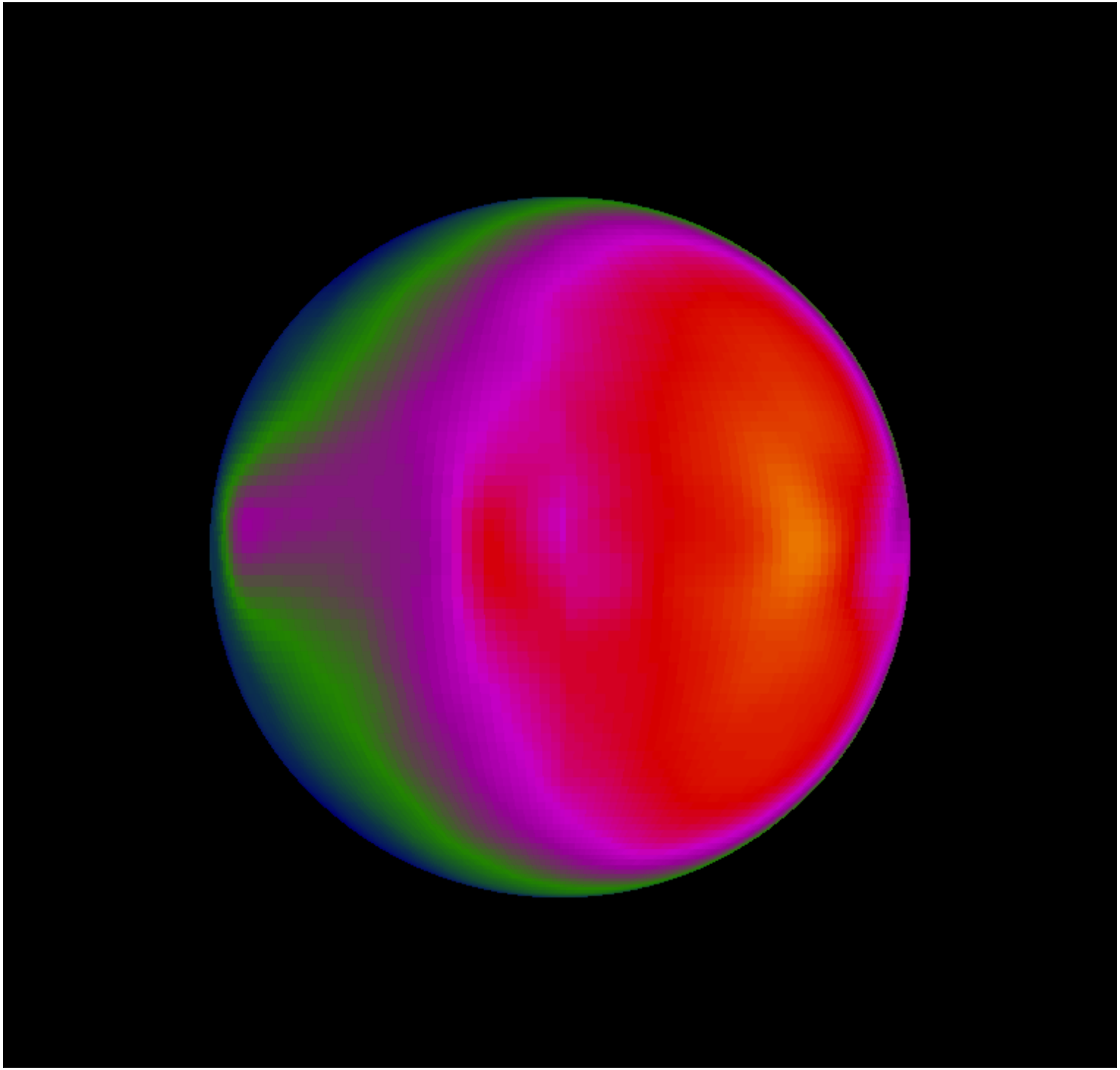

Burrows et al. 2010

HD 209458b: Integrated Phase Light Curves: With inversion / hot upper atmosphere

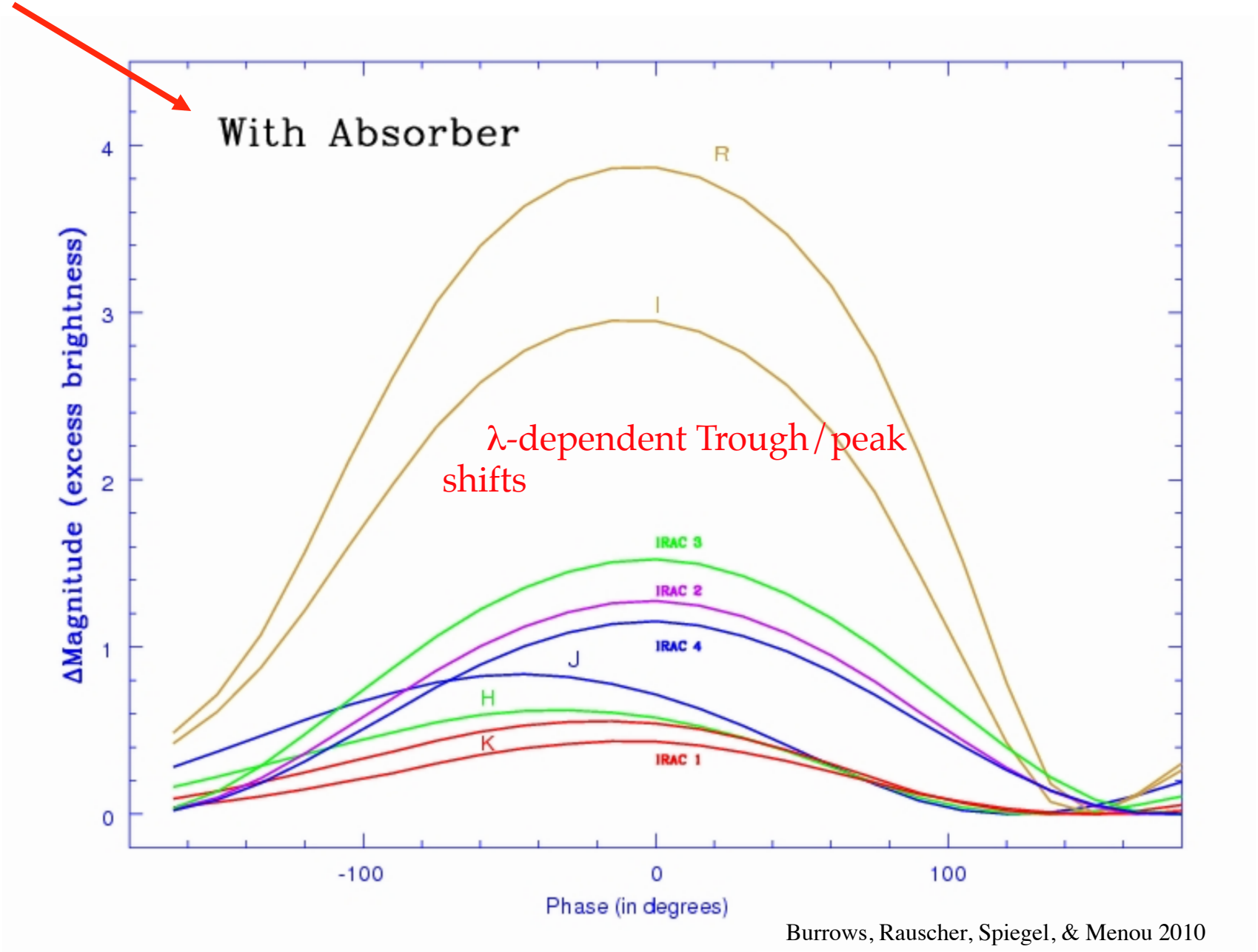

Burrows, Rauscher, Spiegel, & Menou 2010

HD 209458b: Integrated Phase Light Curves: No upper atmosphere absorber

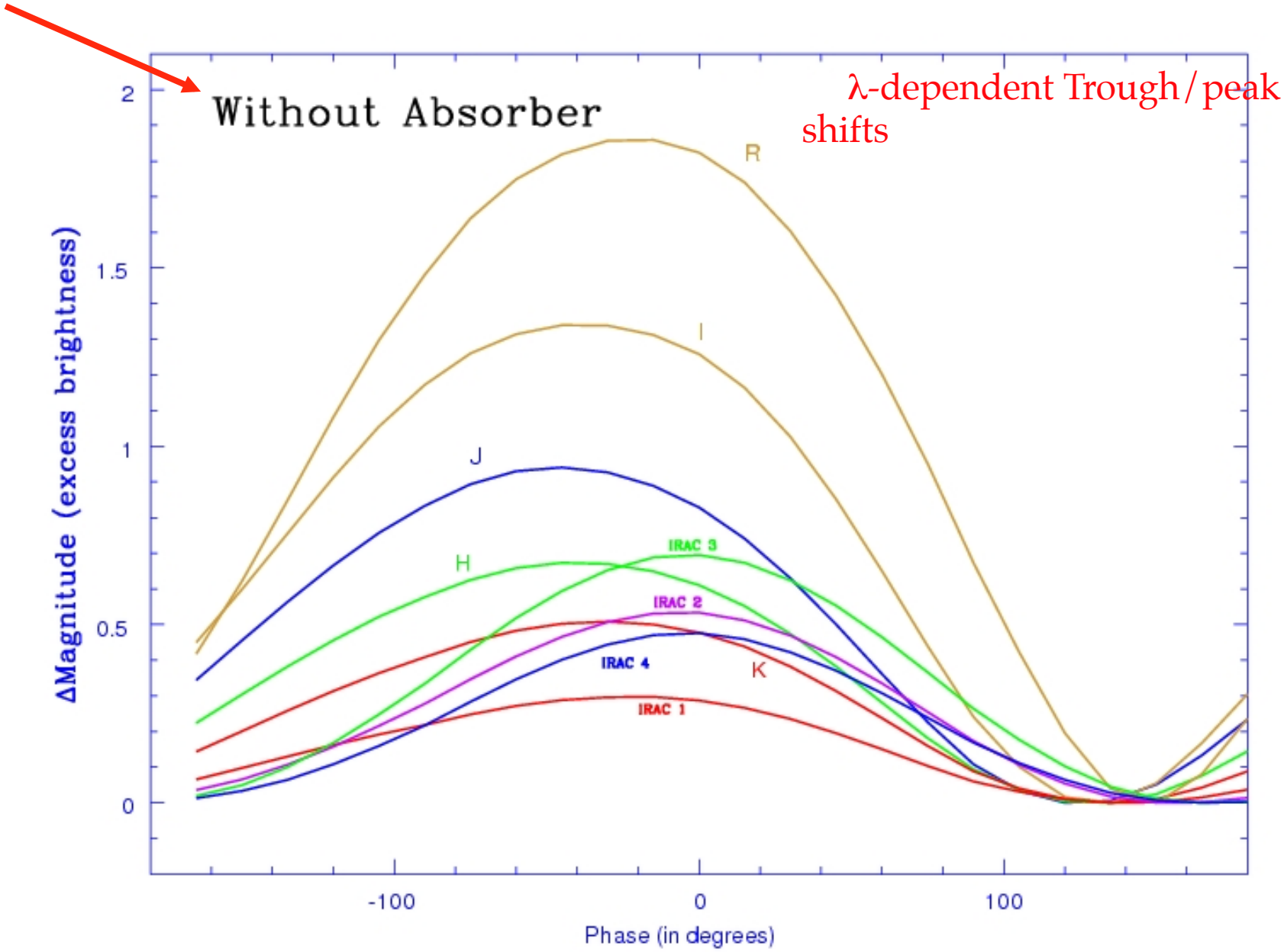

Burrows, Rauscher, Spiegel, & Menou 2010

High-Contrast Imaging

The Planet/Star Flux Ratio for wide-separation extra-solar giant planets (EGPs) depends upon:

- Geometric albedo (A_g), Phase Function ($\Phi(\alpha)$), Keplerian elements, Epoch
- Both A_g and $\Phi(\alpha)$ depend upon wavelength (!) - planet color a function of phase
- Temperature-pressure-composition profiles are needed
- Clouds (NH_3 and H_2O) are crucial determinants, as are Hazes (polyacetylenes, tholins, …)
- For clouds and hazes: Need particle-size distributions, complex indices, vertical extent
- Polarization can be a useful adjunct for physical interpretation
- Detailed models, simple models, and analytic approximations are available, but work is needed to develop analysis pipeline and reverse modeling protocols to extract physical parameters, with error bars.

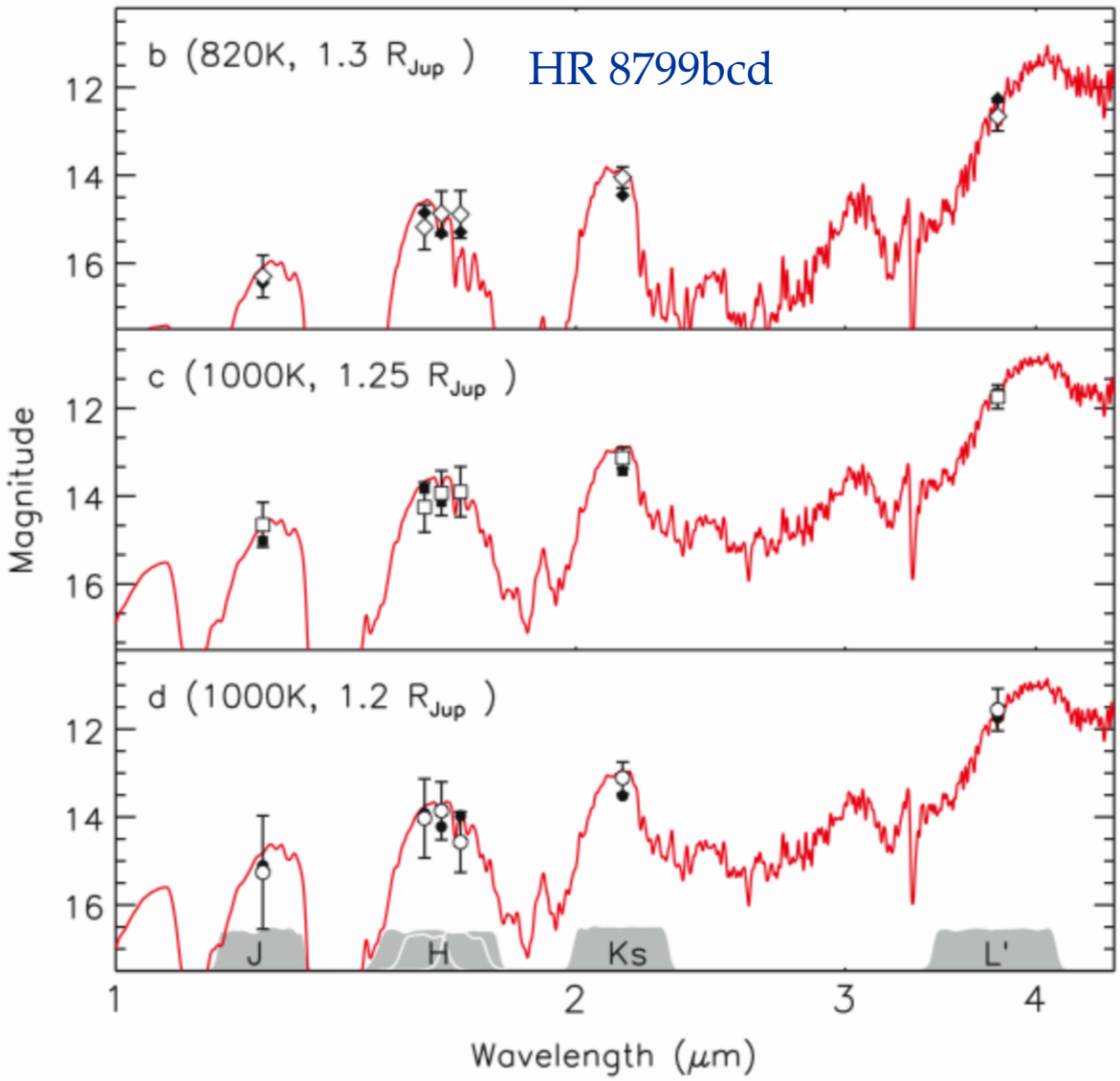
HR 8799bcd
b (820K, 1.3 R$_{Jup}$)
c (1000K, 1.25 R$_{Jup}$)
d (1000K, 1.2 R$_{Jup}$)
Magnitude
12
14
16
J
H
Ks
L'
1
2
3
4
Wavelength (μm)

Very Dusty Atmospheres - low gravity?

HR 8799b

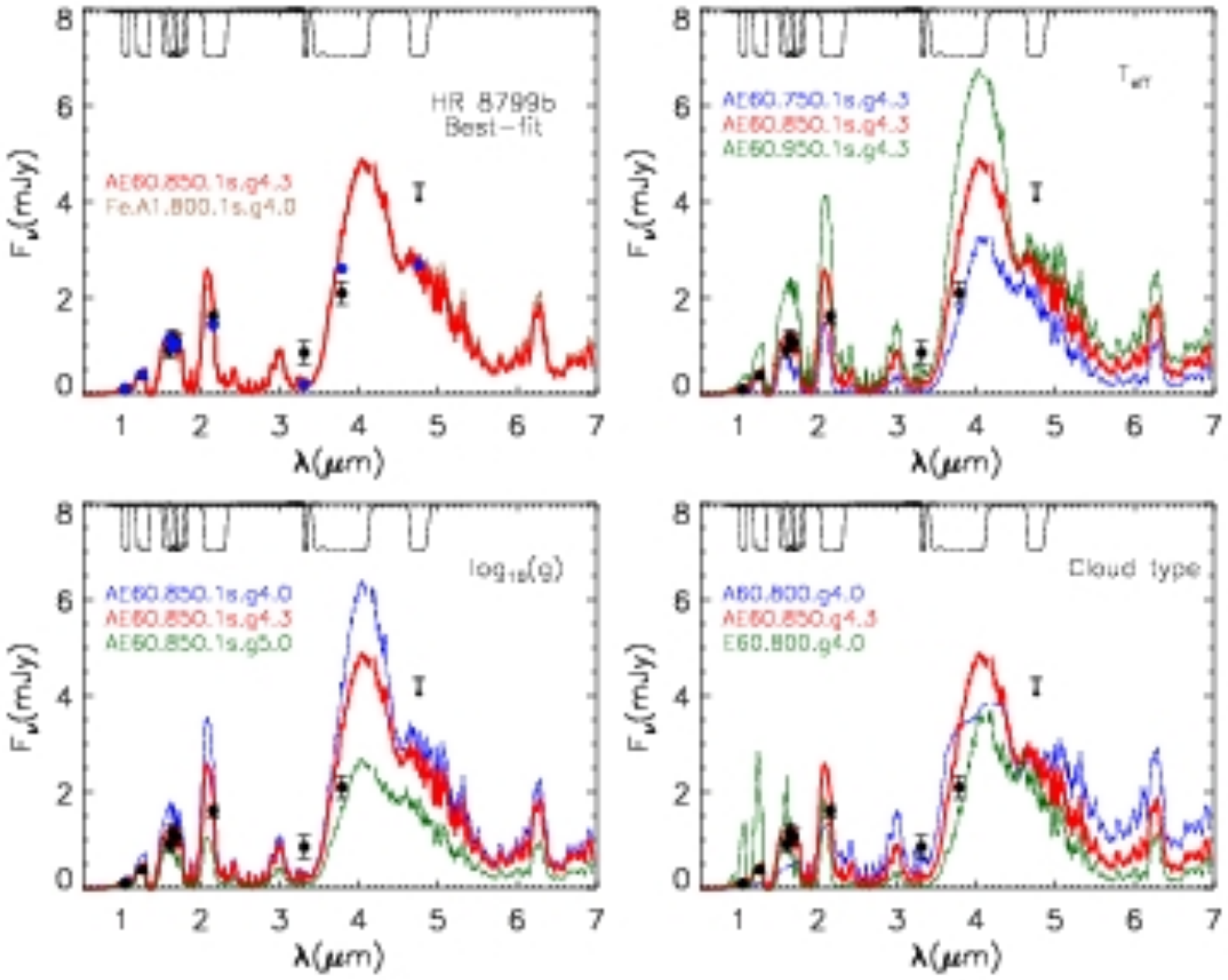

Madhusudhan, Burrows, & Currie 2011

See also Barman et al.

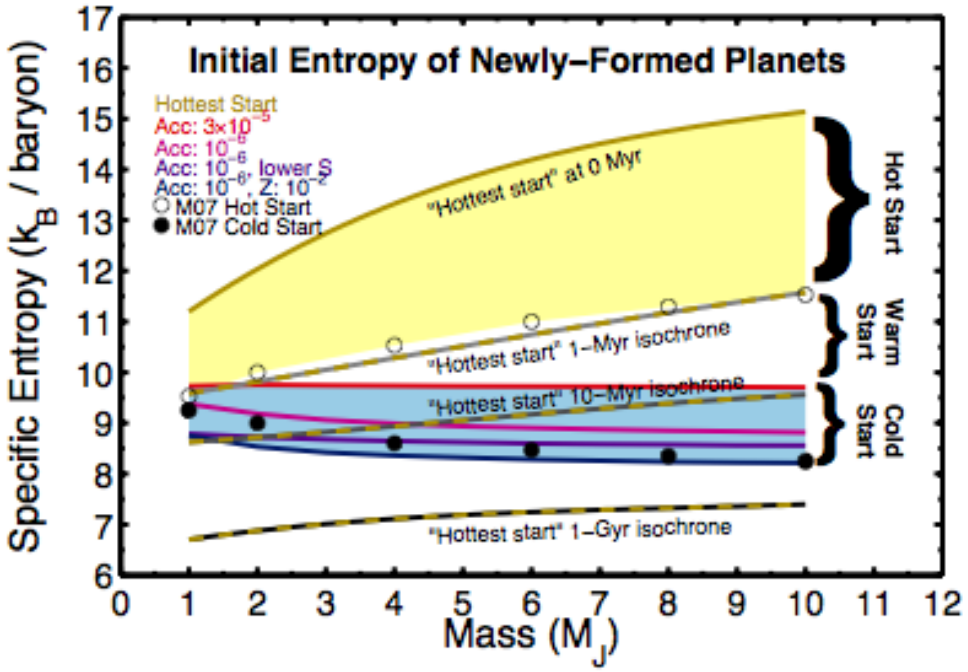
Initial Entropy of Newly–Formed Planets
Specific Entropy (k_B / baryon)
Mass (M_J)
Hottest Start
Acc: 3×10^{-5}
Acc: 10^{-6}
Acc: 10^{-6}, lower S
Acc: 10^{-6}, Z: 10^{-2}
M07 Hot Start
M07 Cold Start
"Hottest start" at 0 Myr
"Hottest start" 1–Myr isochrone
"Hottest start" 10–Myr isochrone
"Hottest start" 1–Gyr isochrone
Hot Start
Warm Start
Cold Start

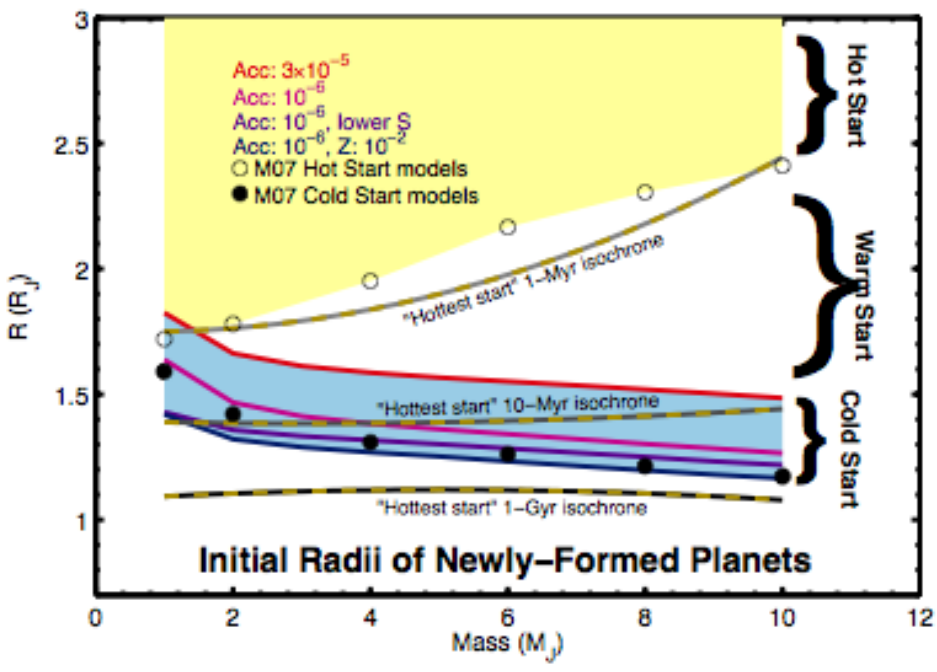
Initial Radii of Newly–Formed Planets
R (R_J)
Mass (M_J)
Acc: 3×10^{-5}
Acc: 10^{-6}
Acc: 10^{-6}, lower S
Acc: 10^{-6}, Z: 10^{-2}
M07 Hot Start models
M07 Cold Start models
"Hottest start" 1–Myr isochrone
"Hottest start" 10–Myr isochrone
"Hottest start" 1–Gyr isochrone
Hot Start
Warm Start
Cold Start

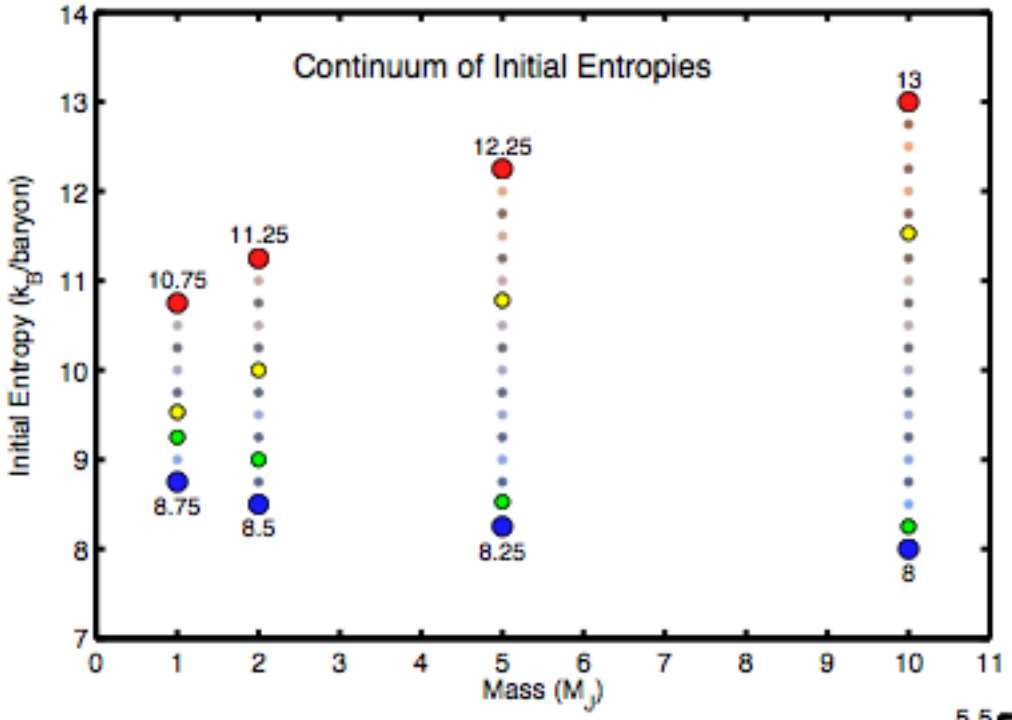
Continuum of Initial Entropies
Initial Entropy (k_B/baryon)
Mass (M_J)
10.75
11.25
12.25
13
8.75
8.5
8.25
8

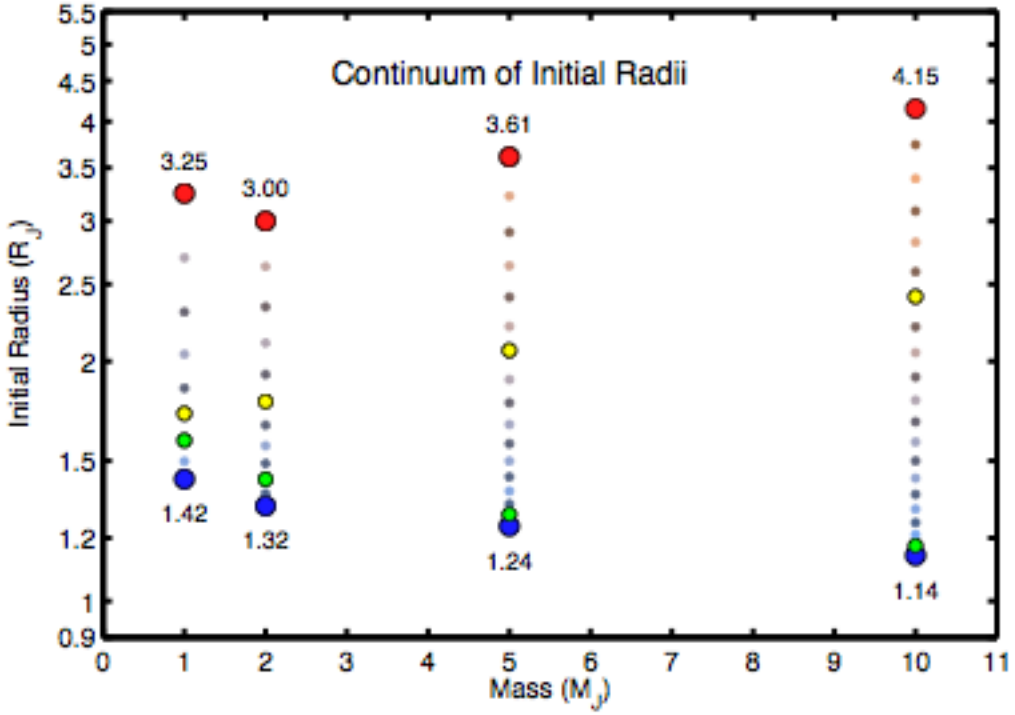
Continuum of Initial Radii
Initial Radius (R_J)
Mass (M_J)
3.25
3.00
3.61
4.15
1.42
1.32
1.24
1.14

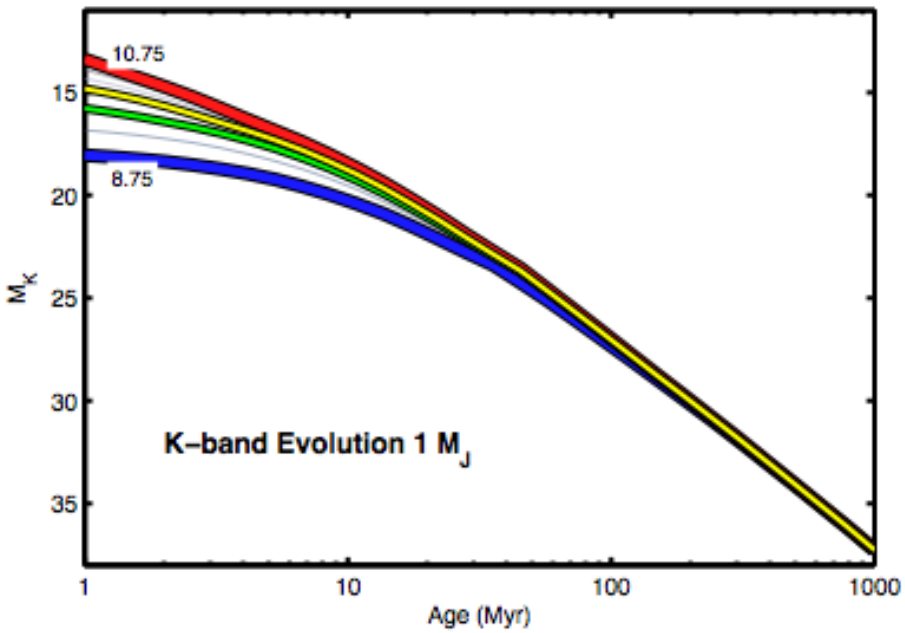
10.75
8.75
K–band Evolution 1 M_J
M_K
Age (Myr)

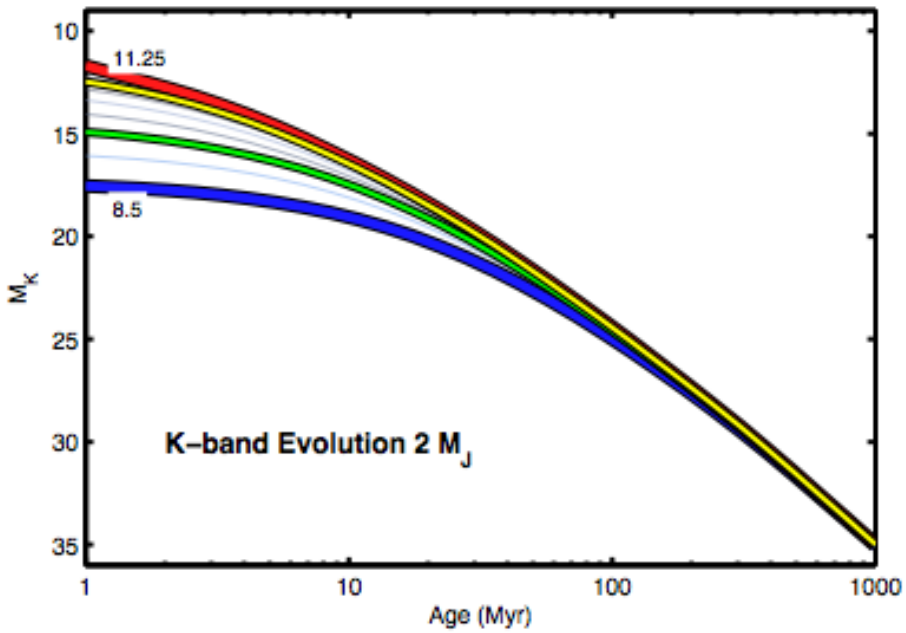
11.25
8.5
K–band Evolution 2 M_J
M_K
Age (Myr)

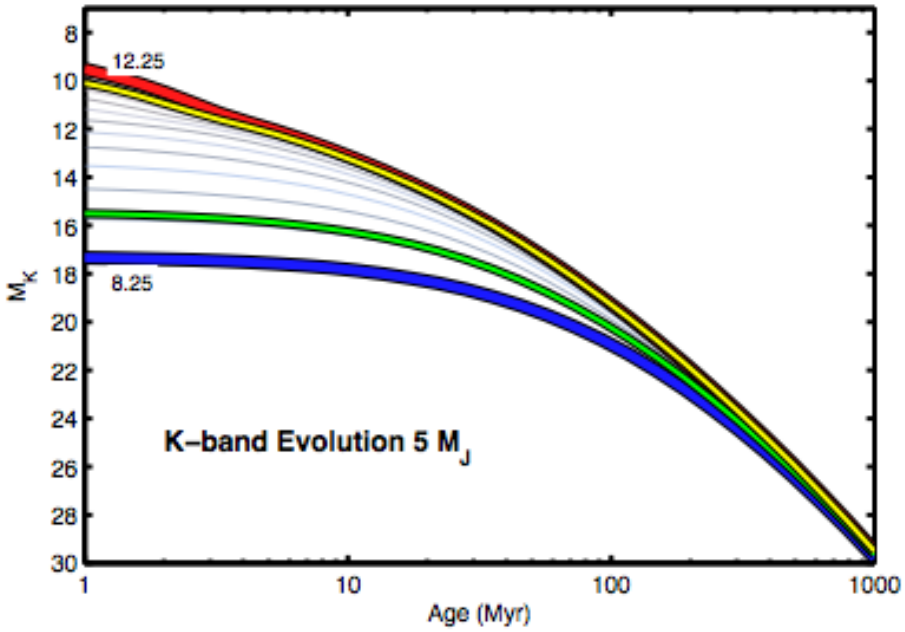
12.25
8.25
K–band Evolution 5 M_J
M_K
Age (Myr)

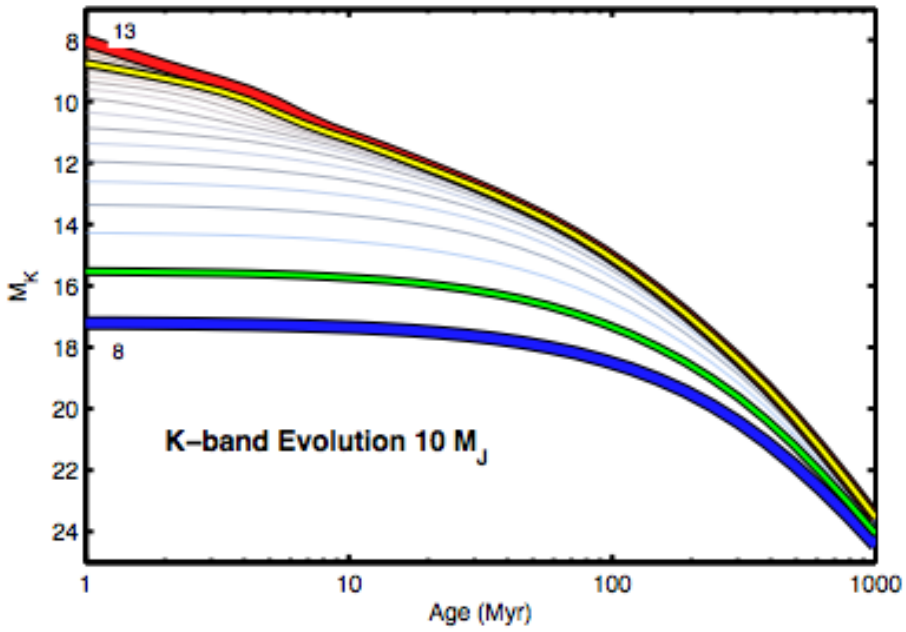
13
8
K–band Evolution 10 M_J
M_K
Age (Myr)

JWST

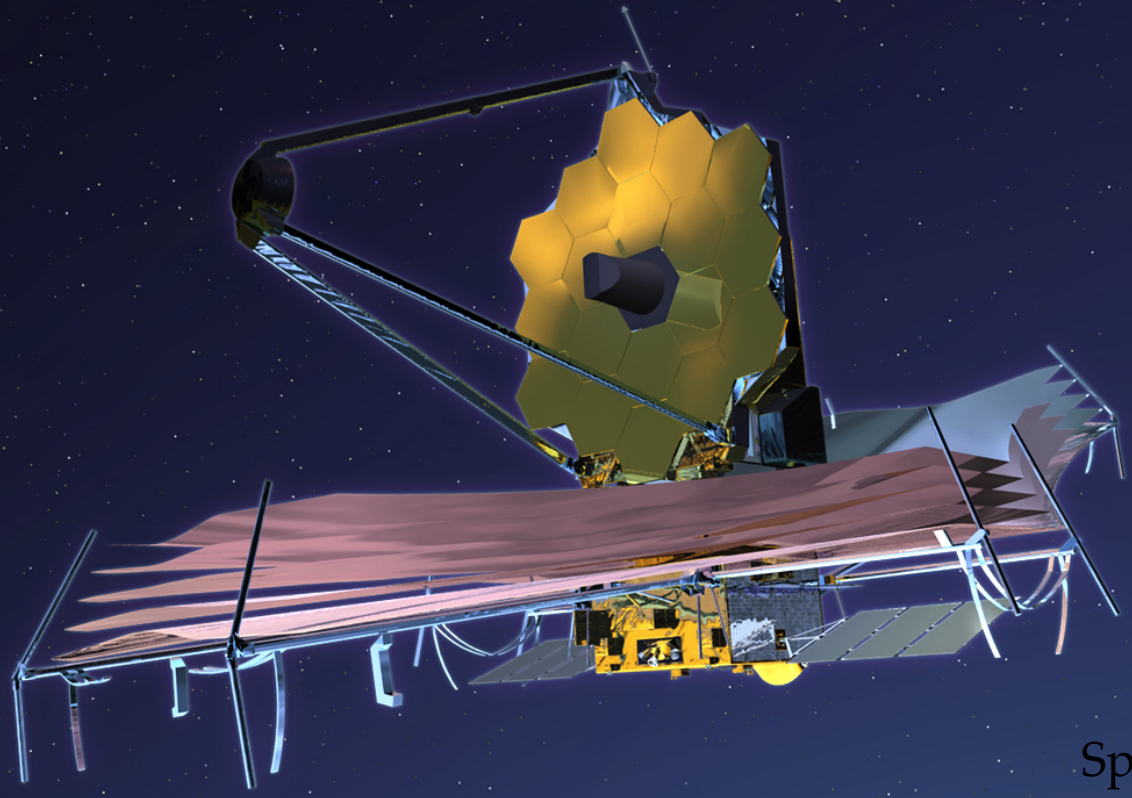

Spitzer

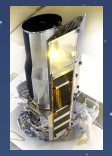

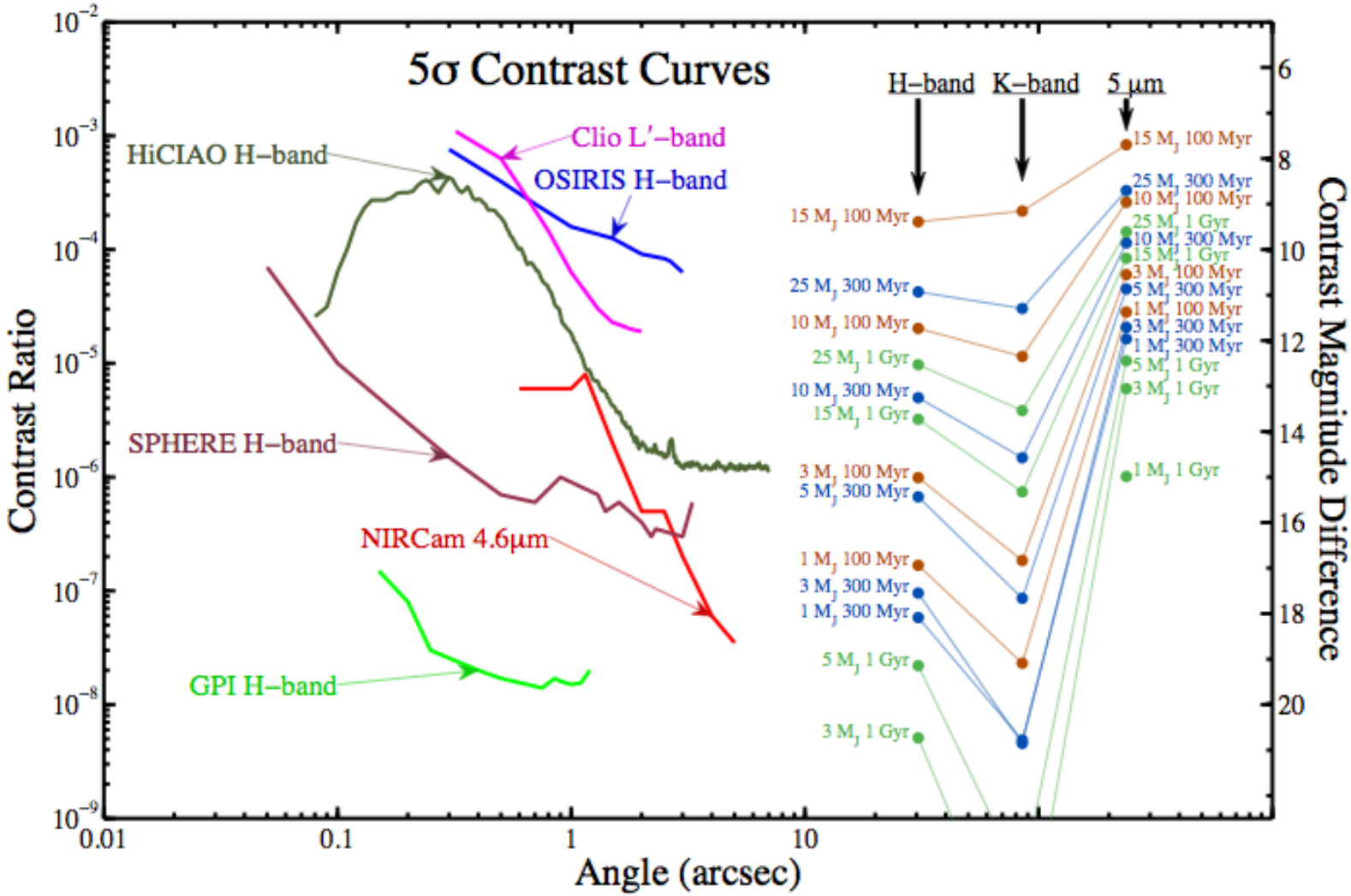
5σ Contrast Curves
HiCIAO H–band
Clio L′–band
OSIRIS H–band
SPHERE H–band
NIRCam 4.6μm
GPI H–band
H–band
K–band
5 μm
15 M_J 100 Myr
25 M_J 300 Myr
10 M_J 100 Myr
25 M_J 1 Gyr
10 M_J 300 Myr
15 M_J 1 Gyr
3 M_J 100 Myr
5 M_J 300 Myr
1 M_J 100 Myr
3 M_J 300 Myr
1 M_J 300 Myr
5 M_J 1 Gyr
3 M_J 1 Gyr
Contrast Ratio
Contrast Magnitude Difference
Angle (arcsec)
0.01
0.1
1
10
6
8
10
12
14
16
18
20

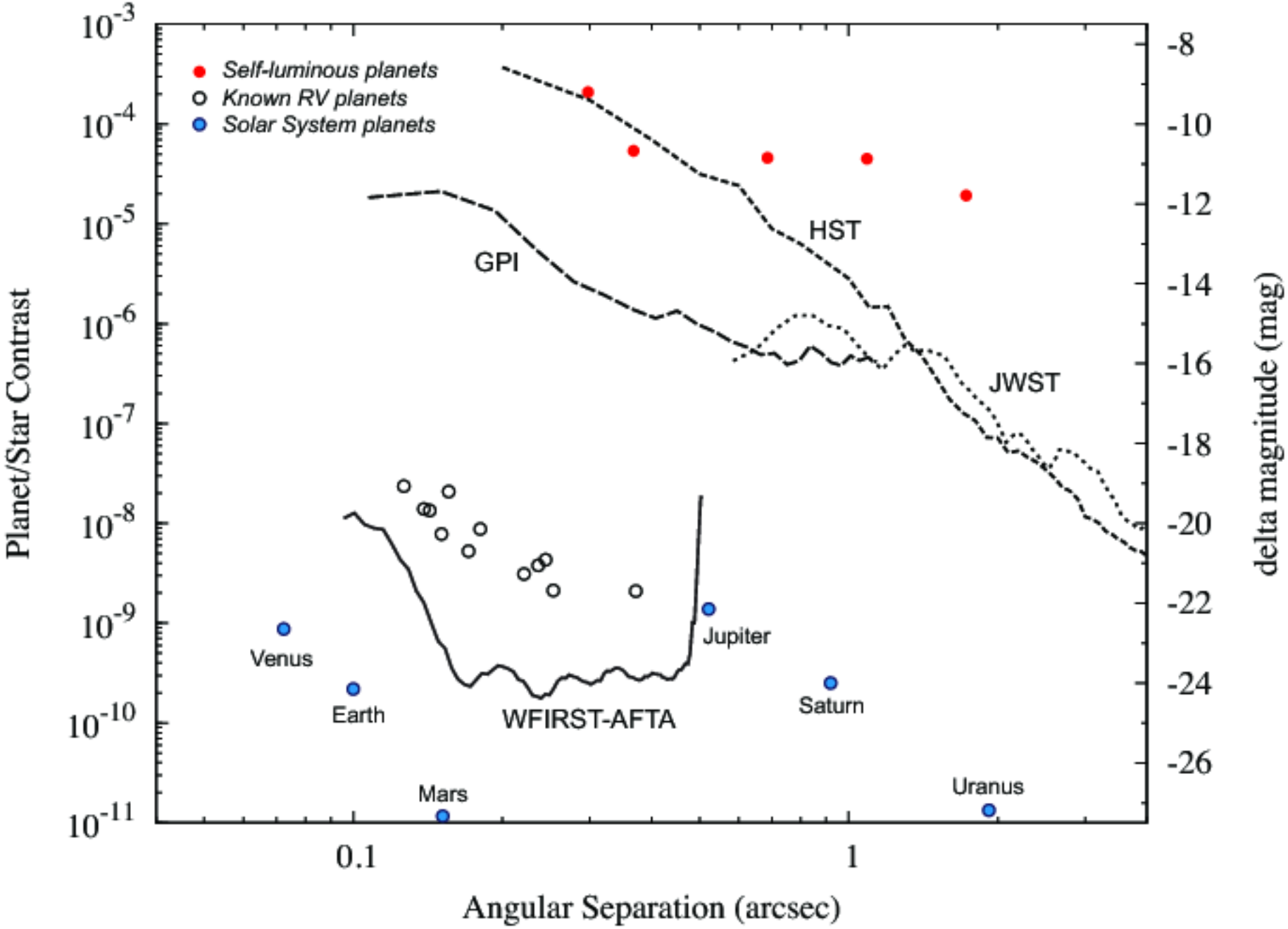
Self-luminous planets
Known RV planets
Solar System planets
HST
GPI
JWST
WFIRST-AFTA
Venus
Earth
Mars
Jupiter
Saturn
Uranus
Planet/Star Contrast
delta magnitude (mag)
Angular Separation (arcsec)
10^-3
10^-4
10^-5
10^-6
10^-7
10^-8
10^-9
10^-10
10^-11
-8
-10
-12
-14
-16
-18
-20
-22
-24
-26
0.1
1

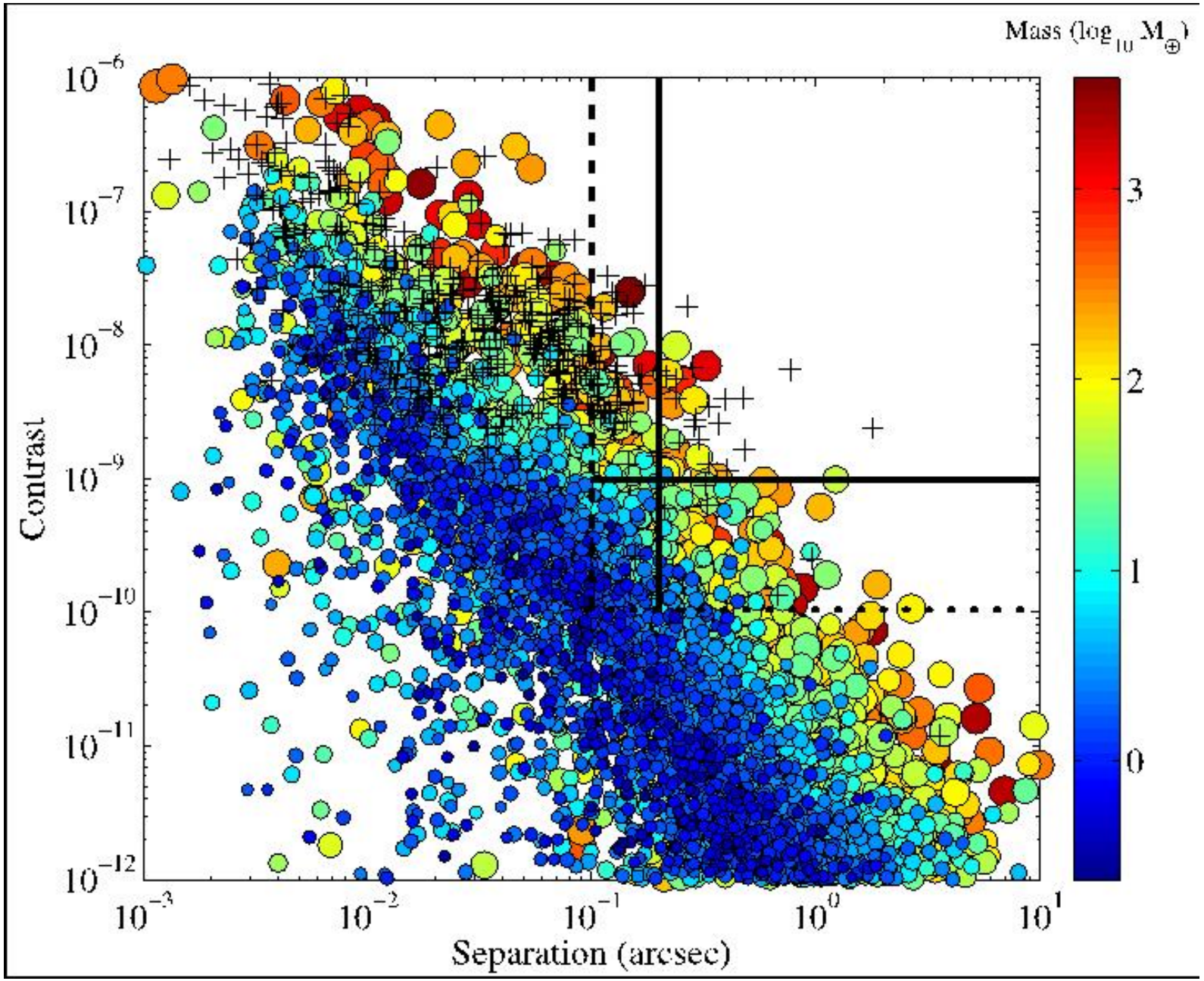
Mass ($\log_{10} M_\oplus$)
3
2
1
0
Contrast
10^{-6}
10^{-7}
10^{-8}
10^{-9}
10^{-10}
10^{-11}
10^{-12}
10^{-3}
10^{-2}
10^{-1}
10^{0}
10^{1}
Separation (arcsec)

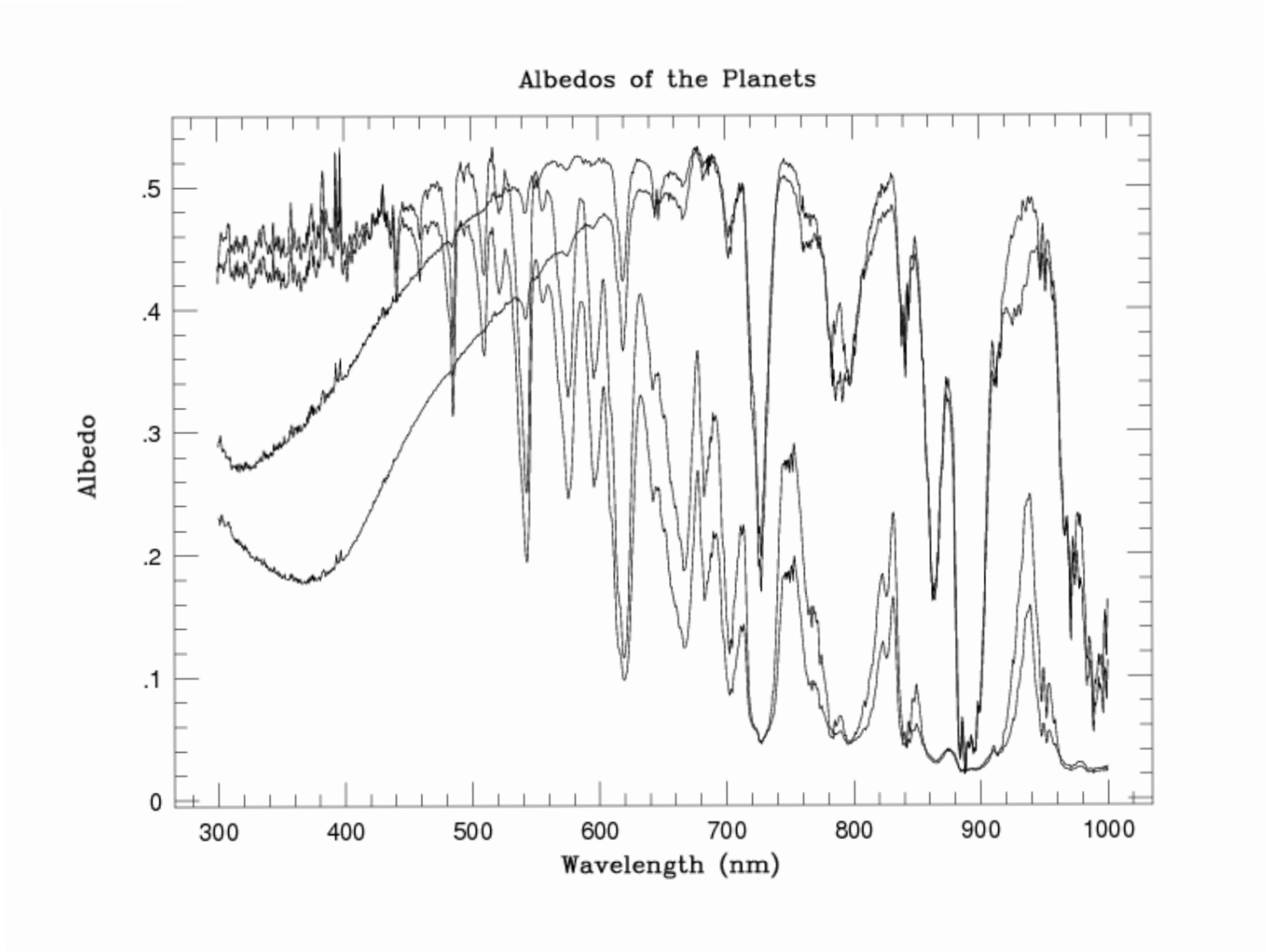

Geometric albedos of Jupiter, Saturn, Uranus, and Neptune in the optical (from Karkoscha 1994).

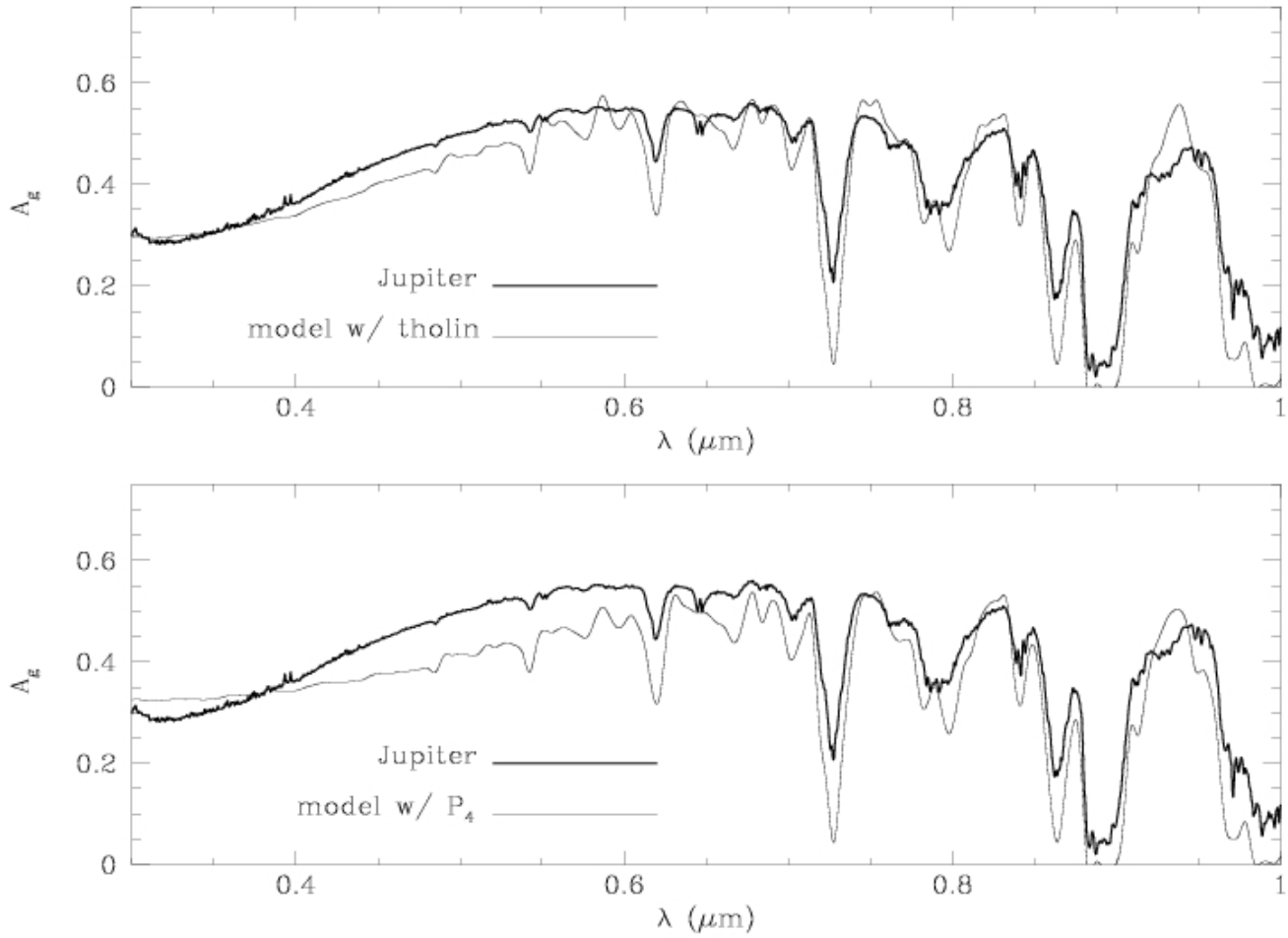

The geometric albedo spectrum of Jupiter compared with models (thin curves). The top model utilizes tholin as a chromophore, while the bottom model uses P_4.

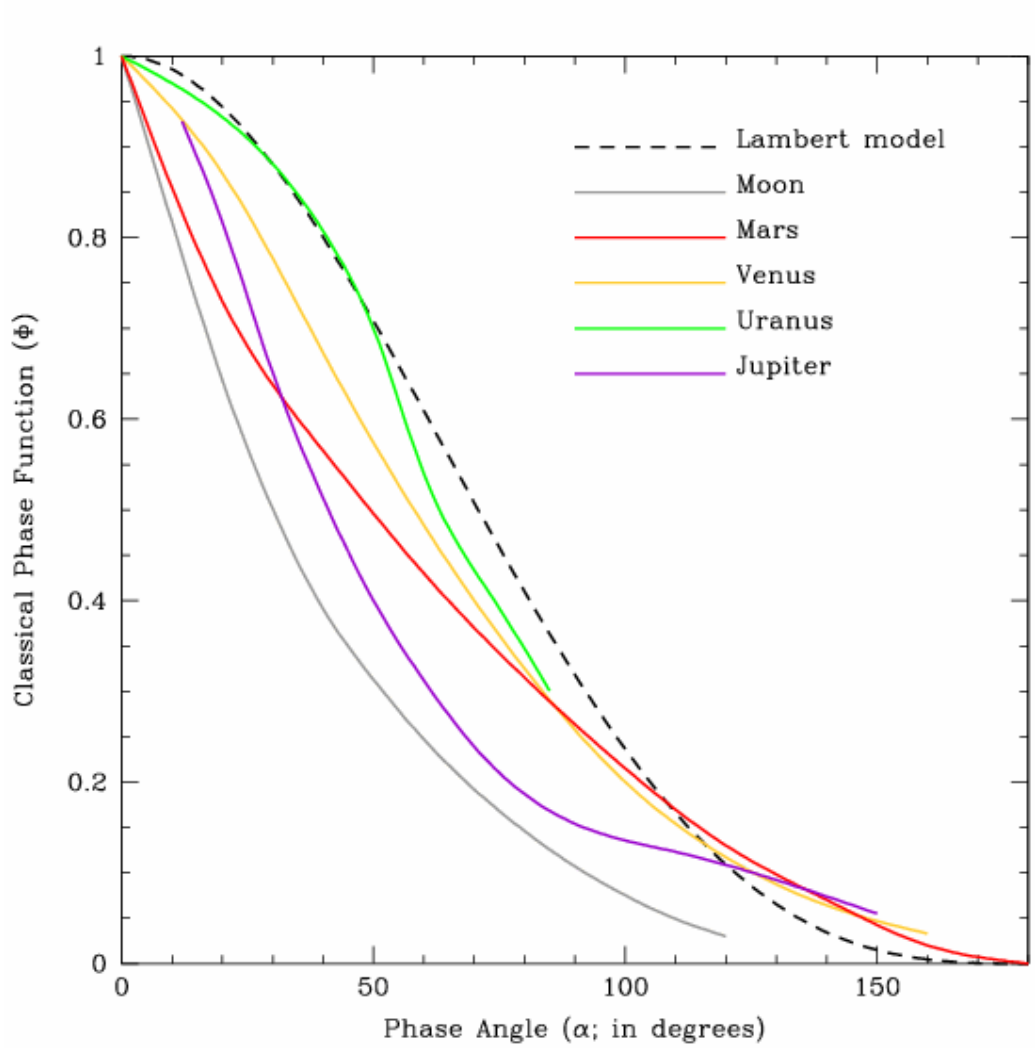

The measured visual phase functions for a selection of Solar System objects. A Lambert scattering phase curve, for which radiation is scattered isotropically off the surface regardless of its angle of incidence, is shown for comparison. The phase functions of the Moon and Mars peak near full phase (the so-called "opposition effect"). A red bandpass Jupiter phase function, taken from Dyudina et al. (2004), is also plotted.

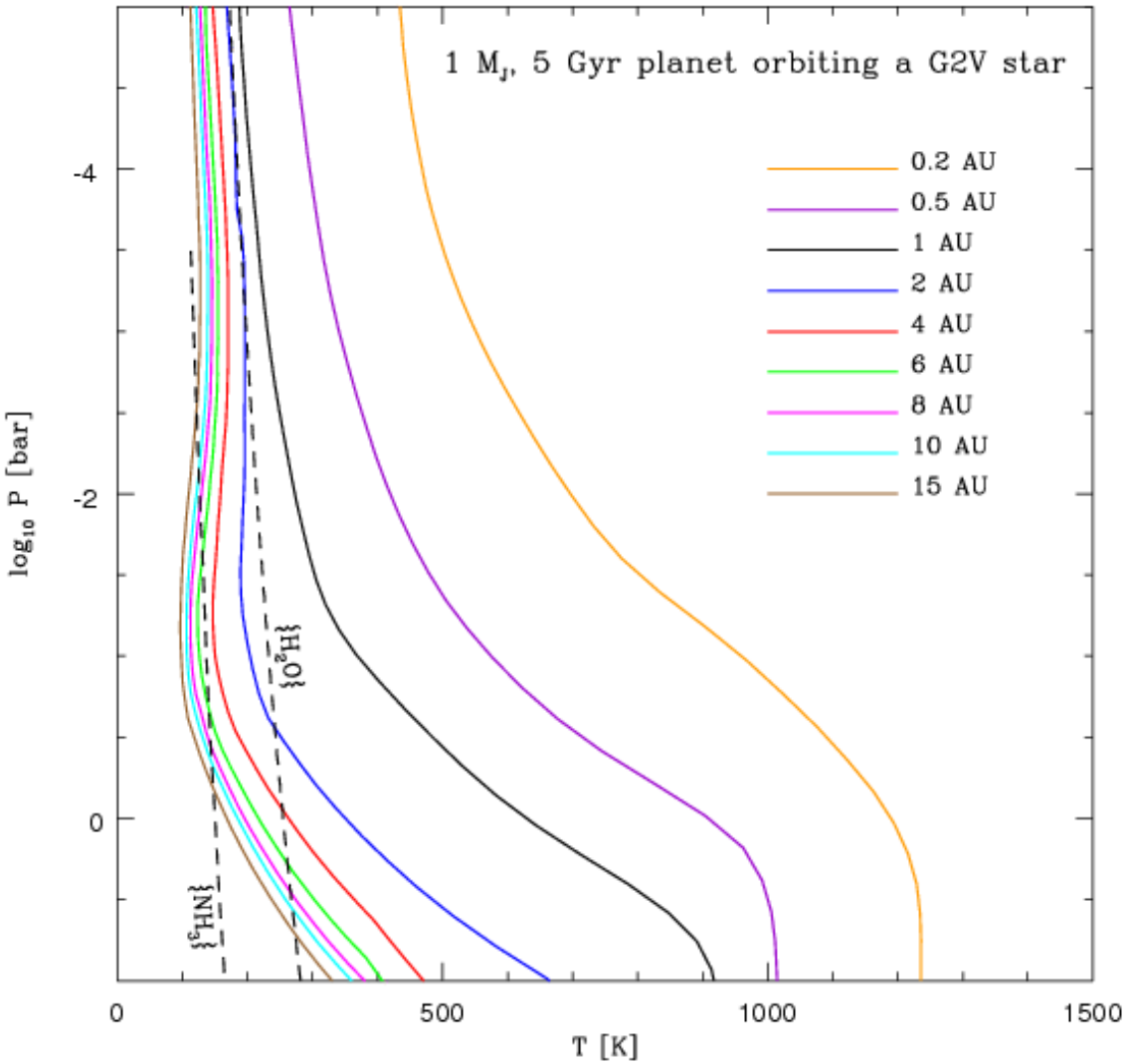

The temperature-pressure (T-P) profiles for a selection of model EGPs. Condensation curves for water and ammonia are shown.The deeper intersections of these condensation curves with the T-P profiles indicate the positions of the cloud bases.

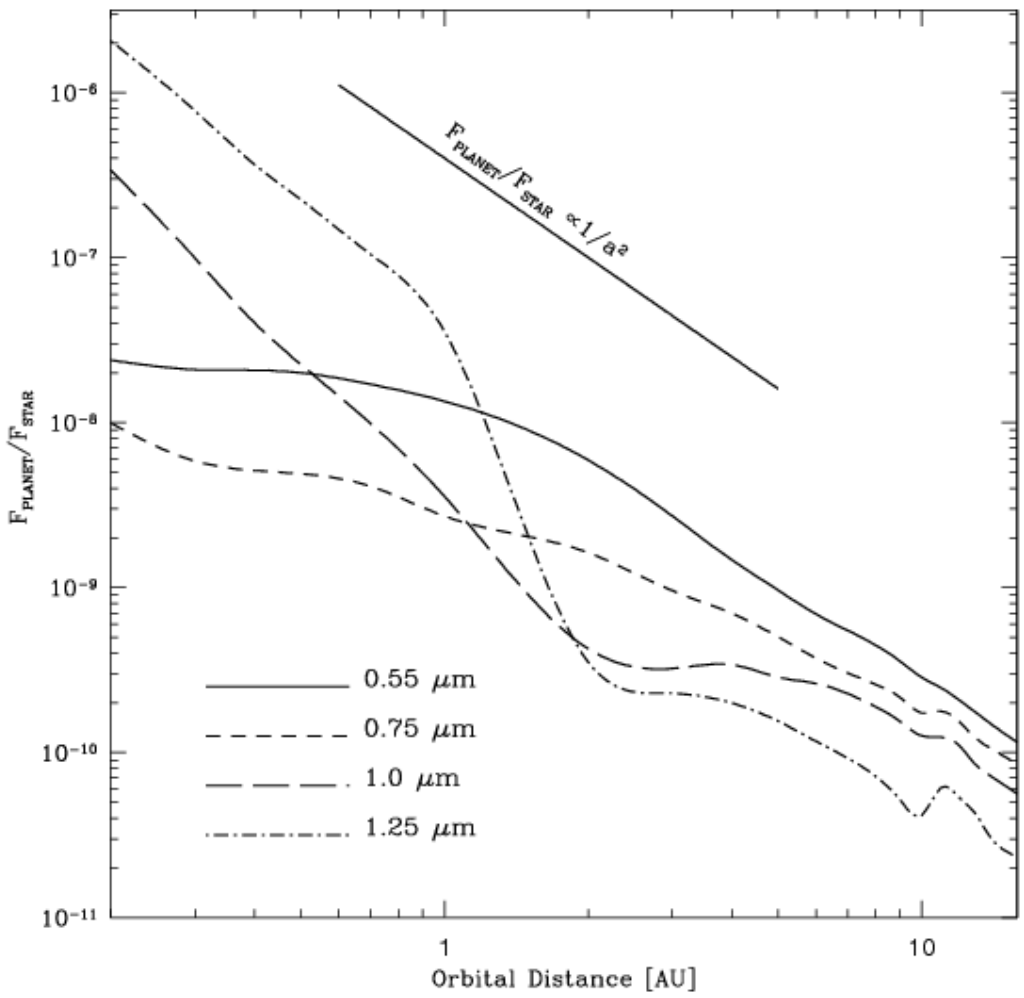

Planet/star flux ratio as a function of orbital distance at 0.55, 0.75, 1.0, and 1.25 microns assuming a G2V central star. In each case, the plotted value corresponds to a planet at greatest elongation with an orbital inclination of 80 degrees. Note that the planet/star flux ratios do not follow a simple $1/a^2$ law.

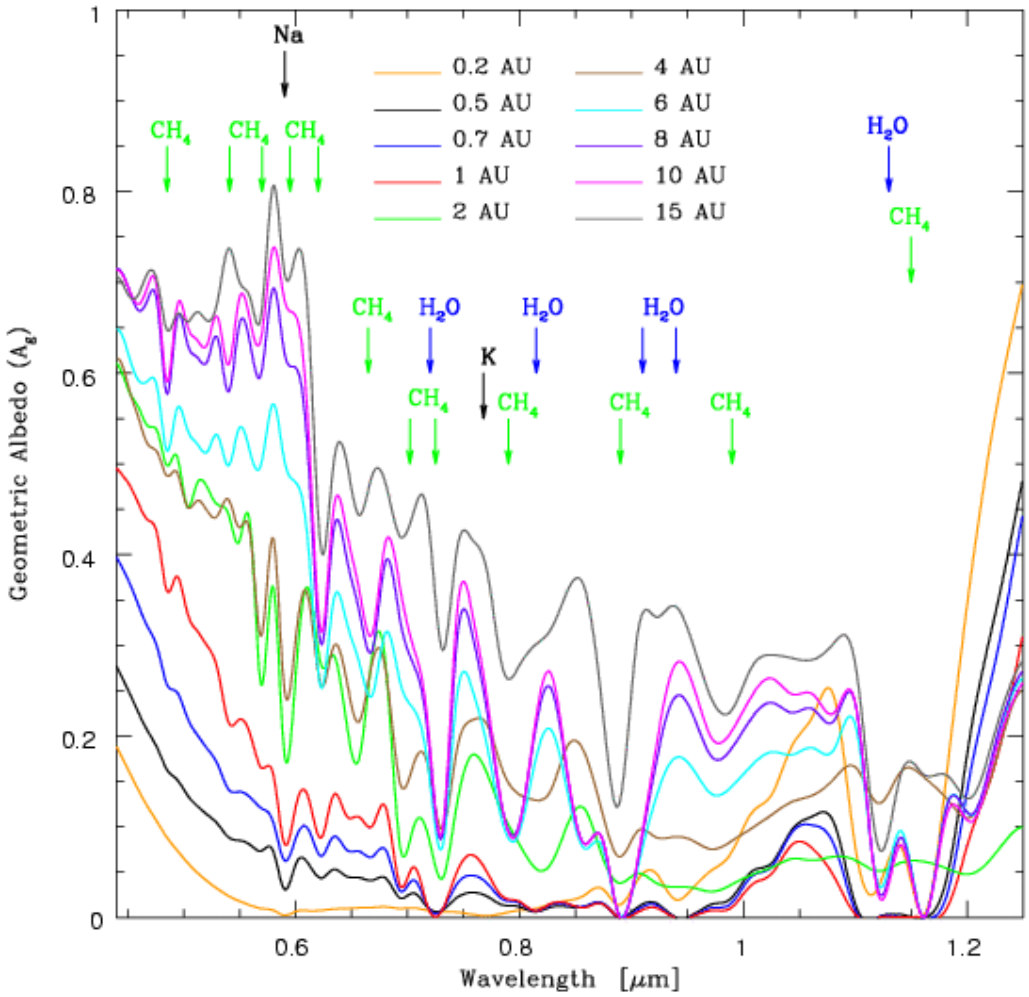

Low-resolution, wavelength-dependent geometric albedos of 1-M_J, 5 Gyr EGPs ranging in orbital distance from 0.2 AU to 15 AU about a G2V star. Cubic splines are fit to all albedo data. Reddening effects of photochemical hazes are not incorporated.

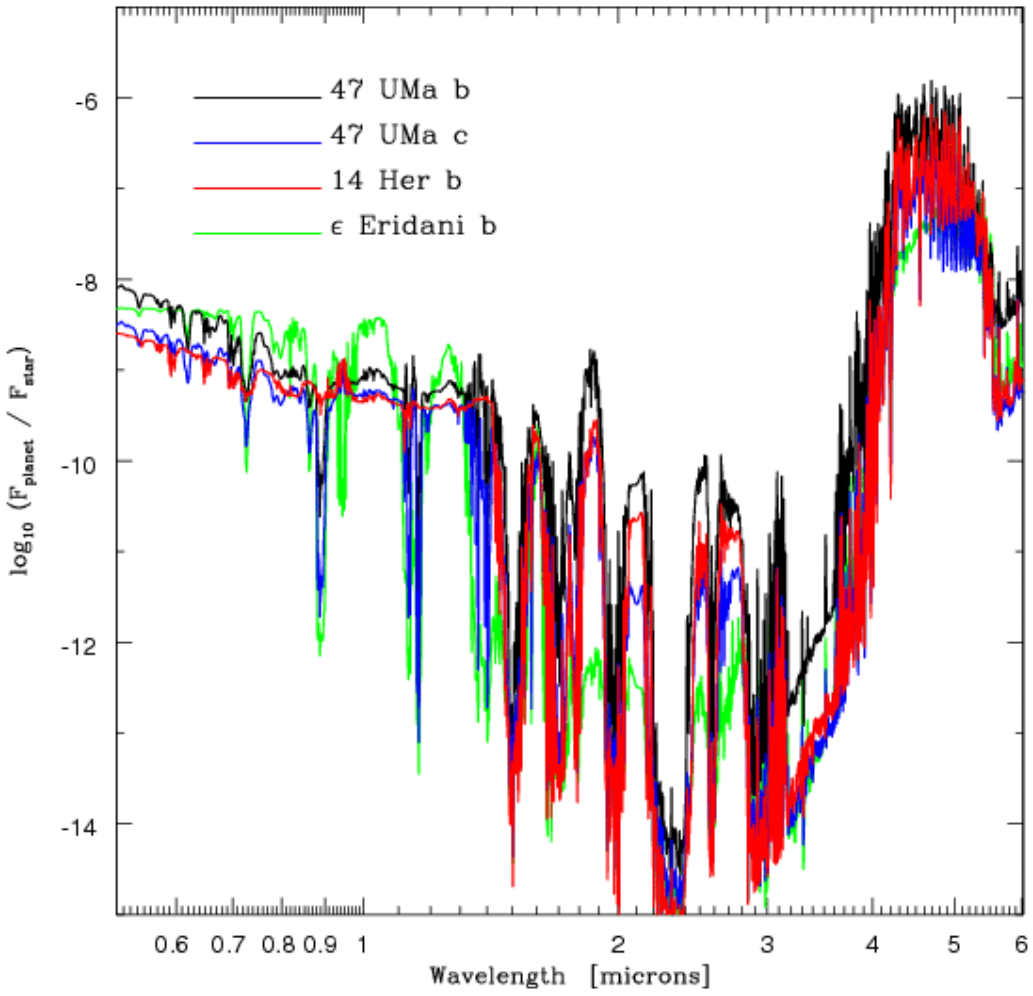

Average Planet/Star flux ratios for some representative non-transiting EGPs.

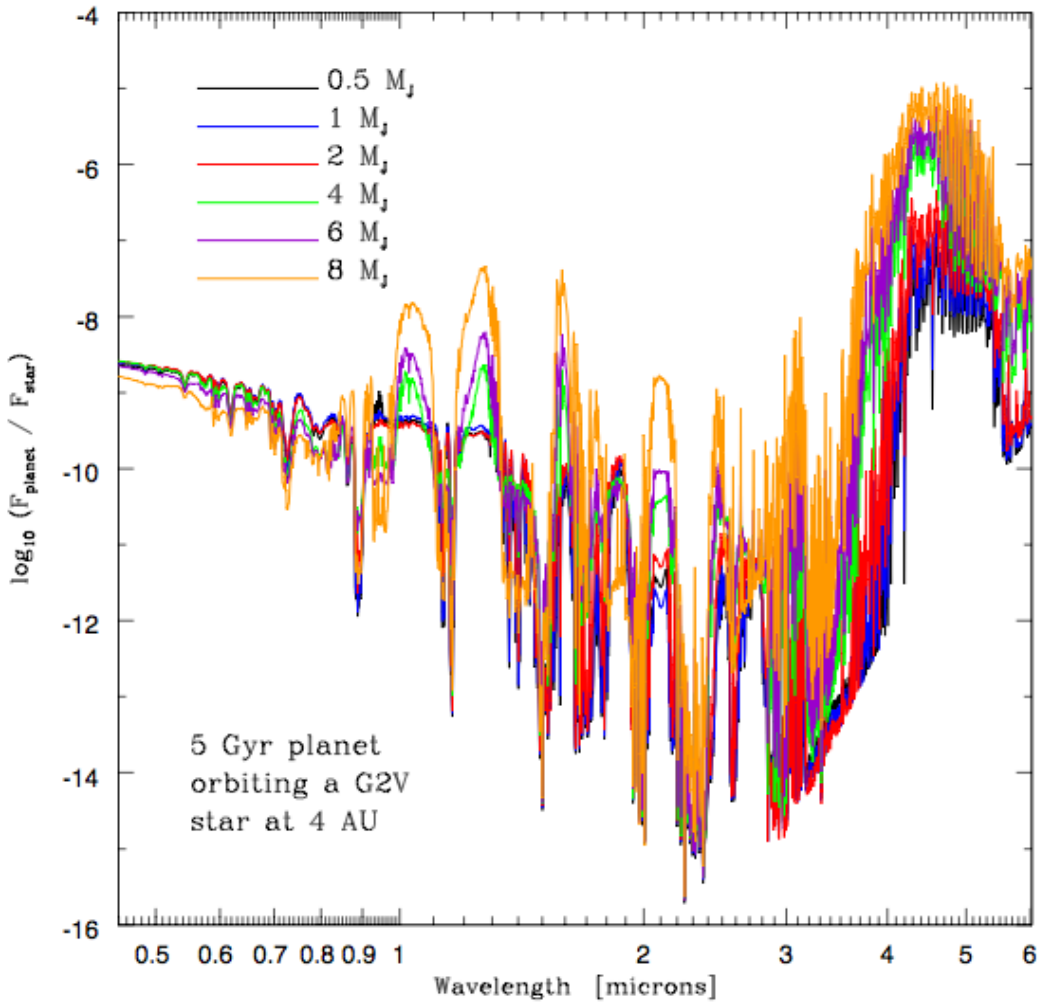

Planet/Star flux ratios as a function EGP mass at an age of 5 Gyrs, orbiting a G2V star at 4 AU.

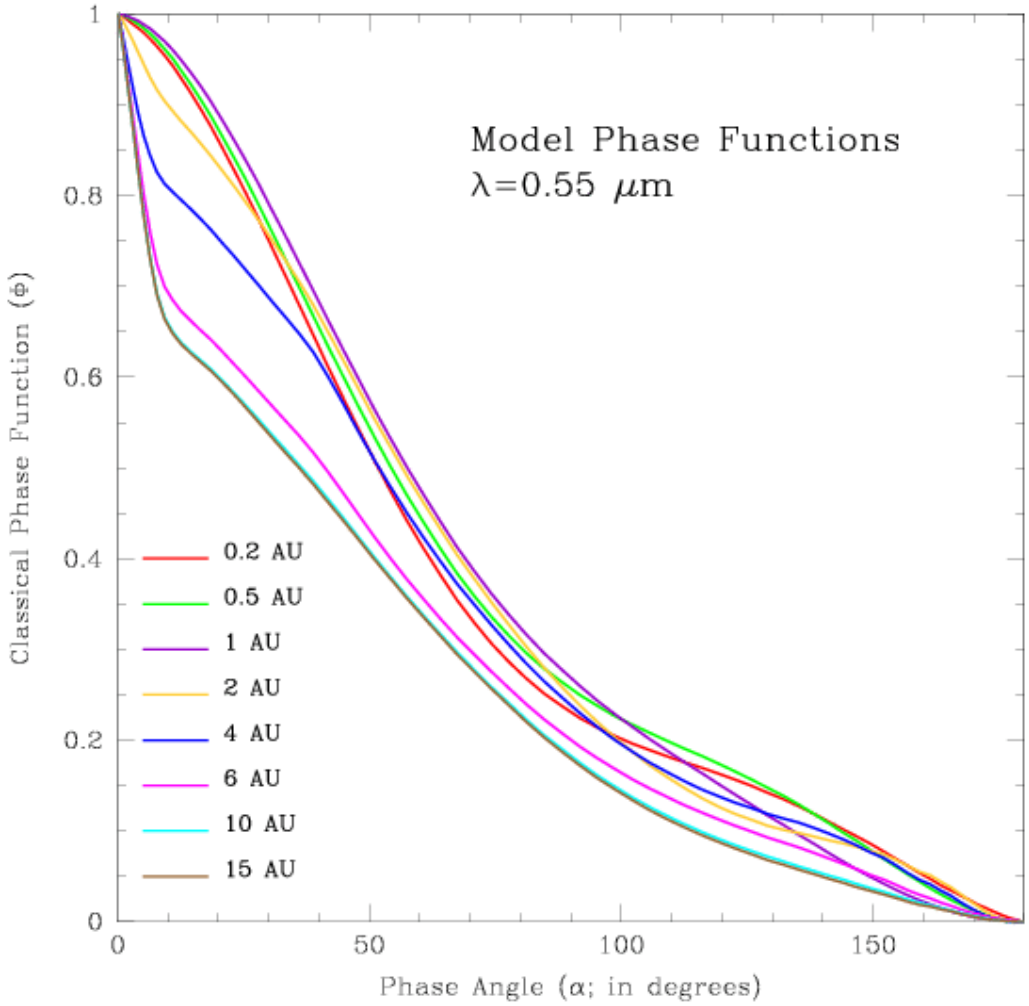

Theoretical optical phase functions of 1-M_J, 5-Gyr EGPs ranging in orbital distance from 0.2 AU to 15 AU from a G2V star. Near full phase, the phase functions for our baseline models at larger orbital distances peak most strongly. For the cloud-free EGPs at smaller orbital distances (0.2 AU, 0.5 AU, and 1 AU), the phase functions are more rounded near full phase.

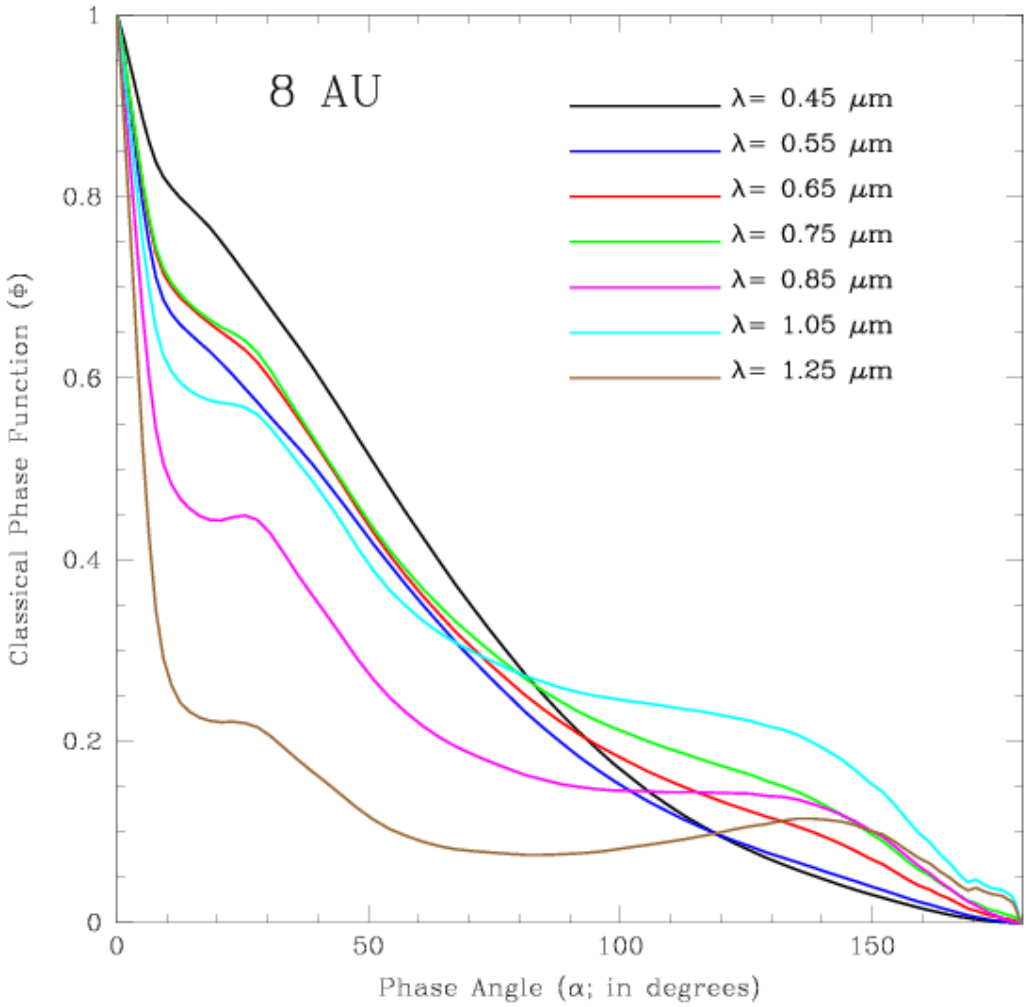

Wavelength dependence of the phase function for an EGP orbiting at a distance of 8 AU from its G2V central star. The EGP contains an ammonia cloud layer above a deeper water cloud.

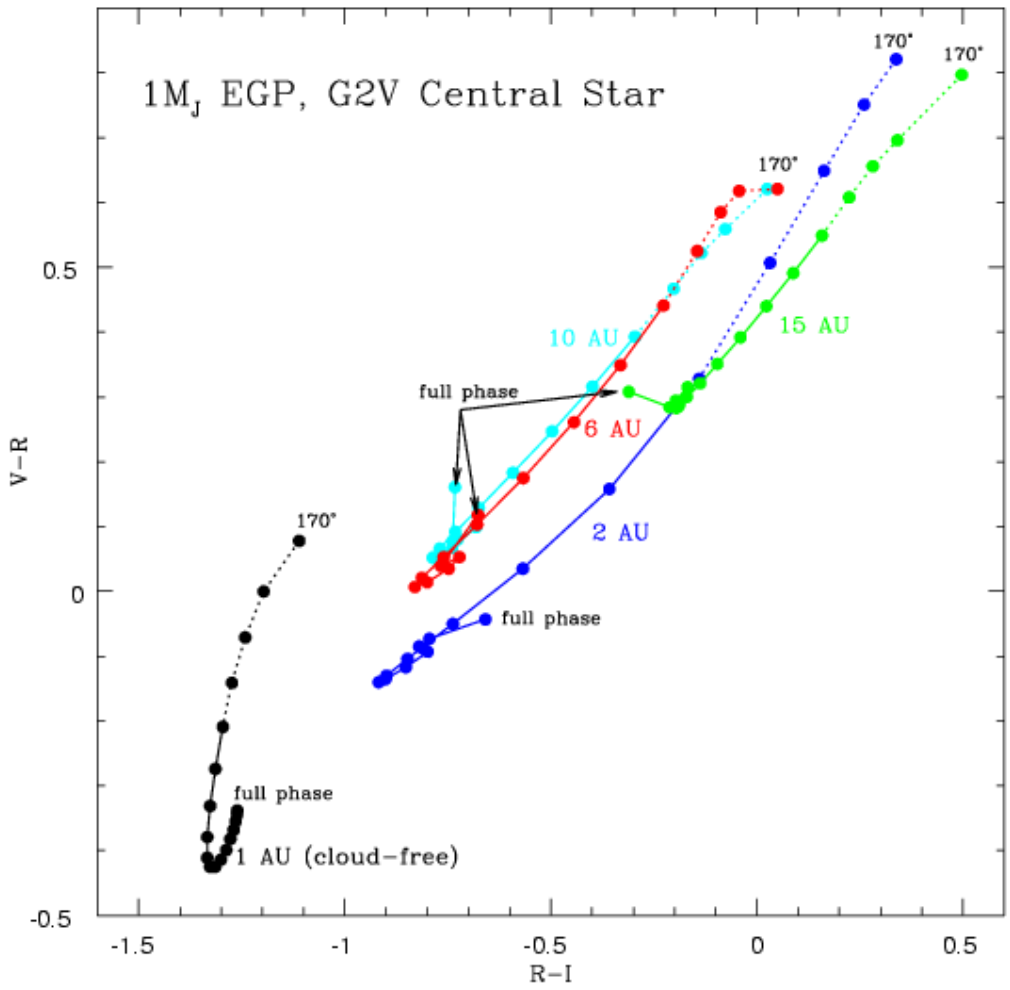

V-R vs. R-I color-color diagram detailing variations with planetary phase for a variety of orbital distances. Each of the curves depicts an orbit from full phase (0 degrees) to a thin crescent phase (170 degrees) in increments of 10 degrees (as indicated by the filled circles). Cloud-free EGPs are bluest near greatest elongation, while cloudy EGPs tend to be bluest in a gibbous phase. As full phase is approached, the colors redden somewhat. However, the crescent phases appear to be far redder, varying by as much as a full astronomical magnitude from their blue gibbous-phase colors in some cases. See text for details and a discussion of the accuracy at large phase angles (denoted by dotted lines).

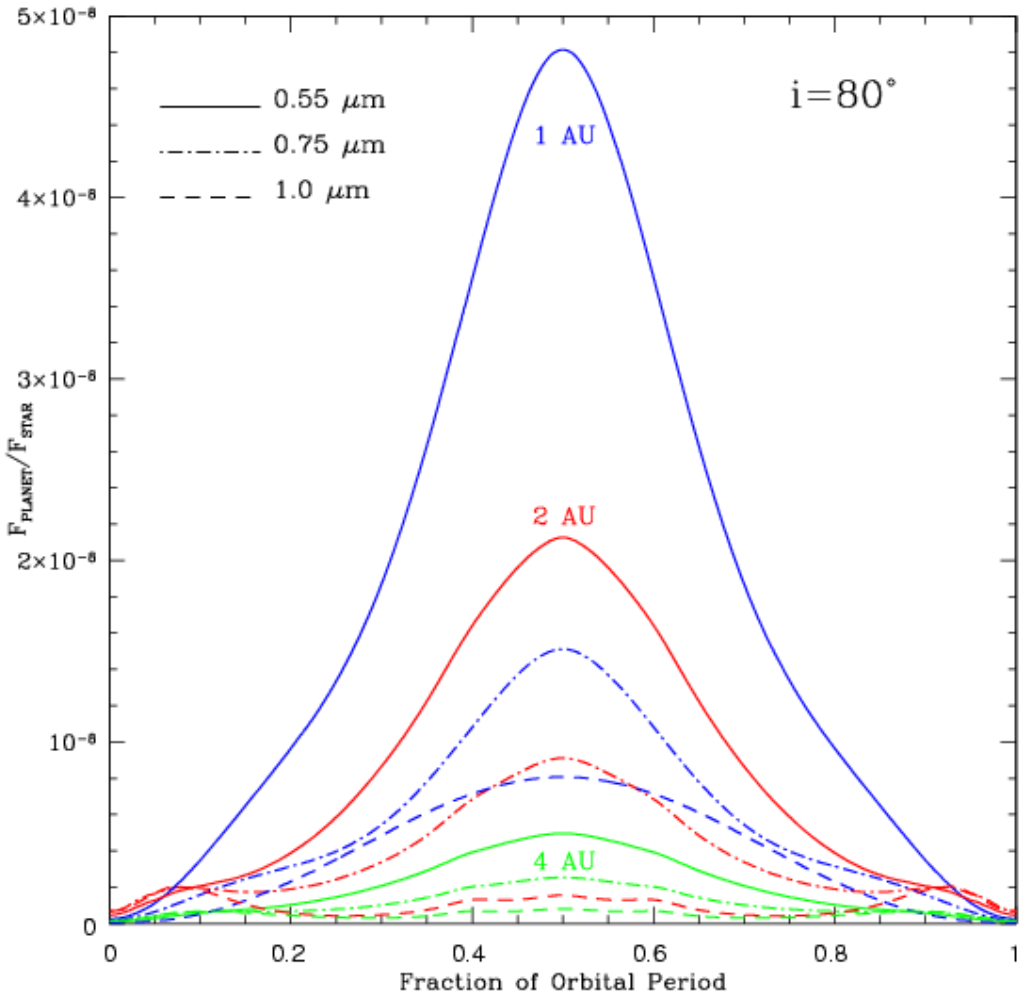

Light curves at 0.55, 0.75, and 1.0 microns for our model EGPs in circular orbits inclined to 80 degrees at distances of 1 AU, 2 AU, and 4 AU from a G2V star. The logarithm of the planet/star flux ratio is plotted. The models at 2 AU and 4 AU contain water ice clouds in their upper atmospheres, while the 1 AU model does not.

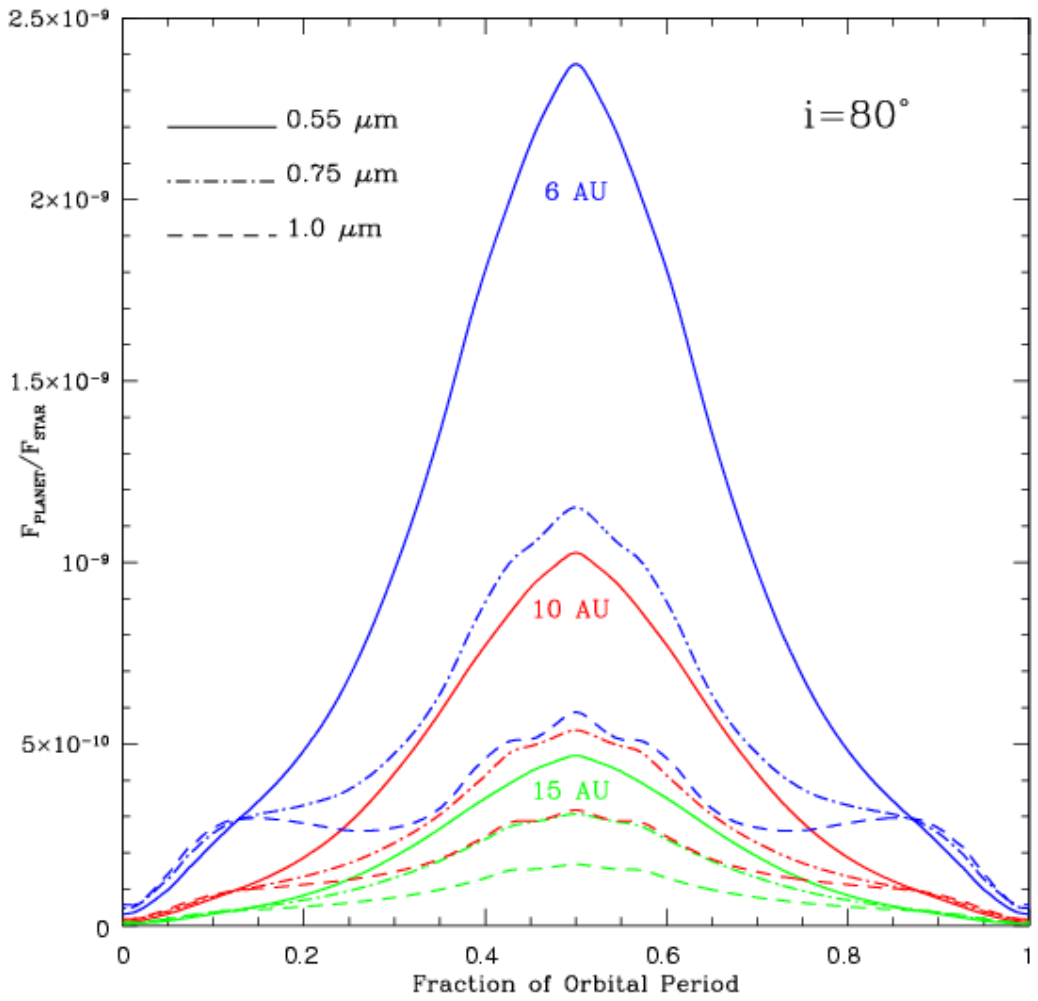

Light curves at 0.55, 0.75, and 1.0 microns for our model EGPs in circular orbits inclined to 80 degrees at distances of 6 AU, 10 AU, and 15 AU from a G2V star. The logarithm of the planet/star flux ratio is plotted. Each of these models contains an ammonia ice cloud layer above a deeper water cloud deck.

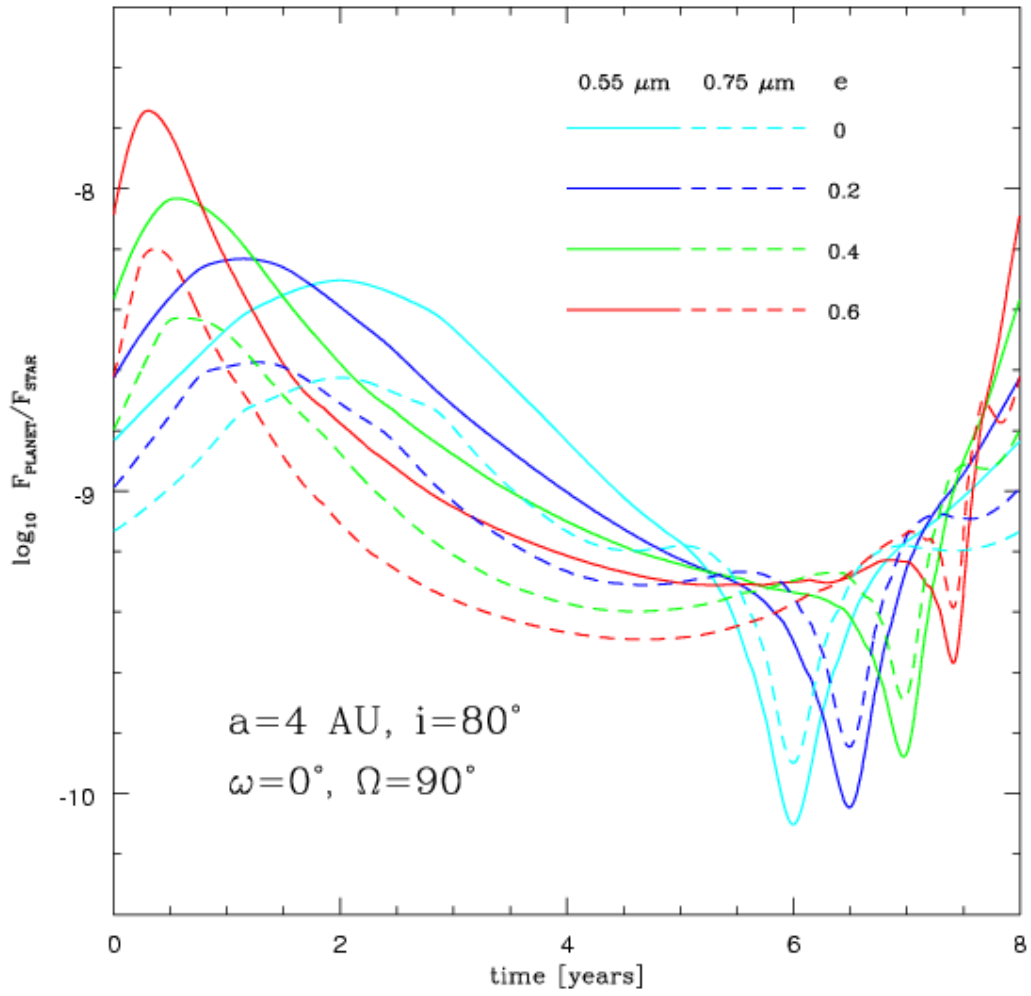

The logarithm of the optical (at 0.55 microns) and far red (0.75 microns) planet/ star flux ratios as a function of eccentricity for a = 4 AU, fixing i at 80 degrees and ω is zero. The planet/star flux ratio is a factor of 2 to 3 greater at 0.55 microns than in the far red at most planetary phases.

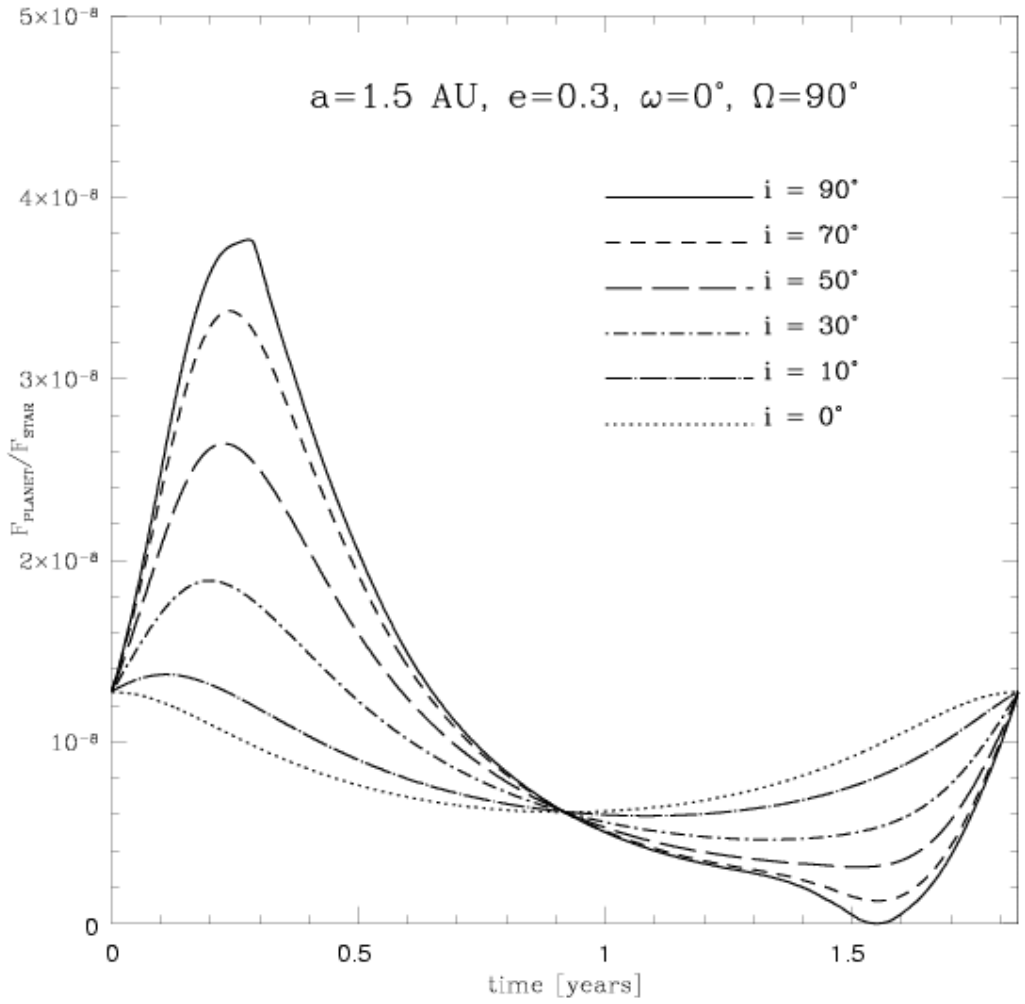

Variation with inclination of the optical light curve for an elliptical orbit (G2V central star, a = 1.5 AU, e = 0.3). For a highly-inclined orbit, the peak of the planet/star flux ratio is a factor of ~3 greater than for a face-on (i=0 degrees) orbit. The (symmetric) variation for the face-on case is due entirely to the variation in the planet-star distance over an eccentric orbit.

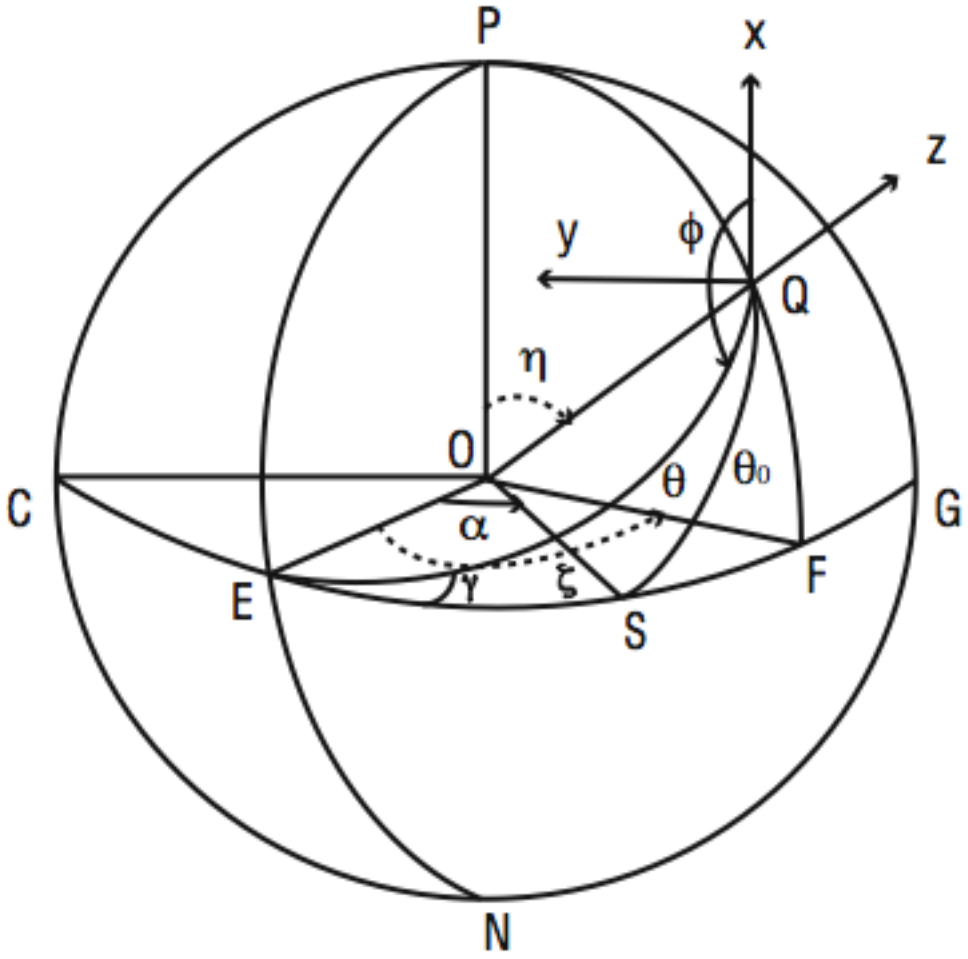

Coordinate system for calculating polarization due to reflection off planet. (from Madhusudhan and Burrows 2011)

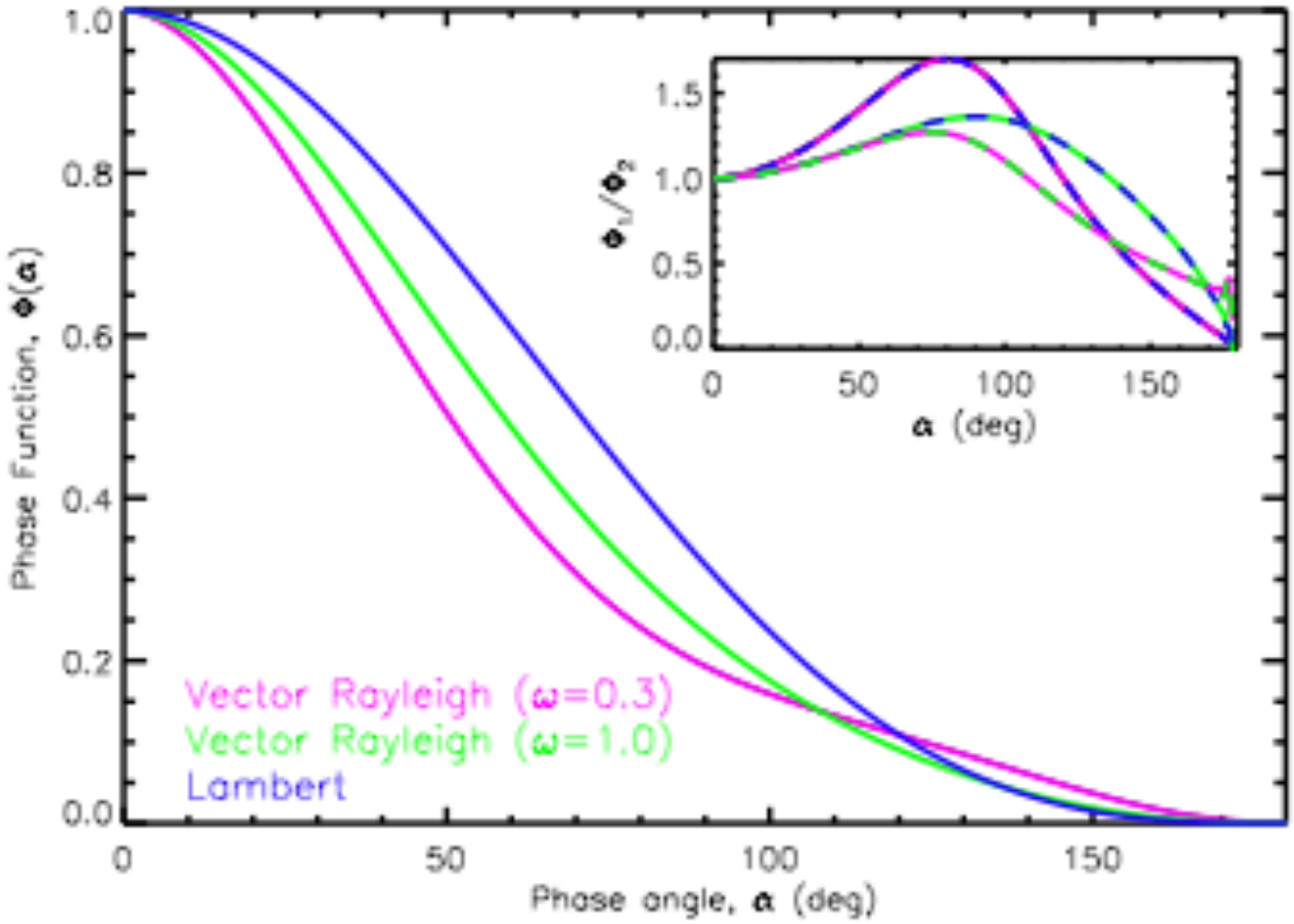

Comparison between phase curves due to Rayleigh scattering (with vector formulation) and Lambert scattering. The solid curves in the main panel show three phase curves for the cases described in the legend. The multi-colored dashed curves in the inset show the ratios between pairs of solid curves, e.g. the magenta-green dashed curve is the ratio between the magenta and green solid curves.

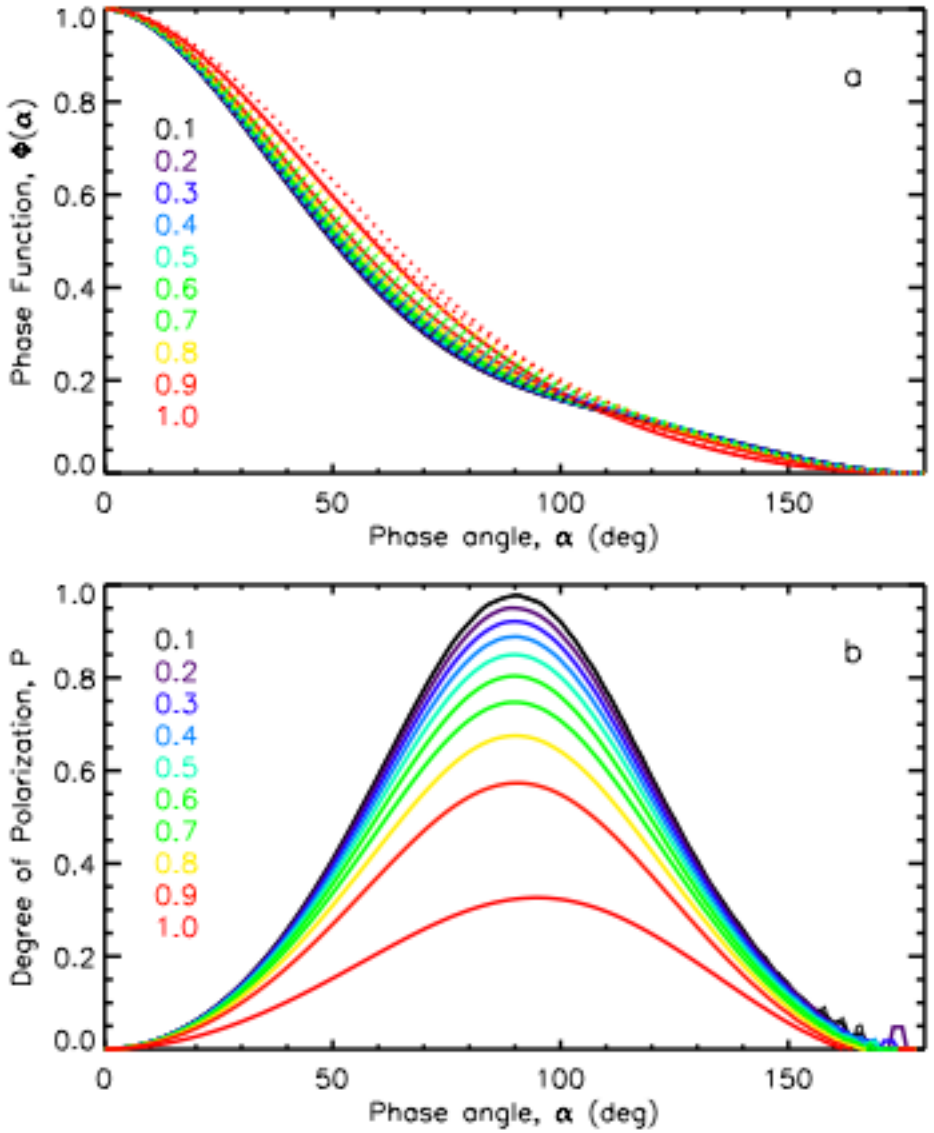

Phase curves and polarization for Rayleigh scattering. The different curves in each panel correspond to the different scattering albedos shown in the legend. In the upper panel, the solid curves show the phase curves for Rayleigh scattering using the vectorial Rayleigh phase matrix, whereas the dotted curves show those with the scalar phase function which does not incorporate polarization. The lower panel shows the degree of polarization (P), using the Rayleigh phase matrix. P is defined as $P = (Q^2 + U^2)^{1/2}/I$, where Q and U are the two Stokes parameters for linear polarization and I is the total intensity. For all the curves shown here, the orbit is assumed to be edge on (i = 90 degrees), in which case U = 0 and, hence, effectively P = Q/I.

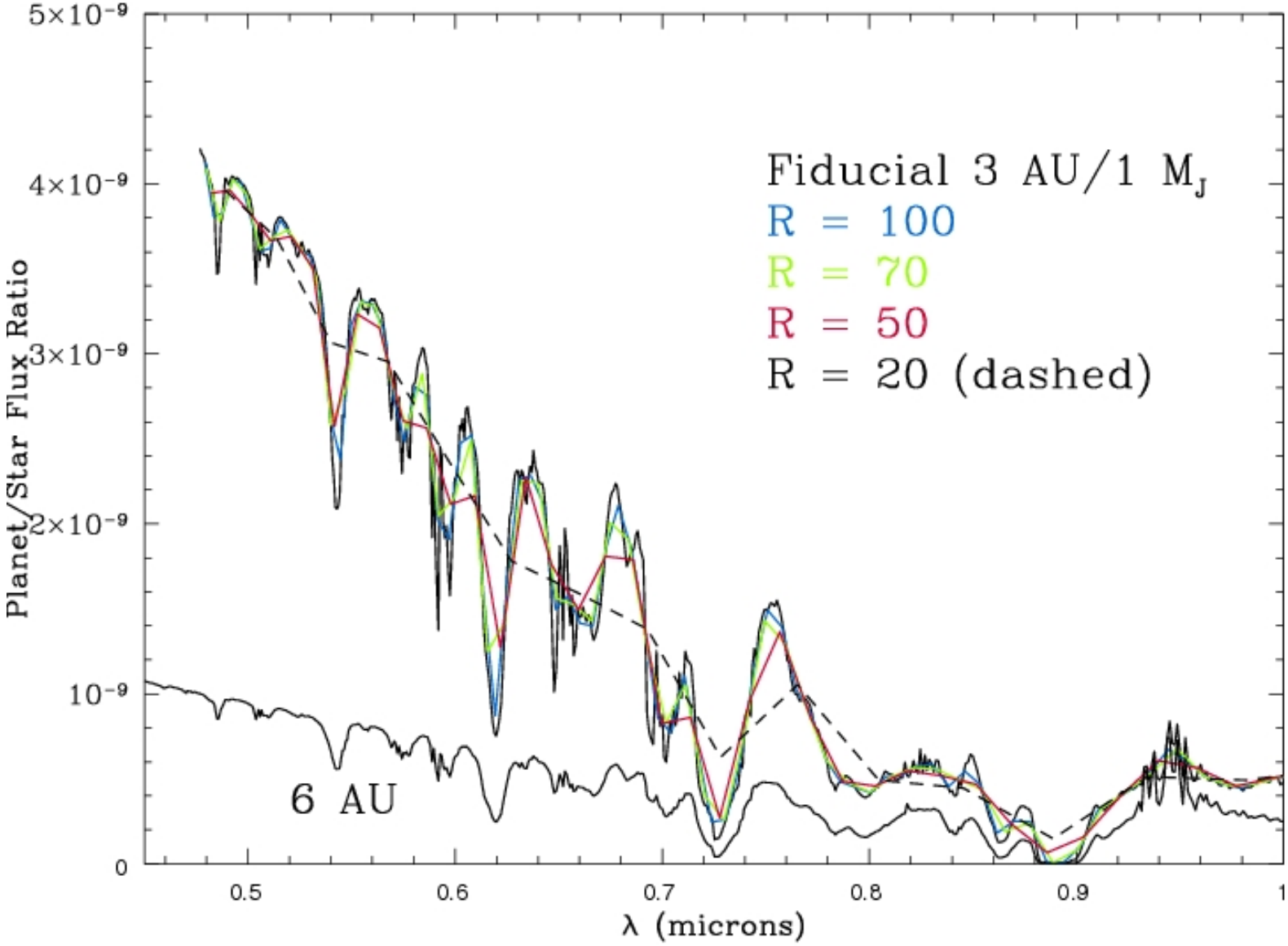
5×10⁻⁹
4×10⁻⁹
3×10⁻⁹
2×10⁻⁹
10⁻⁹
0
Planet/Star Flux Ratio
0.5
0.6
0.7
0.8
0.9
1
λ (microns)
Fiducial 3 AU/1 M_J
R = 100
R = 70
R = 50
R = 20 (dashed)
6 AU

Extra Slides

References:

"Spectra and Diagnostics for the Direct Detection of Wide-Separation Extrasolar Giant Planets," (A. Burrows, D. Sudarsky, and I. Hubeny), Astrophys. J., 609, 407, 2004.

"Theoretical Spectra and Atmospheres of Extrasolar Giant Planets" (D. Sudarsky, A. Burrows, and I. Hubeny), Astrophys. J., 588, 1121, 2003.

"Phase Functions and Light Curves of Wide Separation Giant Planets," (David Sudarsky, Adam Burrows, Ivan Hubeny, and Aigen Li), Astrophys. J. 627, 520, 2005 (astro-ph/0501109).

"Albedo and Reflection Spectra of Extrasolar Giant Planets," (D. Sudarsky, A. Burrows, and P. Pinto) Astrophys. J., 538, 885, 2000.

"The Theory of Brown Dwarfs and Extrasolar Giant Planets," (A. Burrows, W.B. Hubbard, J.I. Lunine, and J. Liebert), Rev. Mod. Phys}, 73, 719 (2001).

"Spectral and Photometric Diagnostics of Giant Planet Formation Scenarios," (D. Spiegel & A. Burrows), Astrophys. J., 745, 174, 2012 (arXiv:1108.5172).

"Analytic Models for Albedos, Phase Curves, and Polarization of Reflected Light from Exoplanets," (N. Madhusudhan & A. Burrows), Astrophys. J., 747, 25, 2011 (arXiv:1112.4476).

"A theoretical look at the direct detection of giant planets outside the Solar System," (A. Burrows) Nature 433, pp. 261 - 268, 2005 (astro-ph/0501484).

Table 1. Interesting EGPs Listed by Angular Separation

EGP	separation ($''$)	star	a (AU)	d (pc)	P	Msini (M_J)	e
ϵ Eri b	1.0	K2V	3.3	3.2	6.85 yrs.	0.86	0.61
55 Cnc d	0.44	G8V	5.9	13.4	14.7	4.05	0.16
47 UMa c	0.28	G0V	3.73	13.3	7.10	0.76	0.1
Gl 777A b	0.23	G6V	3.65	15.9	7.15	1.15	$\sim$0
υ And d	0.19	F8V	2.50	13.5	3.47	4.61	0.41
HD 39091b	0.16	G1IV	3.34	20.6	5.70	10.3	0.62
47 UMa b	0.16	G0V	2.09	13.3	2.98	2.54	0.06
γ Cephei b	0.15	K2V	1.8	11.8	2.5	1.25	$\sim$0
HD 160691c	0.15	G3IV-V	2.3	15.3	3.56	$\sim$1	$\sim$0.8
14 Her b	0.15	K0V	2.5	17	4.51	3.3	0.33
HD 33636b	0.12	G0V	3.56	28.7	4.43	7.71	0.41
HD 10647b	0.12	F9V	2.10	17.3	2.89	1.17	0.32
HD 70642b	0.11	G5IV-V	3.3	29	4.79	2.0	0.10
HD 216437b	0.10	G4V	2.7	26.5	3.54	2.1	0.34
HD 147513b	0.098	G3V	1.26	12.9	1.48	1.0	0.52
HD 160691b	0.097	G3IV-V	1.48	15.3	1.74	1.7	0.31
HD 168443c	0.087	G5V	2.87	33	4.76	17.1	0.23
HD 50554b	0.077	F8V	2.38	31.03	3.50	4.9	0.42
HD 106252b	0.070	G0V	2.61	37.44	4.11	6.81	0.54
HD 10697b	0.067	G5IV	2.0	30	2.99	6.59	0.12
υ And c	0.061	F8V	0.83	13.5	241 days	2.11	0.18
GJ 876b	0.045	M4V	0.21	4.72	61.0	1.89	0.1
GJ 876c	0.028	M4V	0.13	4.72	30.1	0.56	0.27
HD 114762b	0.013	F9V	0.35	28	84.0	11.0	0.34
55 Cnc b	8.2×10^{-3}	G8V	0.12	13.4	14.7	0.84	0.02
υ And b	4.4×10^{-3}	F8V	0.059	13.5	4.62	0.71	0.034
51 Peg b	3.4×10^{-3}	G2V	0.05	14.7	4.23	0.44	0.01
τ Boo b	3.3×10^{-3}	F7V	0.05	15	3.31	4.09	$\sim$0
HD 209458b	9.6×10^{-4}	G0V	0.045	47	3.52	0.69	$\sim$0
HD 83443b	8.7×10^{-4}	K0V	0.038	43.5	2.99	0.35	0.08

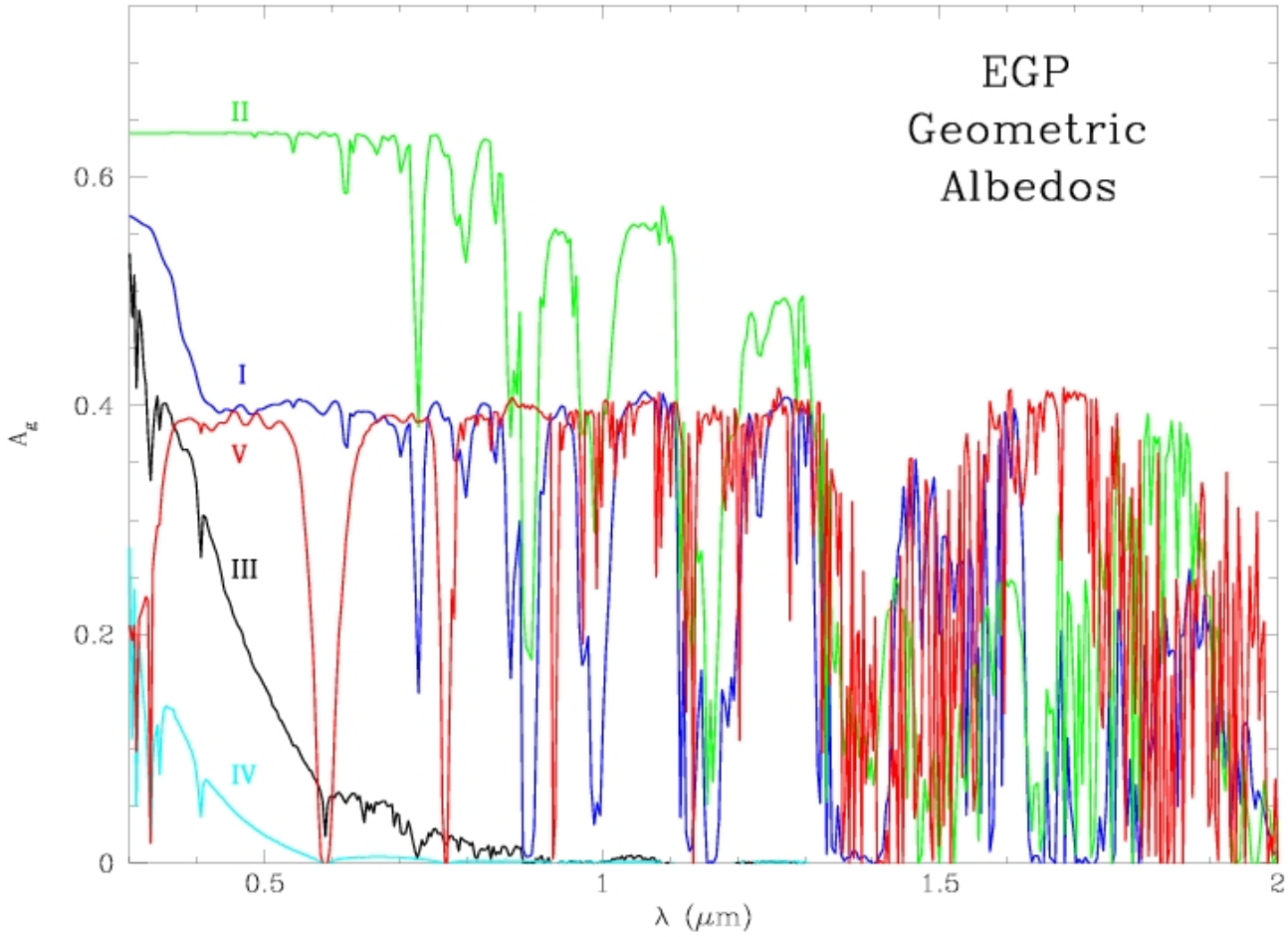

Estimated geometric albedos of Class I through V EGPs.

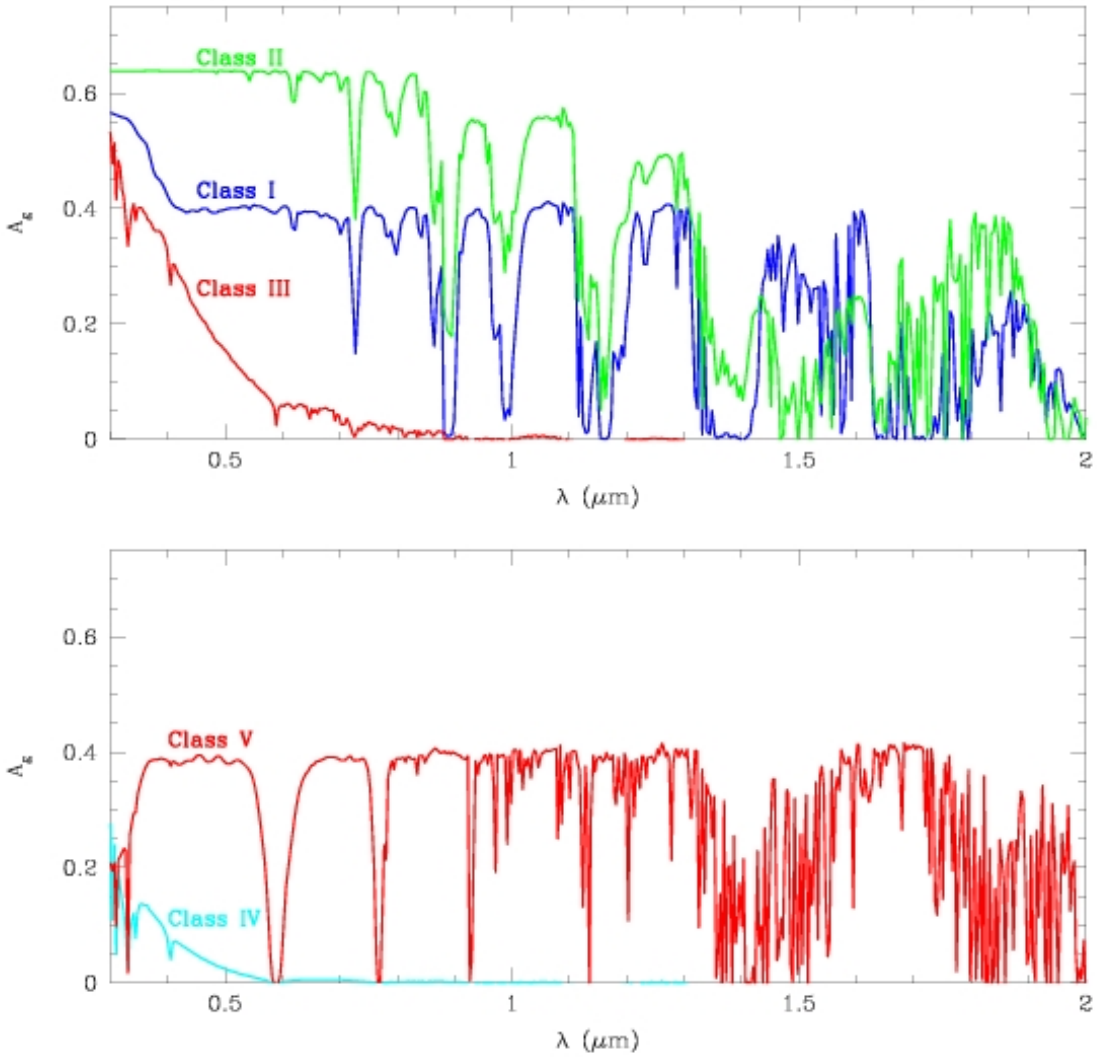

(a) Estimated geometric albedos of Class I, II and III EGPs. A modified T-P profile model is used in each case. These conversions from spherical albedos are made by approximating the phase integral based on the single scattering albedo and scattering asymmetry factor at an atmospheric depth equal to the mean free path of incident radiation. (b) Estimated geometric albedos of Class IV and V EGPs.

Planet diversity

→ fractional radius

→ inclination

→ planetary mass

- Solid planets:

=> Diversity

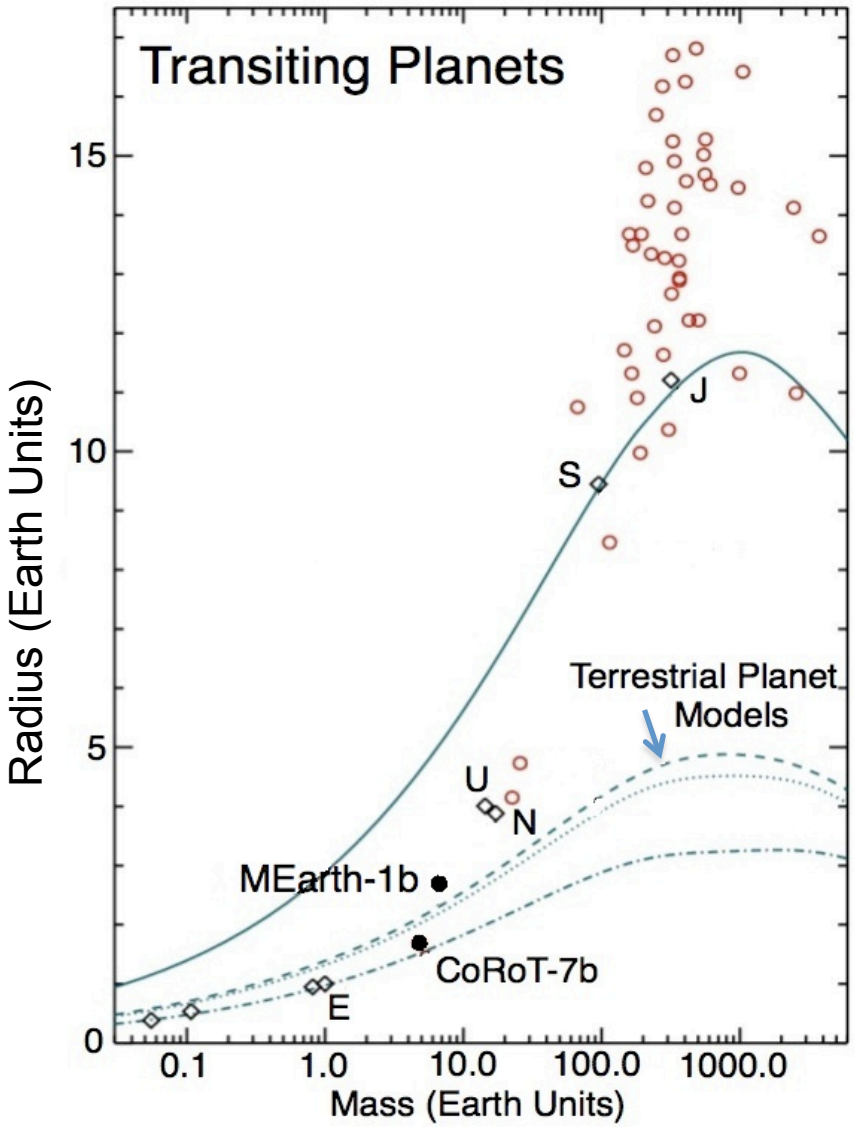

~A Thousand Planets Are Known to be Transiting.

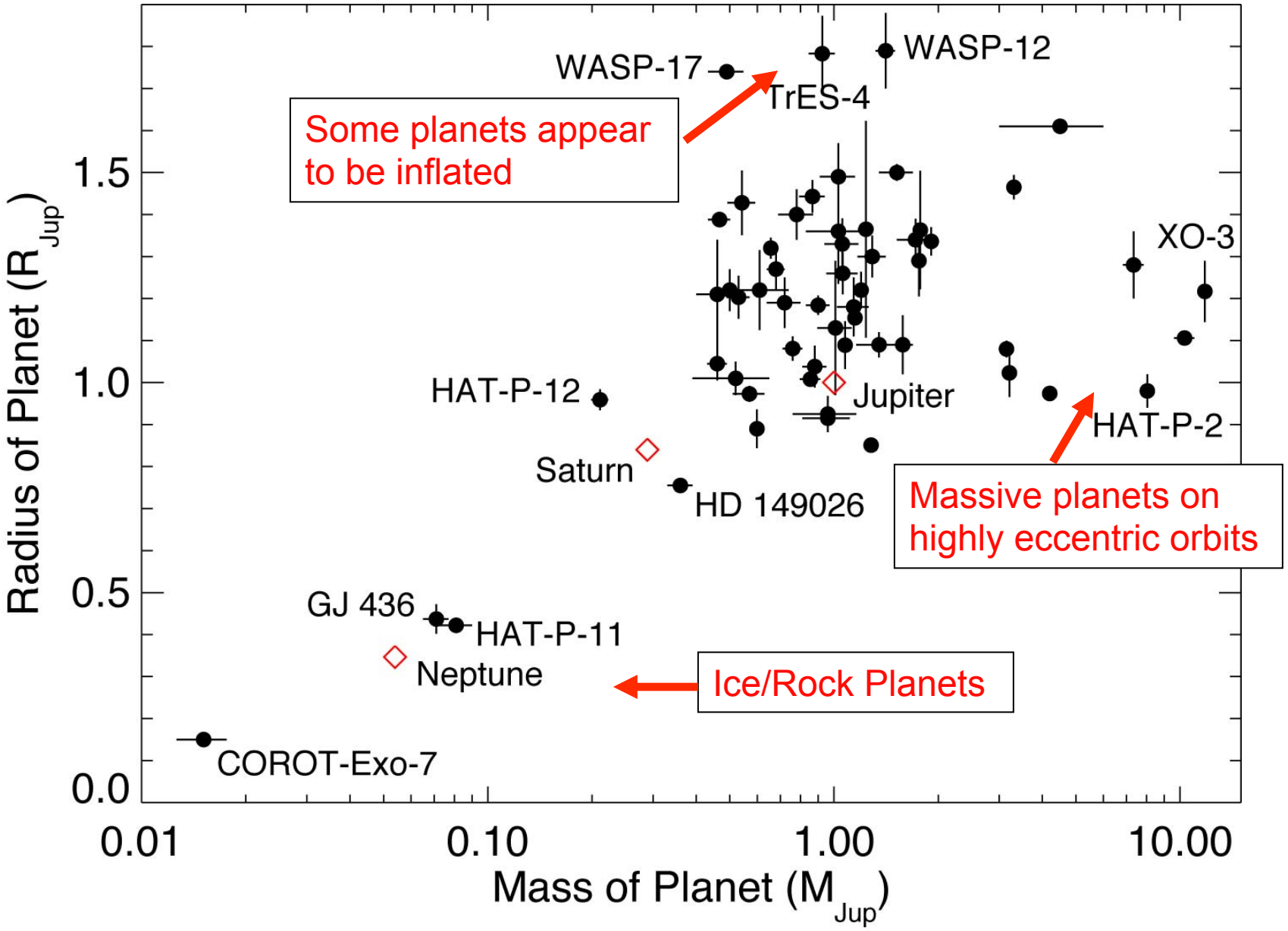

Spitzer ST:

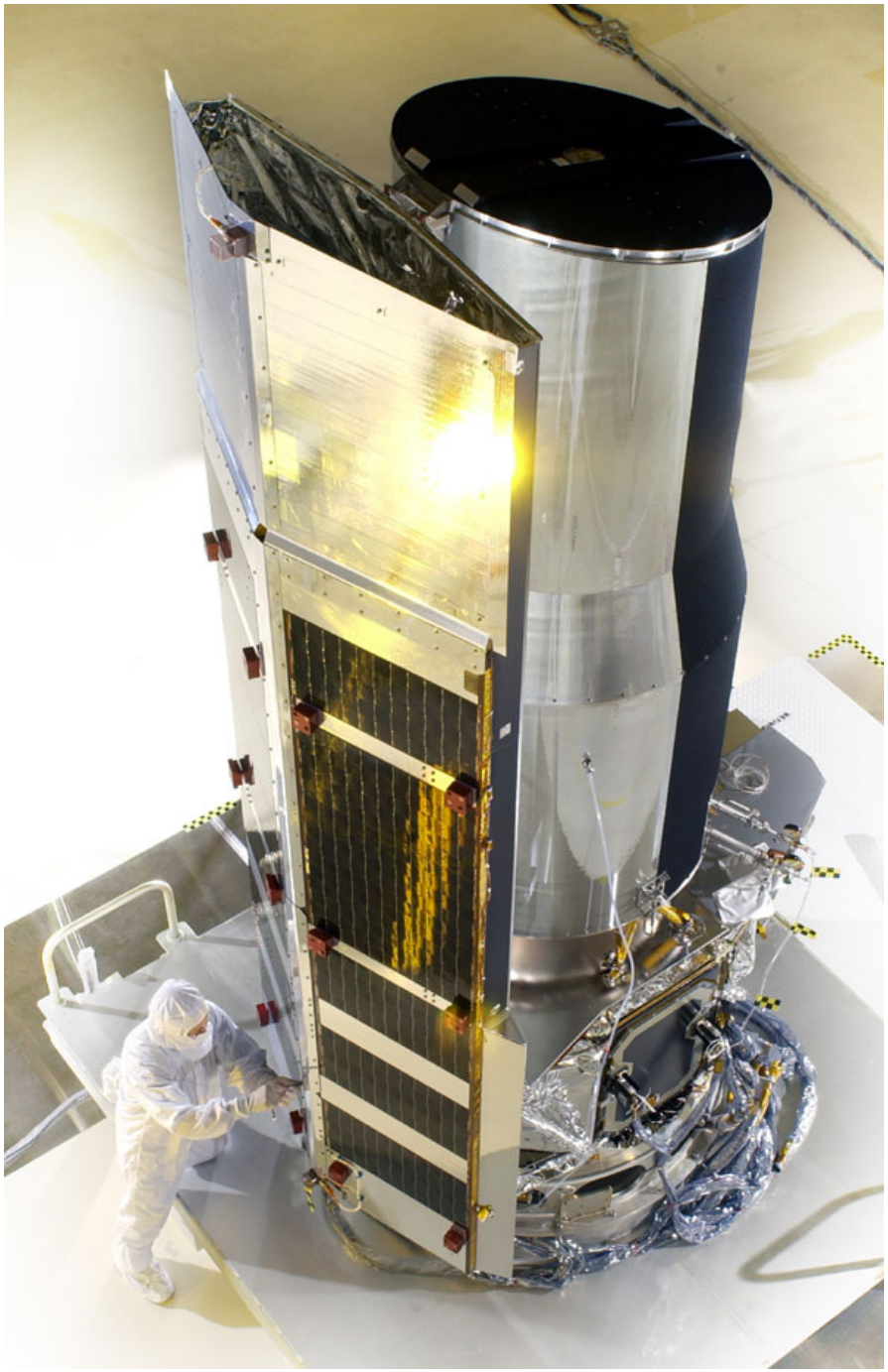

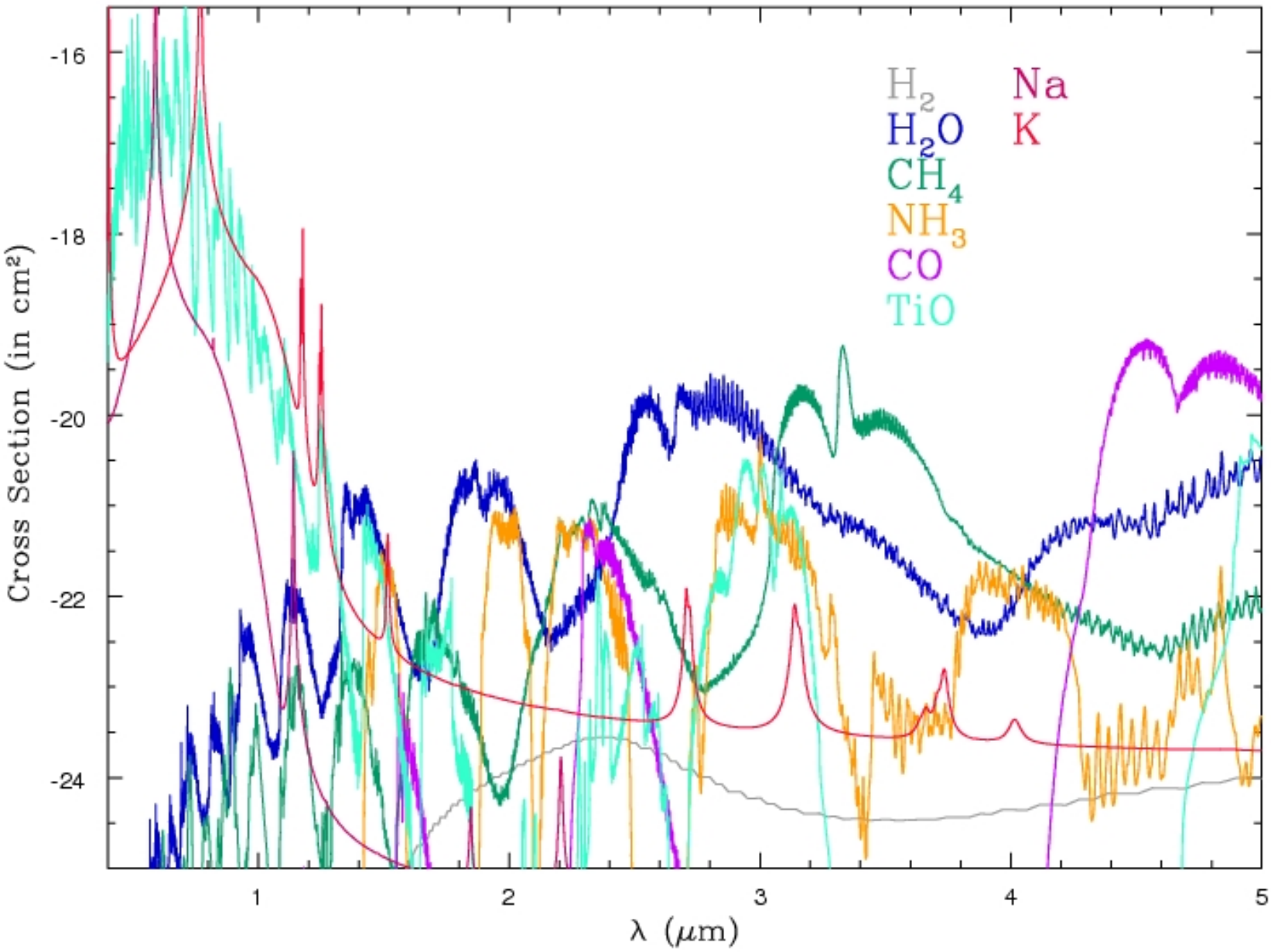
-16
-18
-20
-22
-24
Cross Section (in cm²)
1
2
3
4
5
λ (μm)
H2
H2O
CH4
NH3
CO
TiO
Na
K

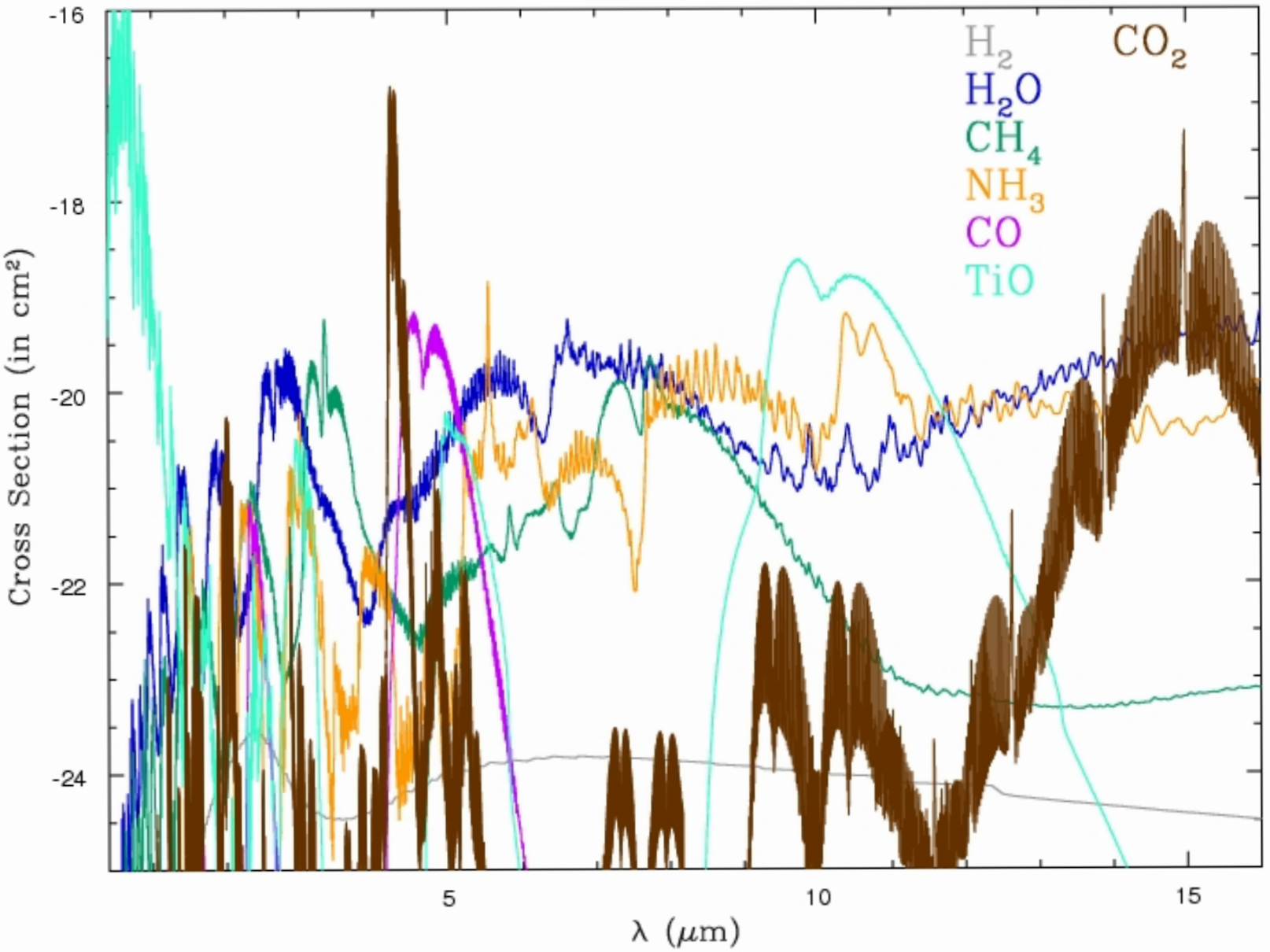
-16
-18
-20
-22
-24
Cross Section (in cm²)
5
10
15
λ (μm)
H2
H2O
CH4
NH3
CO
TiO
CO2

WFIRST-2.4 Exoplanet Imaging Sensitivity

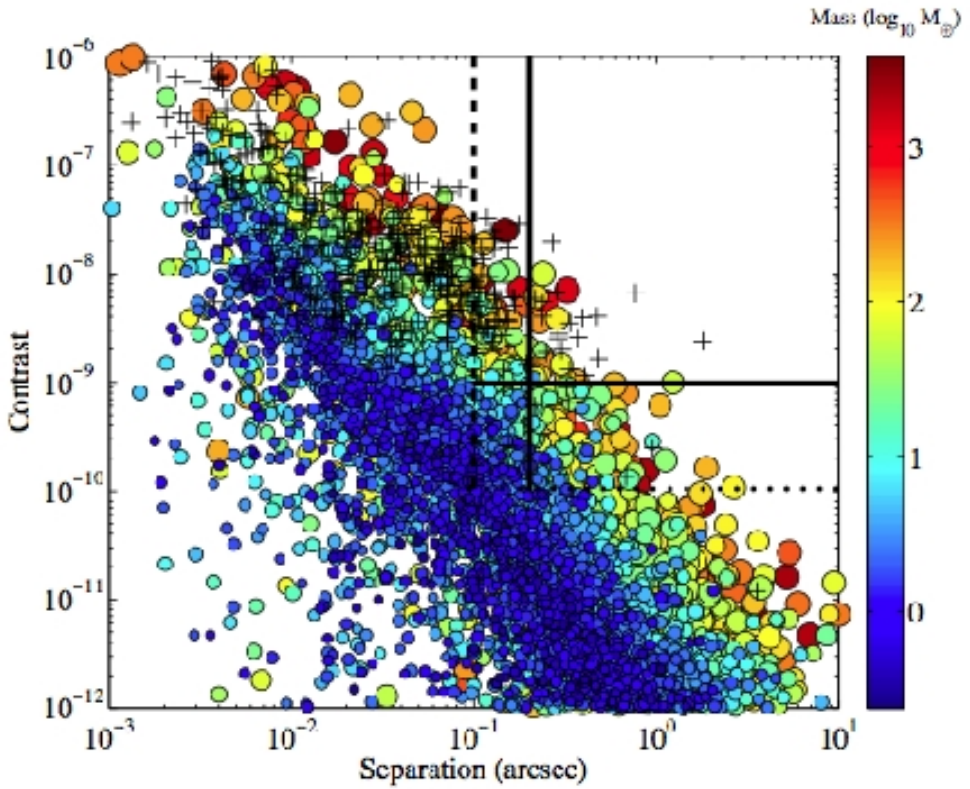

- Very sensitive to contrast limit (& IWA)

AFTA SDT report

Figure 2-21: This figure is a snapshot in time of contrast and separation for model planets, ranging in size from Mars-like to several times the radius of Jupiter, for about 200 of the nearest stars within 30 pc. Color indicates planet mass while size indicates planet radius. Crosses represent known radial velocity planets. Solid black lines mark the baseline technical goal of 1 ppb contrast and 0.2 arcsec IWA, while the dotted lines show the more aggressive goals of 0.1 ppb and 0.1 arcsec IWA.

Theoretical Questions

- What limits super-rotational atmospheric flows?
- Day/Night Contrasts?
- What is the "extra absorber" in many hot-EGP atmospheres?
- Why are some "Hot Jupiters" so large (R_p vs. M_p)?
- Is there a dynamical, structural, and/or thermal role for B-fields?
- What condensates reside in planetary atmospheres?
- Winds and Evaporation?
- Tidal Effects?
- Atmospheric, Envelope, and Core compositions?
- Mode(s) of Formation (and Signatures!)?

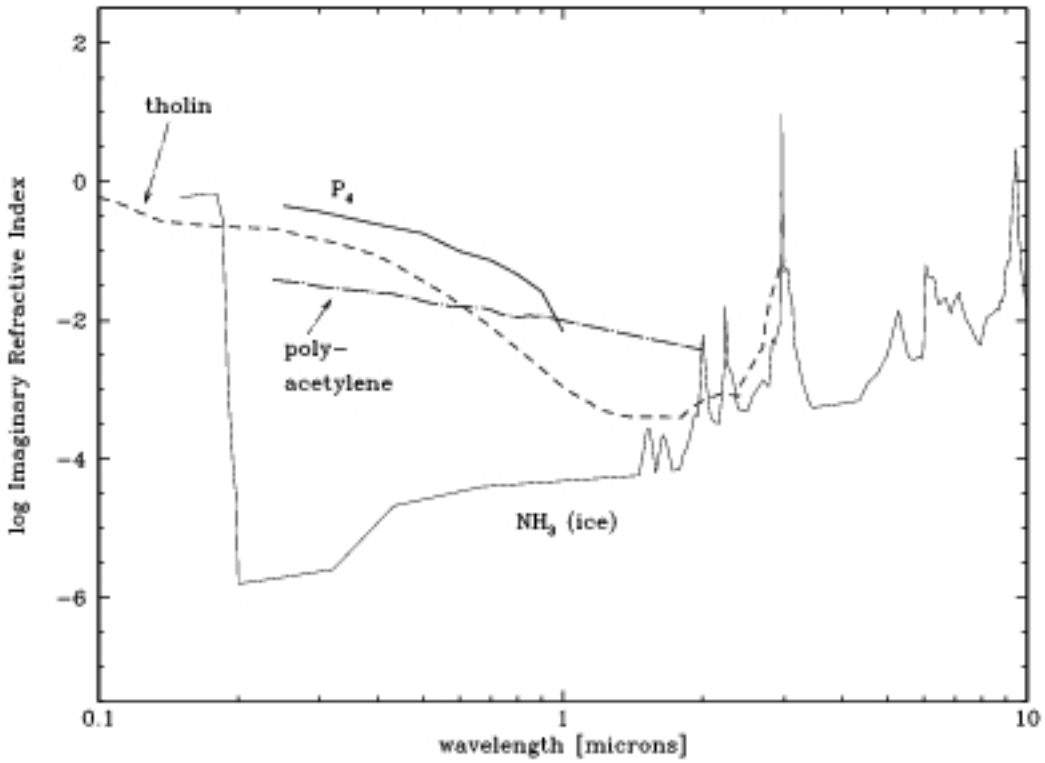

Imaginary indices of refraction for possible haze chromophores, in comparison to that for NH_3 (ice).

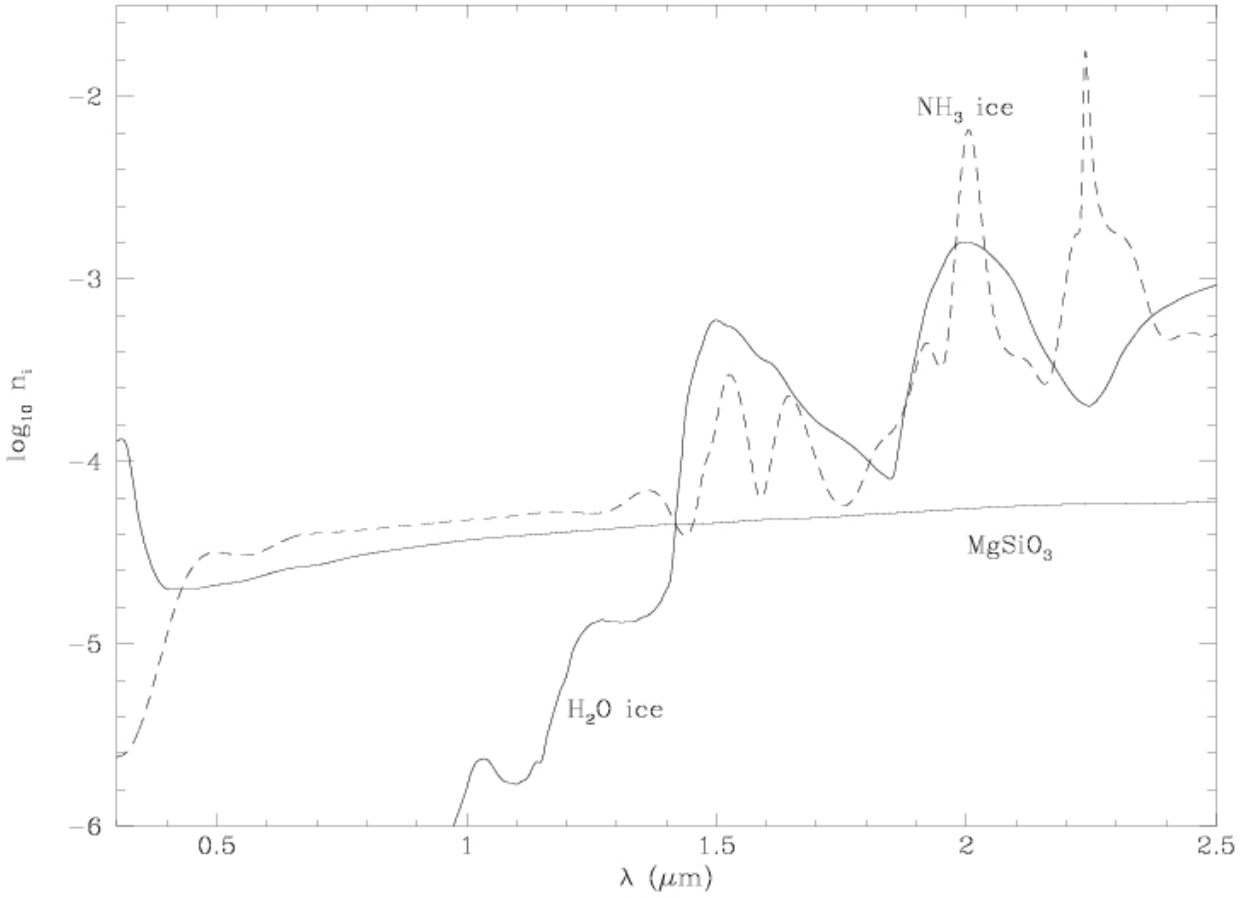

Imaginary refractive indices of the principal condensates.

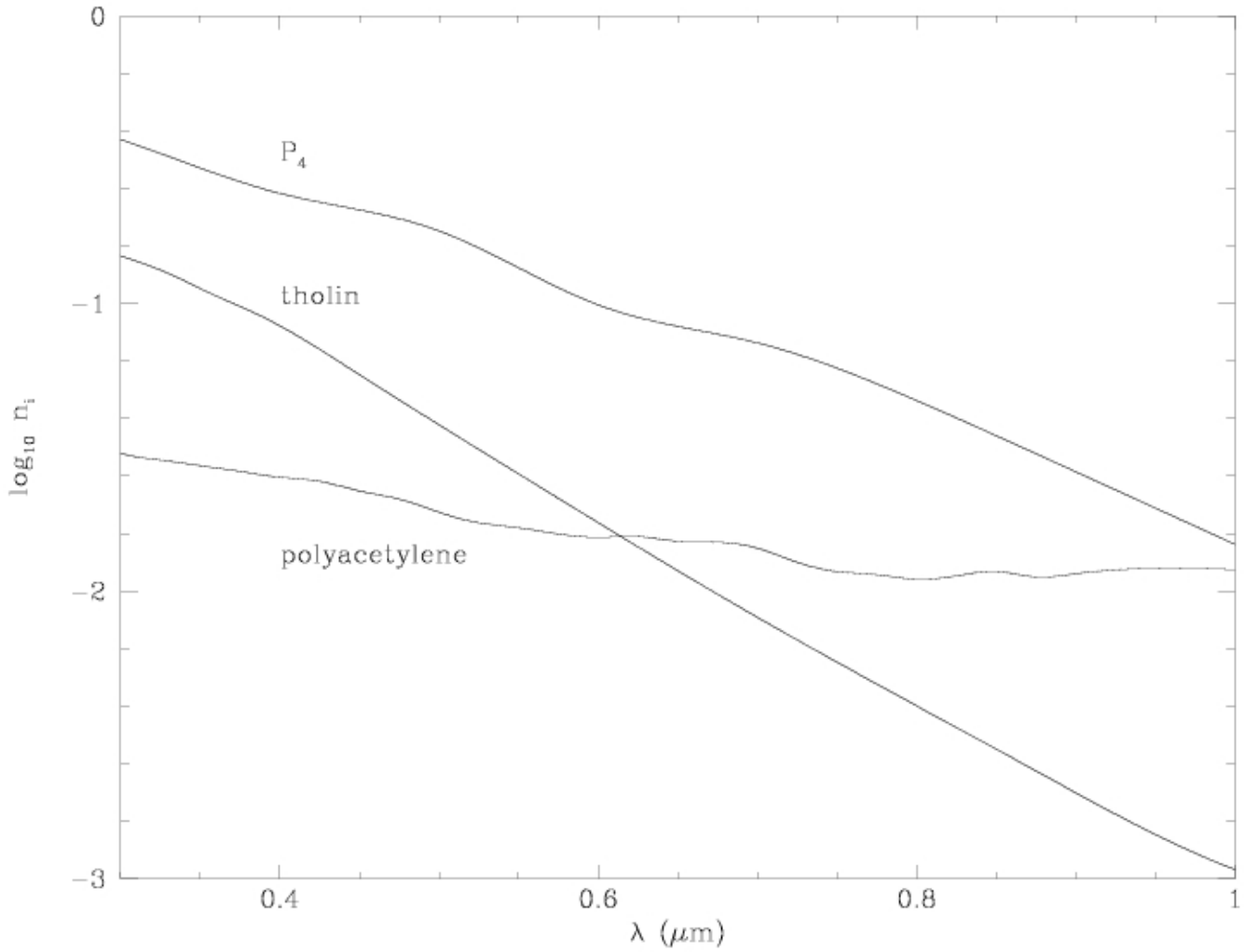

Imaginary refractive indices of stratospheric haze and tropospheric chromophore candidates. Tholin and P_4 provide a great deal of absorption in the UV/blue.

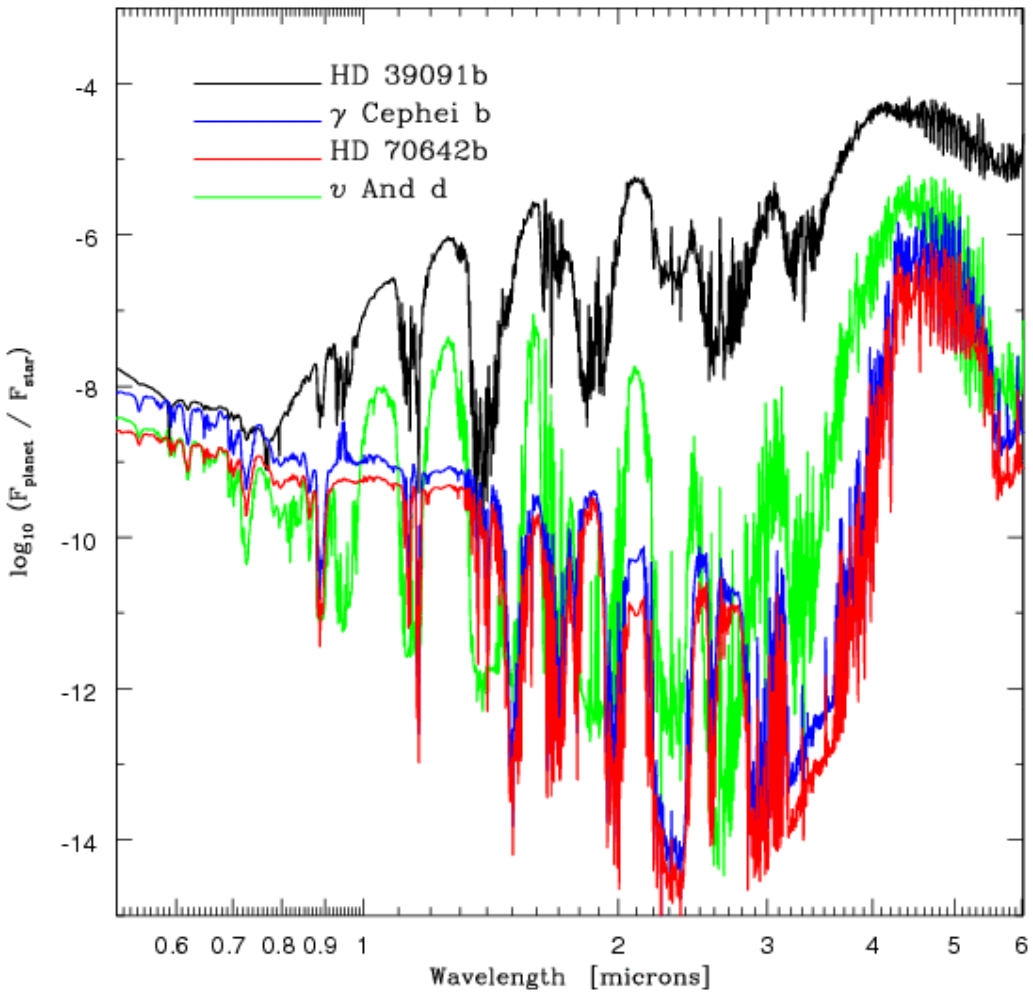

Average Planet/Star flux ratios for some other representative non-transiting EGPs.

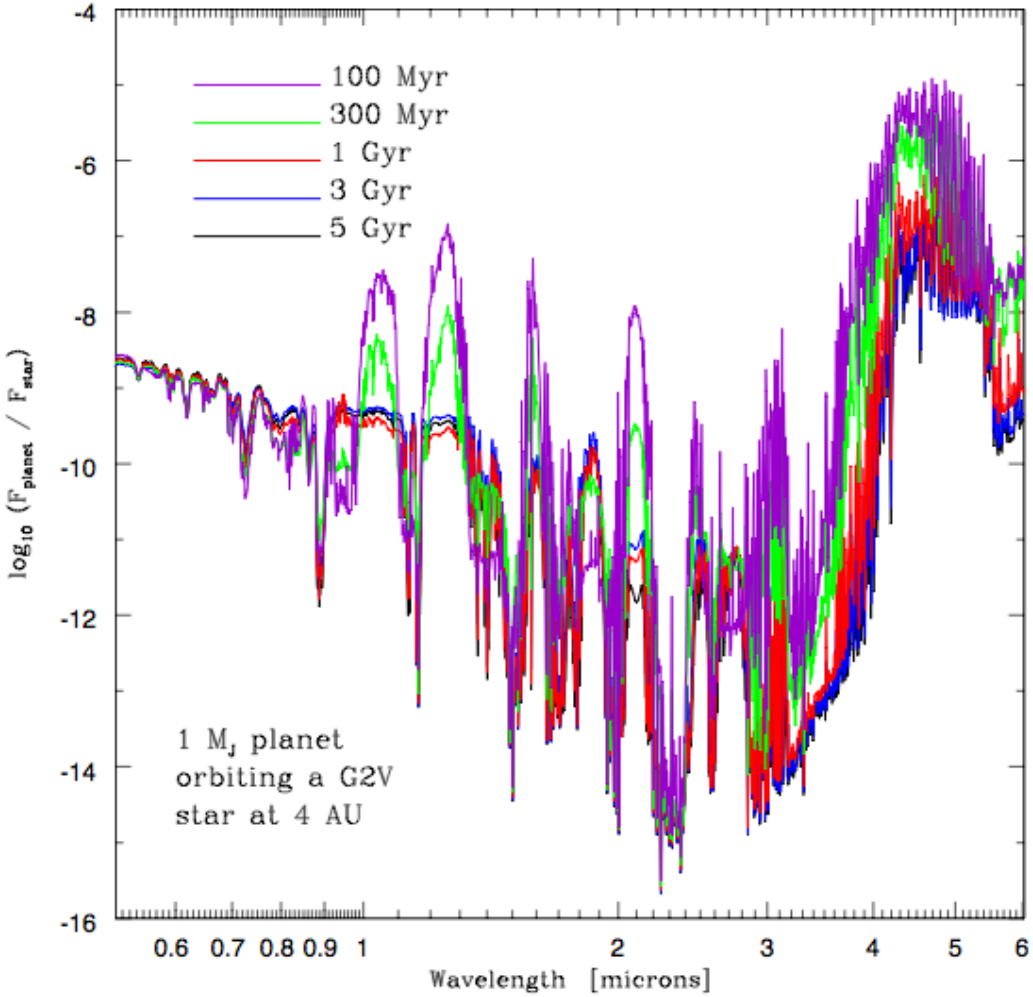

Planet/Star flux ratios as a function of age for a given EGP mass (1 M_J) orbiting a G2V star at 4 AU.

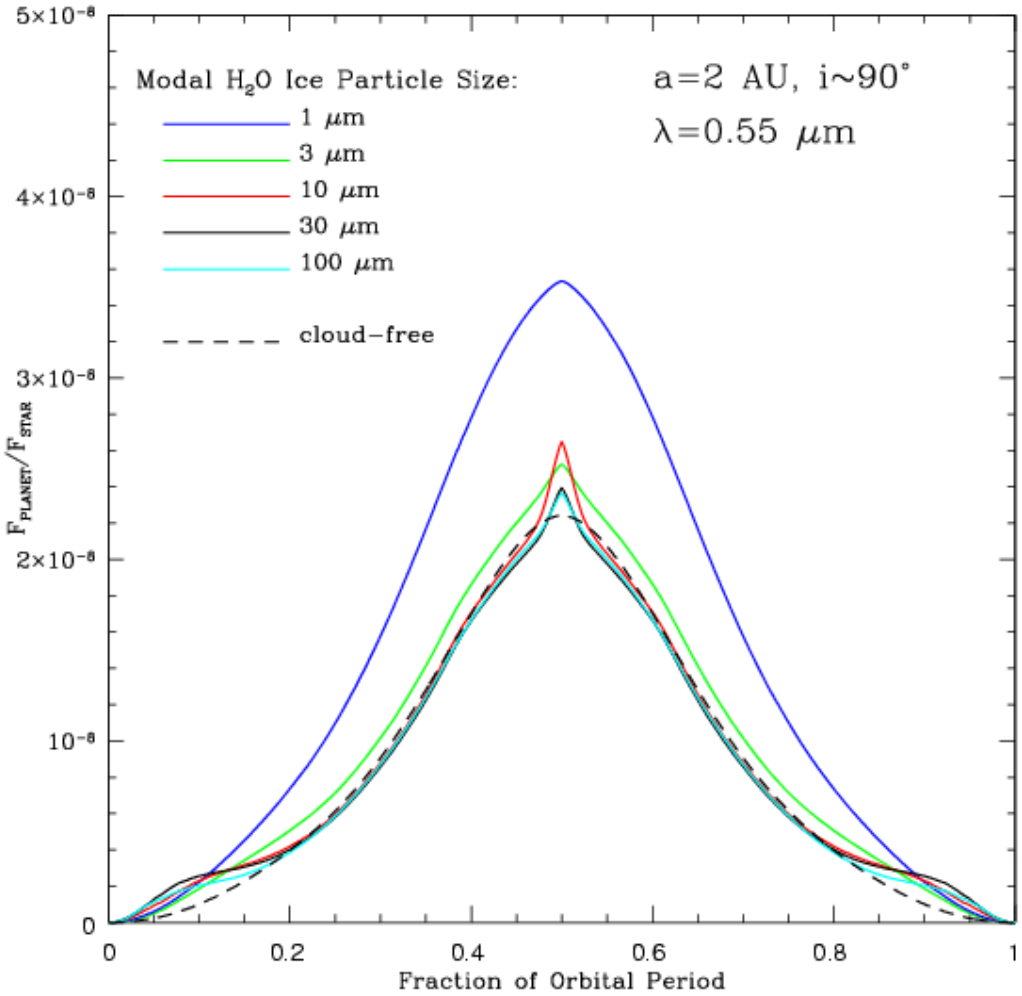

The dependence of the planet/star flux ratio on condensate particle size at a wavelength of 0.55 microns. Model light curves for EGPs at 2 AU with modal H_2O ice particle sizes of 1, 3, 10, 30, and 100 microns are depicted. Shown for comparison is a cloud-free model (black dashed curve). In order to show the full variation in the shapes and magnitudes of the light curves with particle size, we have set the orbital inclination to approximately 90 degrees so that the opposition effect, present for many of the models, can be seen in full.

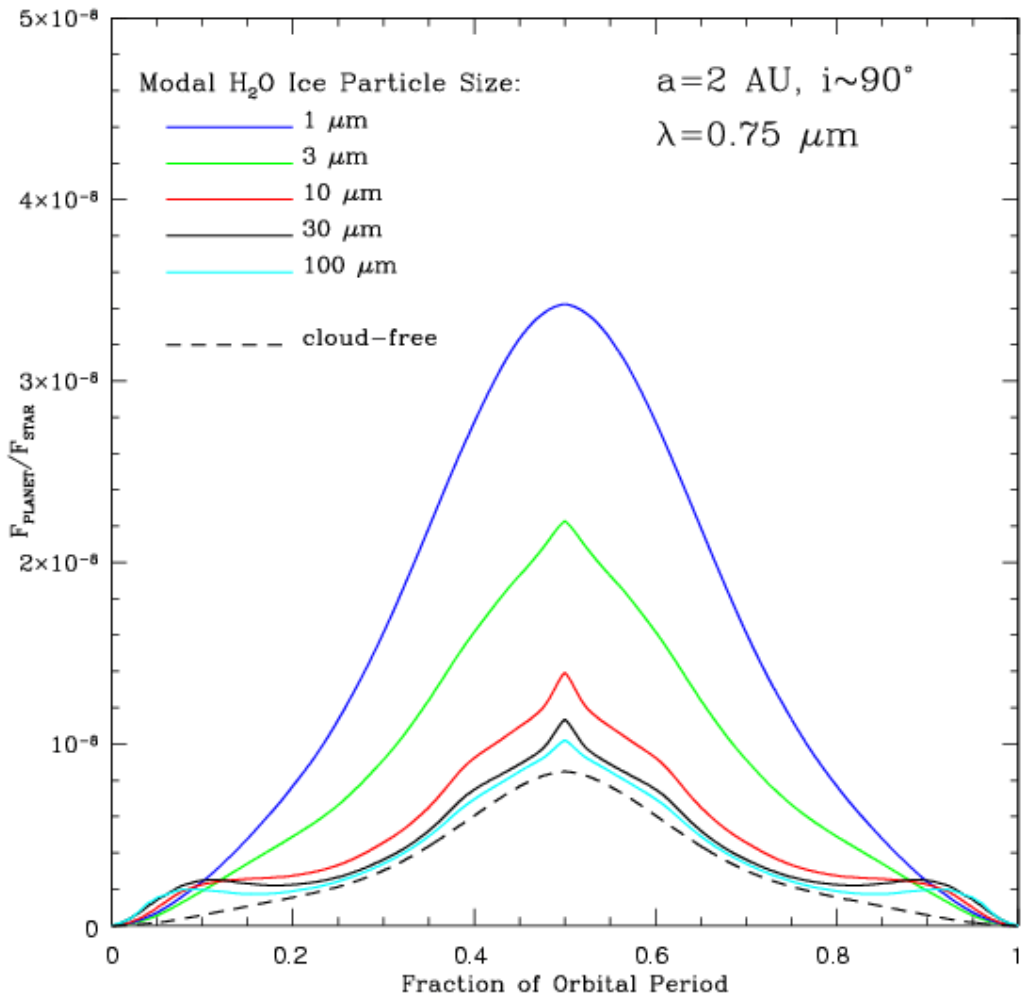

The dependence of the planet/star flux ratio on condensate particle size at a wavelength of 0.75 microns. Model light curves for EGPs at 2 AU with modal H_2O ice particle sizes of 1, 3, 10, 30, and 100 microns are depicted. Shown for comparison is a cloud-free model (black dashed curve).

In order to show the full variation in the shapes and magnitudes of the light curves with particle size, we have set the orbital inclination to approximately 90 degrees so that the opposition effect, present for many of the models, can be seen in full.

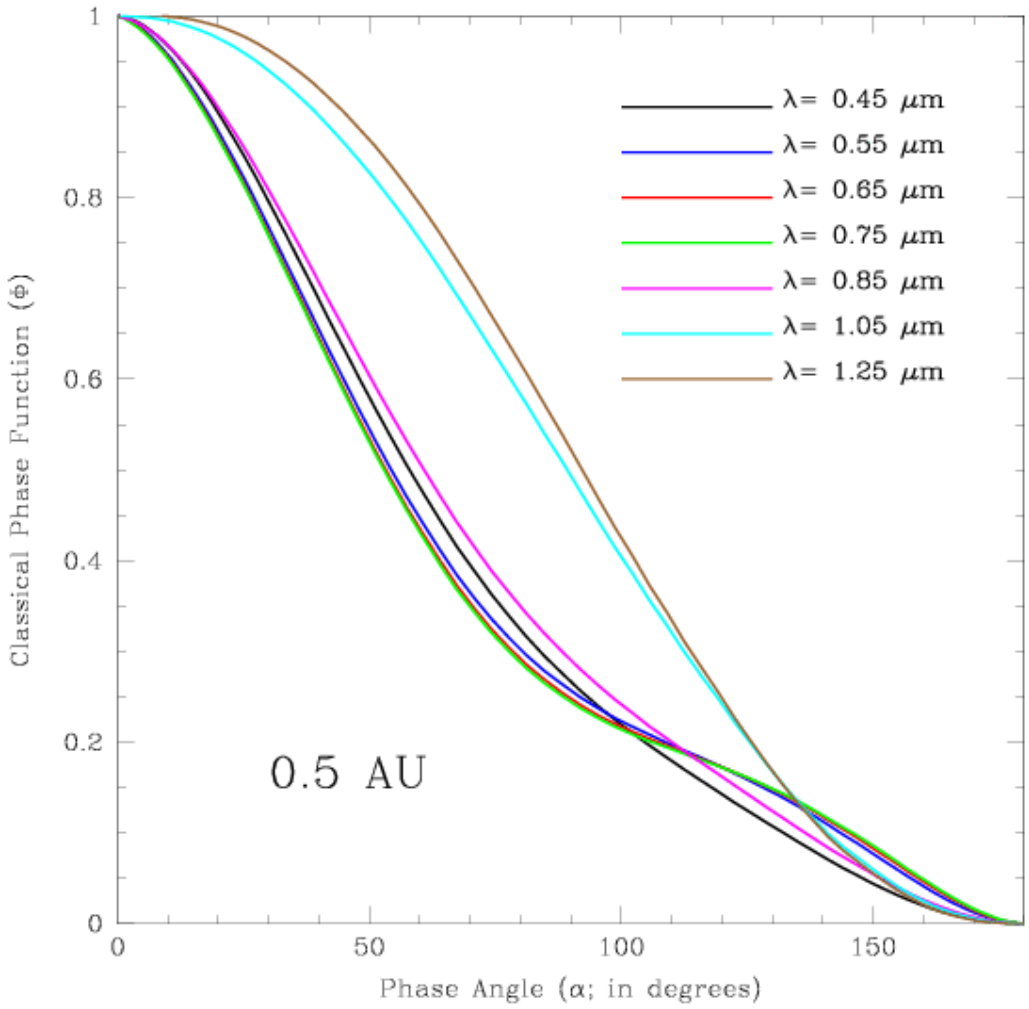

Wavelength dependence of the phase function for a cloud-free EGP orbiting at a distance of 0.5 AU from its G2V central star. The 1.05 microns and 1.25 microns phase curves are outliers because they contain a mix of thermally re-emitted and reflected radiation.

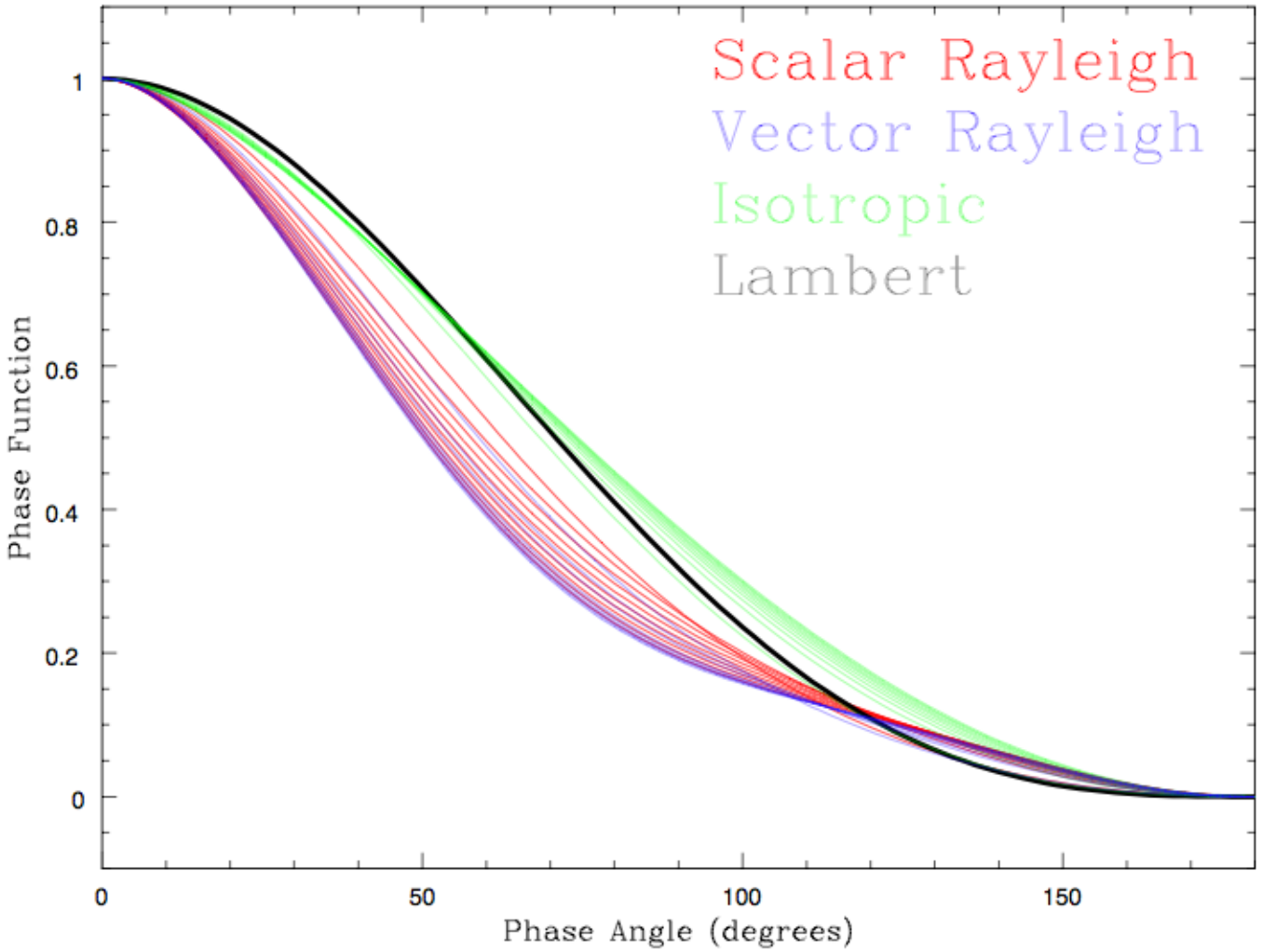

Comparison of phase curves for different scattering phase functions. The phase curves for Rayleigh scattering (both scalar and vector) and isotropic scattering are shown for several ω values between 0 and 1; higher phase curves correspond to larger ω. For Lambert scattering, the phase curve is independent of ω.

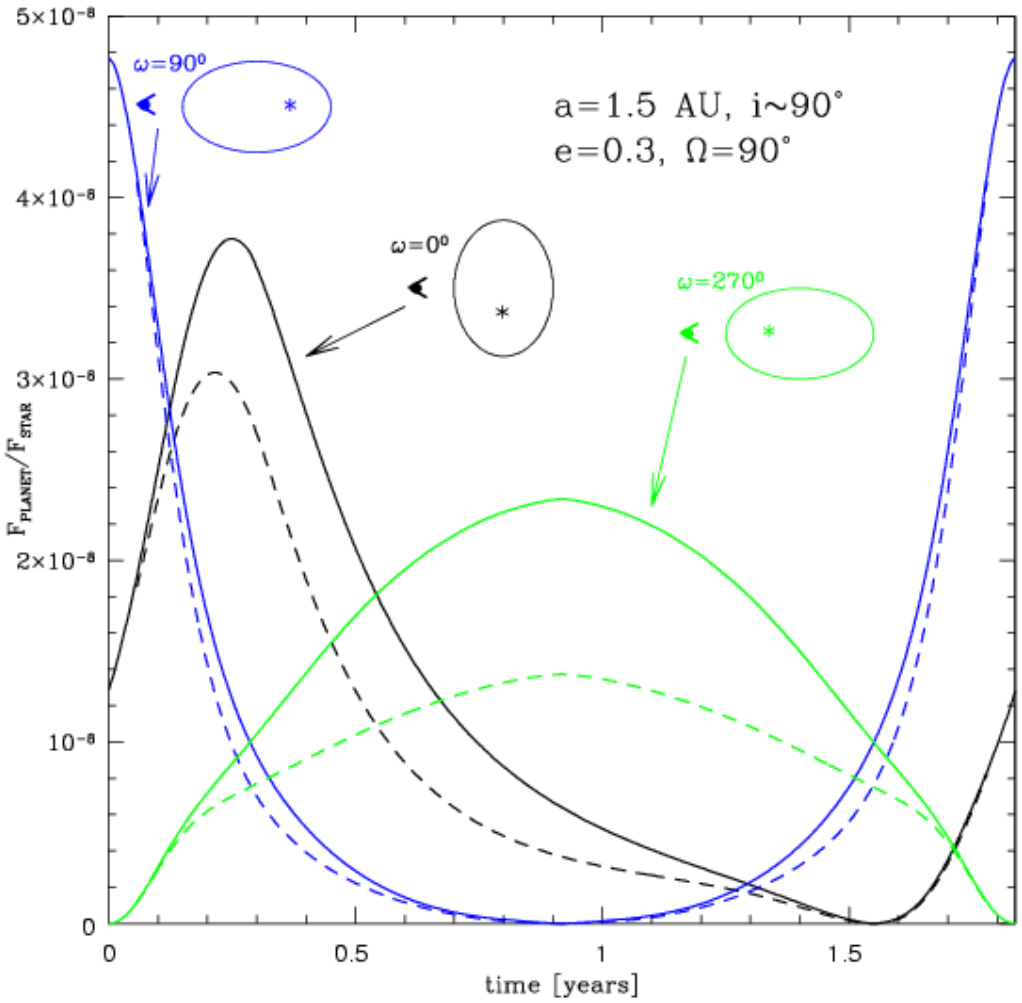

The optical light curve of an EGP with a=1.5 AU and e=0.3, assuming a G2V central star (a system similar to HD 160691; Jones et al. 2002) and an inclination of 80 degrees (with no transit effects). Three different possible viewing angles are shown (solid curves). Clouds condense and sublimate throughout each orbit as the planet-star distance varies in time. Shown for the sake of comparison are the light curves that would result if the object were to remain artificially cloud-free throughout its entire orbit (dashed curves).

Doppler Imaging Map of Luhman 16B: Crossfield et al. 2014

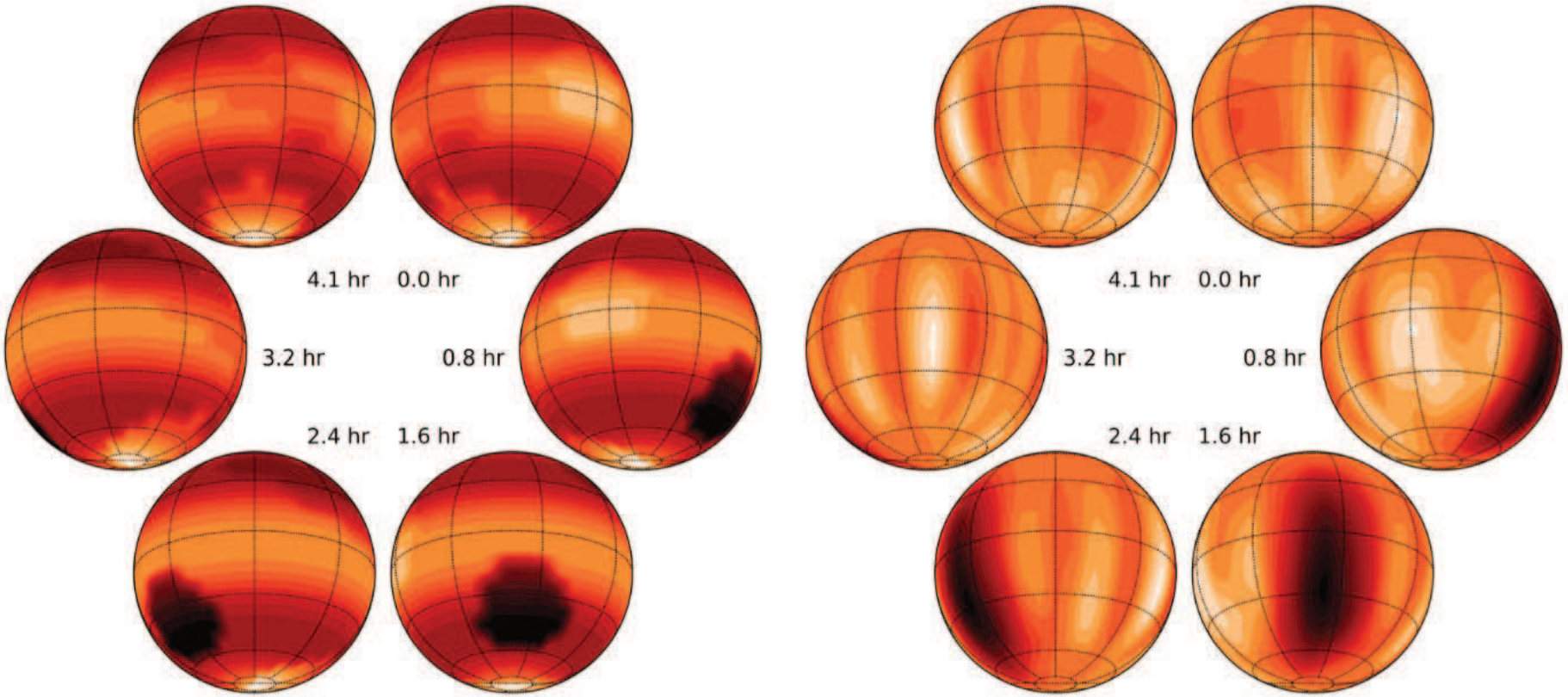

WASP-43b Planet Flux vs. Wavelength and Phase